

STABILITY AND STRESS ANALYSIS OF PARABOLIC PIPE-REDUCERS

By

MUHAMMAD ASHIQUR RAHMAN
B. Sc. Engg. (Mech.)

A thesis submitted to the department of Mechanical Engineering
in partial fulfillment of the requirements for
the degree of Master of Science
in
Mechanical Engineering.



APRIL, 1994

BANGLADESH UNIVERSITY OF ENGINEERING AND TECHNOLOGY,

DHAKA, BANGLADESH.



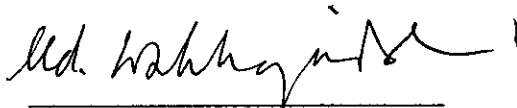
#87538#

"R"
621.8672
1994
ASH

RECOMMENDATION BY THE BOARD OF EXAMINERS

The board of examiners hereby recommends to the Department of Mechanical Engineering, BUET, Dhaka, acceptance of the thesis, "STABILITY AND STRESS ANALYSIS OF PARABOLIC PIPE-REDUCERS", submitted by M. Ashiqur Rahman, in partial fulfillment of the requirements for the degree of Master of Science in Mechanical Engineering.

Chairman :



Dr. Md. Wahhaj Uddin
Professor
Dept. of Mech. Engg.
BUET, Dhaka

Member :



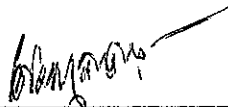
Dr. Md. Abdur Razzaq Akhanda
Professor and Head
Dept. of Mech. Engg.
BUET, Dhaka

Member :



Dr. R. G. M. Hasan
Assistant Professor
Dept. of Mech. Engg.
BUET, Dhaka

Member (External) :



Dr. A. M. M. T. Anwar
Associate Professor
Dept. of Civil Engg.
BUET, Dhaka

ACKNOWLEDGEMENT

The author expresses his gratefulness to his supervisor, Dr. Md. Wahhaj Uddin, Professor, Department of Mechanical Engineering for his constant and sincere guidance and invaluable suggestions during the whole period of this research work. Special thanks are for Md. Raisuddin Khan, Assistant Professor, BIT, Chittagong, who helped the author in sorting out the critical problems and overcoming them during the research work.

ABSTRACT

For joining pipes of unequal diameters, truncated parabolic shells can be used as pipe reducers instead of the traditional conical frustums, as the doubly curved parabolic shell elements are superior to the conical shells in withstanding high pressure. The present investigation analyses the stability and stresses in the truncated parabolic shells to be used as pipe reducers and also compares the results with those of conical reducers obtained by Ali.

The analysis is based on the nonlinear governing equations for axisymmetric deformations of shells of revolution. The multisegment method of integration is used for obtaining the solutions of the governing nonlinear differential equations. Numerical solutions are obtained by using a modified computer program, developed by Uddin, for solving the governing equations by the multisegment method of integration. The interpretation of instability of the parabolic reducers is based on Thompson's theorems I and II.

Critical pressures for the parabolic reducers are calculated varying the thickness ratio and the diameter ratio. Critical pressures and the stress distributions are presented graphically and their dependence on different parameters are discussed.

It is found that long parabolic reducers are prone to local instability near the larger end of the reducer but this critical zone shifts towards the smaller end as the two ends of the reducer are brought closer. Comparison between a parabolic reducer and a conical reducer with identical parameters shows that the former one develops uniform stresses of lower magnitude. Consequently, it is found that they are much more stable than their counter parts under uniform external pressure.

NOTATIONS

a	=	distance between the vertex and the focus of the parabola
b_1, b_{m+1}	=	(m,1) matrices, contain prescribed variables at the boundary, defined in Eq. (4.13a)
C	=	Eh : extensional rigidity
\bar{C}	=	$(1-\nu^2)\xi_e/R$
D	=	$Eh^3/[12(1-\nu^2)]$: bending rigidity
\bar{D}	=	$1/[12(1-\nu^2)\bar{P}\bar{T}^2\bar{R}]$
E	=	Young's modulus
F	=	$a/(R-R_1)$, ratio to define the geometry of the reducer
H	=	horizontal stress resultant
\bar{H}	=	H/PR : nondimensional horizontal stress resultant
h	=	shell thickness
I	=	(m,m) unit matrix
k_θ, k_ξ	=	changes of curvature of the middle surface of shell
\bar{k}_θ	=	$k_\theta\xi_e$: nondimensional value of k_θ
\bar{k}_ξ	=	$k_\xi\xi_e$: nondimensional value of k_ξ
\bar{L}	=	$\bar{R}/\bar{P}\bar{T}$
M	=	number of segment
m	=	order of system of differential equations
M_ξ	=	meridional couple resultant
M_θ	=	circumferential couple resultant
\bar{M}_ξ	=	M_ξ/PRh : nondimensional value of M_ξ
\bar{M}_θ	=	M_θ/PRh : nondimensional value of M_θ
N_ξ	=	meridional stress resultant
N_θ	=	circumferential stress resultant
\bar{N}_ξ	=	N_ξ/PR : nondimensional value of N_ξ
\bar{N}_θ	=	N_θ/PR : nondimensional value of N_θ
P	=	outward normal pressure
\bar{P}	=	P/E : nondimensional value of P
P_v	=	vertical component of surface load
P_H	=	horizontal component of surface load
Q	=	transverse shear stress resultant
R	=	larger radius of the reducer
R_1	=	smaller radius of the reducer

\bar{R}	=	ξ_e/R
R_ξ, R_θ	=	principal radii of curvature of middle surface of shell
r_o	=	radial distance of a point on undeformed middle surface from axis of symmetry
r	=	r_o+u : radial distance of a point on deformed middle surface from axis of symmetry
\bar{r}_o	=	r_o/ξ_e : nondimensional value of r_o
S_i	=	i th segment
T_1, T_{m+1}	=	(m,m) matrices, given by boundary conditions
\bar{T}	=	R/h : thickness ratio
u	=	radial (horizontal) displacement
\bar{u}	=	uEh/PR^2 : nondimensional horizontal displacement
V	=	vertical stress resultant
\bar{V}	=	V/PR : nondimensional vertical stress resultant
w	=	axial (vertical) displacement
\bar{w}	=	wEh/PR^2 : nondimensional axial displacement
x	=	independent variable
x_i	=	end point of segment
x_l	=	R_1/R : diameter ratio
$y(x)$	=	$(m,1)$ matrix, contains m variables
z_o	=	axial distance of a point on undeformed middle surface of shell
z	=	z_o+w : axial distance of a point on deformed middle surface
α	=	parameter of meridian of deformed shell, defined in Eq. (3.1c), or semi-apex angle of conical shell
α_o	=	value of α corresponding to undeformed shell
β	=	angle of rotation of normal after deformation
$\bar{\beta}$	=	β
$\epsilon_\xi, \epsilon_\theta$	=	middle surface strains
$\bar{\epsilon}_\xi$	=	$\epsilon_\xi Eh \xi_e/PR^2$: nondimensional value of ϵ_ξ
$\bar{\epsilon}_\theta$	=	$\epsilon_\theta Eh \xi_e/PR^2$: nondimensional value of ϵ_θ
ζ	=	normal distance of a point in the shell from middle surface
ξ	=	parameter of shell meridian, or distance measured along meridian
$\bar{\xi}$	=	ξ/ξ_e : nondimensional meridional distance between the centre of the smaller end and the larger end junction

- ξ_e = total meridional length, between the centre of the smaller end and the larger end junction.
- ϕ_o = angle between normal and axis of symmetry before deformation (meridional angle)
- ϕ = $\phi_o - \beta$: angle between normal and axis of symmetry after deformation
- ν = Poisson's ratio
- σ_{ai} = $N_\xi/h + 6M_\xi/h^2$: meridional stress at the extreme inner fiber
- σ_{ao} = $N_\xi/h + 6M_\xi/h^2$: meridional stress at the extreme outer fiber
- σ_{ci} = $N_\theta/h + 6M_\theta/h^2$: circumferential stress at the extreme inner fiber
- σ_{co} = $N_\theta/h + 6M_\theta/h^2$: circumferential stress at the extreme outer fiber
- $\bar{\sigma}_{ai}$ = σ_{ai}/E : nondimensional value of σ_{ai}
- $\bar{\sigma}_{ao}$ = σ_{ao}/E : nondimensional value of σ_{ao}
- $\bar{\sigma}_{ci}$ = σ_{ci}/E : nondimensional value of σ_{ci}
- $\bar{\sigma}_{co}$ = σ_{co}/E : nondimensional value of σ_{co}
- $(...)'$ = derivative with respect to ξ or $\bar{\xi}$

CONTENTS

	Page Nos.
ABSTRACT	i
NOTATIONS	ii
CHAPTER 1 INTRODUCTION	
1.1 Preliminary	1
1.2 The problem of instability or buckling	2
1.3 Resume of nonlinear shell analysis	4
1.4 Objectives of this investigation	5
1.5 Methods of solving nonlinear differential equations	8
CHAPTER 2 LITERATURE REVIEW	
2.1. General	14
2.2 Some analytical, numerical and experimental investigations of shell problems	17
CHAPTER 3 GOVERNING EQUATIONS	
3.1 General	23
3.2 The shell theory	23
3.3 Reissner's theory of axisymmetric deformations of shells of revolution	24
3.4 Derivation of field equations	27
3.5 Linearized equations of axisymmetric shells	30
3.6 Boundary conditions of axisymmetric shells	31
3.7 Equations in non-dimensional forms	33

CHAPTER 4	METHOD OF SOLUTION	
4.1	Introduction to multisegment integration	39
4.2	Derivation of additional equations	41
4.3	Treatment of boundary conditions	46
4.4	Determination of critical pressure	48
CHAPTER 5	RESULTS AND DISCUSSIONS	
5.1	Accuracy and reliability of the analysis	50
5.2	General discussions on results	51
5.3	General discussions on the pattern of stresses	55
5.4	Discussions on the modes of buckling	58
CHAPTER 6	CONCLUSIONS AND RECOMMENDATIONS	
5.1	Conclusions	66
5.2	Recommendations for future work	67
REFERENCES		69
TABLES		80
FIGURES		81
APPENDIX A.	PROGRAMMING FEATURES	
A.1	General features	128
A.2	Treatment of boundary conditions	129
A.3	On the use of the program	130
A.4	Output of the program	132
A.5	Table of input and output variables	134
APPENDIX B.	PROGRAM LISTING	136



CHAPTER 1

INTRODUCTION

1.1 PRELIMINARY

Shell elements, in general, can transmit the surface load primarily through the uniformly distributed in plane membrane forces by virtue of their curved surfaces, without the action of bending or twisting. This property makes them, as a rule, a much more rigid and more economical structure than a plate. Consequently, shell elements are indispensable parts of almost all engineering structures. This is specifically true for the aerospace, nuclear, marine, and petrochemical industries where dramatic and sophisticated uses of shells are currently being made in missiles and space vehicles, nuclear reactor vessels, refinery equipment and the like. Tubular shell members are the most important components in the deep water offshore structures. Also, shell like structures are extensively used as silos and storage tanks.

As the use of shells gains momentum, more and more sophisticated mathematical analysis of shells are being sought. Shell structures can undergo a substantial amount of deformation before failure. This feature of shells submits themselves to the domain of nonlinear mathematical analysis. The nonlinearity is introduced into the governing equations of elasticity in three ways:

- a. through the strain-displacement relations
- b. through the equations of equilibrium of a volume element of the body, and
- c. through the stress-strain relations.

In (a) and (b) the retention of nonlinear terms is conditioned by geometric considerations, that is, the necessity of taking into account the angles of rotation in determining the changes of dimension in the line element and in the formulation of the conditions of equilibrium of a volume element. On the other hand, the nonlinear terms appear in the third set of equations (c) if the material does not behave in a linearly elastic fashion.

Hence, there are two types of nonlinearity:

- i. geometric, and
- ii. physical

In the problems of shell structures, the angles of rotation can be large, but the strains can be quite elastic. An example of this type of problem is the bending of a thin steel strip. It is well known that strips of good steel can be straightened out without traces of residual deformation after having their ends brought together. This bears witness to the fact that in these strips, even for large displacement and angle of rotation, the stresses do not exceed the yield strength. Thus, many shell structures belong to a class of problems which are physically linear but geometrically nonlinear.

1.2 THE PROBLEM OF INSTABILITY OR BUCKLING

Through the blessings of the modern science, the strength of the engineering materials has been increased tremendously. As a result, thinner structures can carry high intensity external loadings. Consequently, today's structures are more prone to failure due to instability than due to strength. The onset of buckling

invariably results abrupt changes in the shape of the structures which ultimately leads to failure as enormous deformations take place that shoot everything away from an initially stable equilibrium position. The concept of stability of equilibrium is thus a strongly intuitive one, and it consequently arises quite early in the development of classical mechanics. The work of Euler [26] appeared in 1744, and the contribution of Lagrange [41] in 1788. A century later a general bifurcation theory was sketched by Poincare [61] in 1885, and the definition of stability was given mathematical rigor in the treatise of Liapunov [43] in 1892.

If at any level of external cause (in the form of displacement, velocity, force etc.), a structure can sustain a small disturbance from its equilibrium condition, then the structure is said to be in stable equilibrium at that level of external cause. It should be noted that sustaining the disturbance means the structure will oscillate with a small amplitude about its equilibrium position. On the other hand, if the structure does not go back to its original equilibrium position or vibrate with ever increasing amplitude due to the disturbance, then the structure is said to be in an unstable equilibrium state at that level of external cause. If the structure remains in the disturbed state without vibration, then the equilibrium is referred to as the neutral equilibrium state.

A close assessment of the critical load for simple mechanical stability models reveals that the system maintains its stable equilibrium states as long as the work done due to internal resisting forces is greater than that due to the external load for any disturbance from the equilibrium position. In other words, it is the balance between the potential energy due to the internal resisting forces, which will be called internal strain energy or simply strain energy from now on, and the potential energy due to the external force, which will be called

external load potential or simply load potential from now on, which accounts for the stability of the system. At a certain level of the external cause, the internal strain energy becomes equal to or less than the external load potential, and the system reaches its unstable equilibrium state. Any disturbance to this equilibrium state will upset equilibrium or bring the system to a new equilibrium state distinct from the previous one, depending on whether the internal strain energy is equal to or less than the load potential. In fact, these are the alternate statements of the energy method used to confirm the mechanical stability of a system.

1.3 RESUME OF NONLINEAR SHELL ANALYSIS

That linear shell analysis fails to give proper information about the shell stresses and deformation in many problems can be seen in recent papers on the nonlinear shell analysis [27, 28, 32, 33, 37, 54, 65, 66, 67, 70, 82, 91, 92, 94-98, 103-106]. For this reason, the use of nonlinear theory has become rather widely accepted as a plausible basis for predictions of elastic strengths of shells of various geometries. Most of the papers currently found in the literature are concerned with the shells of revolution.

The basic concept of finite deflection analysis of Donnel [22] has been employed by numerous investigators to establish collapse loads of cylindrical shells subjected to various loadings. Finite deflection analysis has also been successful in offering reasonable predictions of the elastic buckling loads of shallow spherical caps subjected to uniformly distributed external pressure. Kaplan and Fung [38] have presented a perturbation solution to the nonlinear equations that agrees quite well with the results of their experiments for very shallow clamped

edged shells. Archer [7] extended their results to a greater range of shells. As can be seen from recent papers, very extensive work has been done in this field [32, 33, 37, 38, 66, 91, 92, 105]. Ball [9] has considered the problems of arbitrarily loaded shells of revolution and obtained solution for a clamped shallow spherical shell uniformly loaded over one-half of its surface. A number of papers based on the nonlinear analysis of stiffened shells, multilayered shells and sandwich shells can also be found in the current literature [5, 30, 40, 46, 48, 57, 62, 64, 75, 78, 102]. Based on Reissner's [69] large deflection analysis for general shells of revolution, Uddin [95] has presented large deflection analysis of composite shells of revolution and obtained extensive results for various pressure vessel problems [93-98]. Haque [31] analyzed the stability of ellipsoidal head pressure vessel. Rahman [63] extended this analysis to include imperfect shell geometry. Ali [6] analyzed the stability and stresses of conical reducers. In all these cases the predictions of these theories are in better agreement with experimental evidence than those of the classical investigations based on infinitesimal deformations.

1.4 OBJECTIVES OF THIS INVESTIGATION

Reducers, used as fittings in between two pipes of unequal diameters, often fail due to instability although having sufficient material strength, as these shell elements are often subjected to external pressure or internal suction in such applications. Pointing out that no notable work has been done on the stress and stability analysis of the above mentioned conical reducers, Ali [6] carried out a study on the same. Ali [6] found that the critical load for conical reducers decreases almost linearly as the apex angle of the conical frustums are increased keeping all other parameters constant. Motivated by the fact that the doubly curved parabolic reducers can sustain higher external load by virtue of the

membrane forces, the present analysis investigates whether the parabolic geometry of the shell meridian can improve the stress distribution and as well as the stability of the reducers.

So, the main objective of the present analysis is to compare a parabolic reducer with a conical reducer (having the same thickness ratio and diameter ratio) regarding stability and stress distribution. The set objectives are to be achieved through the following steps:

1. As the properly fabricated parabolic reducers are expected to deform axisymmetrically under pressure, Reissner's large deflection equations for axisymmetric deformations of shells of revolution are to be used as the governing equations for the reducers.
2. As the parabolic reducers are always to be connected to pipes of unequal diameters through the flanges, the boundary conditions at the two edges of the reducers are to be taken as those pertaining to completely fixed edges. This will also help to compare the results with ref. [6] where exactly same boundary conditions are considered.
3. As the governing equations to be used here ensure stationary potential energy ($\delta E_t = 0$), Classical or Bifurcation technique which is based on the identification of a secondary mode of deformation is used to calculate the critical pressure. Thompson's [90] theorems I and II are to be used for ascertaining the critical pressure of the parabolic reducer from the solutions of large deflection equations of the same for progressively increasing pressure.

4. As the governing nonlinear differential equations are not amenable to solutions by the method of direct integration because of its inability in determining the unknown boundary values due to inherent accumulation of truncation errors in the process of integration of shell equations, and as the finite-difference technique sometimes fails to differentiate between the instability of the differential equations and that of the solution process of the resulting algebraic equations, the multisegment method of integration is to be used for solving the differential equations.
5. As a computer program is already available in the literature, incorporating the multi-segment method of integration of the Reissner's equations for general shells, the computer program needed for obtaining the numerical solutions of the present problem is to be adopted from the available one by carrying out the necessary modifications.
6. The solutions are to be presented in nondimensional form to widen the usefulness of the results.
7. To keep the volume of results of stresses a minimum, results are to be presented for pressure-steps of about 50% of the critical pressure and above.
8. For each set of values of parameters, stresses are to be plotted against the entire meridional length of the parabolic reducer, so that critical zones in terms of different stresses can be seen readily.

9. Since, stability analysis is justified for thin shells with large diameters, the results are to be presented for thinner parabolic reducers with larger diameters only.

10. Finally, as critical pressure for conical reducers are already available in ref. [6], the critical pressures for parabolic reducers with the same diameter ratio and thickness ratio and of course with the same boundary conditions as those of the conical reducers are to be calculated for meaningful comparison of results.

1.5 METHODS OF SOLVING NONLINEAR DIFFERENTIAL EQUATIONS

Due to the very nature of the response of shell like structures under loading, their analyses, specifically their stability analyses, are based on the nonlinear mathematical analysis. Unfortunately, the majority of such large deflection and stability problems of practical structural components cannot be solved in closed form. Therefore, one has to resort to approximate analytical and/or numerical discretization techniques for their solution. Prior to the advent of digital computers, various approximate analytical techniques were the standard tools for the nonlinear analysis of structures.

The widespread availability of high speed computing machines, the fascination with numerical techniques due to their versatility in handling complex structures (e.g. shells with cutouts and stiffeners), and the simplicity of computer implementation have resulted in a relative stagnation in the development of effective analytical techniques. Analytical techniques have the major advantages over numerical discretization techniques in providing physical insight into the

nature of response. Moreover, analytical techniques can be used in conjunction with partitioning schemes for nonlinear analysis of individual components of practical (complex) structures.

The most frequently used approximate analytical and numerical techniques in solving nonlinear differential equations are :

1. asymptotic integration [50, 53, 69, 70]
2. perturbation techniques
3. Newton's method
4. method of power series expansion
5. hybrid analytical technique
6. direct numerical integration [28, 44]
7. finite difference method
8. finite element method
9. method of multisegment integration

In addition to the above mentioned methods, there are other methods existing in the literature, namely "Reversion Method" [21, 60], "Variation of Parameter" [21, 45, 53] "Averaging Methods Based on Residuals" - (a) Galerkin's Method [21] and (b) Ritz Method [21], and the principle of harmonic balance.

In the perturbation method, the fundamental unknowns are expanded in perturbation series in terms of unknown functions with preassigned coefficients. The unknown functions are obtained by solving a recursive set of differential equations which are generally simpler than the original governing equations of the problem [55, 99]. By contrast, in the Bubnov-Galerkin and Rayleigh-Ritz

techniques, the fundamental unknowns are sought in the form of series of a priori chosen coordinate functions (or modes) with known coefficients. Reviews of the many applications of these techniques are given in Ref. [85].

The perturbation method has two drawbacks. The first one stems from the fact that as the number of terms in the perturbation series increases, the mathematical complexity of the differential equations builds up rapidly. Therefore, for practical applications, the perturbation series has to be restricted to a few terms. The second drawback is the need to restrict the perturbation parameter to small values in order to obtain solutions of acceptable accuracy. The main difficulty of both the Bubnov-Galerkin and Rayleigh-Ritz techniques, from a practical view point, is the difficulty of selecting good coordinate functions (or modes) for structures with complicated geometry and/or complex response.

The hybrid analytical technique combines both the standard regular perturbation method and the classical Bubnov-Galerkin technique. The technique was shown to overcome the major drawbacks of the two parent techniques and to provide a more effective approximate analysis than either of the two techniques. Ref. 1 demonstrates the effectiveness of this technique by means of numerical examples.

The hybrid analytical technique is particularly useful for predicting nonlinear response of structures with simple geometry but complex construction. Examples of such structures are ring-and stringer-stiffened closed cylindrical shells and shell panels with discrete stiffener and rectangular or circular platform.

Asymptotic integration is not a general method and its scope of application is very limited as can be seen from Refs. [53, 69, 70]. Reissner discusses some of

the solutions and limitations of this method in Ref. [69]. In the application of this method, the solution is expressed in the form of a series where the terms of the series are the inverse powers of the largest parameter in the differential equations [69]. Determination of the terms of the series becomes extremely difficult and the solutions generally contain only the first term approximation.

Though the direct integration approach has certain advantages, it has also a serious disadvantage, that is, when the length of the shell is large, a loss of accuracy invariably occurs. This phenomenon is clearly pointed out in Ref. [80]. The loss of accuracy does not occur from accumulative errors in integration, but it is caused by the subtraction of almost equal numbers in the process of determining the unknown boundary values. It follows that for every set of geometric and material parameters of the shell there is a critical length beyond which the solution loses all accuracy.

Finite difference methods are the most widely used techniques for solving nonlinear differential equations. The advantage of the finite difference technique over direct integration is that it can avoid the above mentioned loss of accuracy. But it also has some drawbacks. Firstly, it ultimately leads to the solution of a large number of nonlinear algebraic equations which have to be solved by iterative techniques and often the solution fails due to nonconvergence. Secondly, bound by the requirement of using regular mesh spacings or the condition that the grid lines must be parallel to the coordinate axes, it was very much restricted to domains of regular geometry. However, curvilinear finite difference (CFD) technique, as proposed in Refs. [71-74], now relaxes these restrictions. Irregular meshes can now be employed in the analysis of shells with irregular boundary geometry.

In the literature, the structural analysis of general thin shells is one of the areas dominated by the finite element methods. One of the main advantages of using finite element methods is the flexibility in making discrete any unusual domain. However, in the course of extending the finite element methods to accommodate geometric nonlinearities, two different algorithms are generally adopted. They are namely: the linearized incremental approach and the Newton-Raphson iterative approach. The linearized incremental approach simplifies the programming works involved, but it has its own drawbacks. As linearized incremental equations are used, it is impossible to obtain the "exact" nonlinear solution for a particular load level. On the other hand, the Newton-Raphson method always converges to "true numerical solutions". However, it requires expensive numerical integration techniques [71], and the use of full Newton-Raphson procedures would be very costly. As a result, various modified versions of Newton-Raphson methods appeared in the literature [10, 84].

Newton's method for solving nonlinear differential equations is the extension of Newton's method for calculating roots of algebraic equations. The approach is to express the solution as the sum of two parts; the first part is a known function and the second one is a correction to the known function. A governing equation for the correction is obtained by substituting the assumed function into the governing equations and neglecting terms which are nonlinear [32]. This method does not require the perturbation parameter to be small as is necessary in the perturbation technique, but it involves the solution of a sequence of linear differential equations as in the latter. These linear equations have variable coefficients and generally cannot be solved in closed form. It is paradoxical that the greatest obstacle in solving nonlinear problems is the inability to solve linear differential equations in closed form.

The multisegment method of integration is a very powerful method developed and used by Kalnins and Lestingi [37] to solve nonlinear differential equations. This method involves:

- a. division of the total interval into a number of segments
- b. initial value integration of a system of first order differential equations over each segment
- c. solution of a system of matrix equations which ensures the continuity of the variables at the ends of the segments
- d. repetition of (b) and (c) until convergence is achieved
- e. integration of an initial value problem to obtain answers at any desired point within each segment

The main advantage of this method over the finite difference method is that the solution is obtained everywhere with uniform accuracy, and the iteration process with respect to mesh size, which is required with the finite difference approach, is eliminated. But the feature which makes this method most attractive is that any discontinuity, either in geometry or in loading, can be easily handled by requiring that the end point of a segment coincides with the location of the discontinuity. As the integration is restricted at the beginning of each segment, the precise effect of the discontinuity is obtained by this method. Moreover, this method is the most accurate of all the numerical methods because the problem is solved in the form of a system of first order differential equations in which no derivatives of geometrical or elastic properties appear and no further numerical derivatives are essential to obtain any desired results in the calculation.

CHAPTER 2

LITERATURE REVIEW

2.1 GENERAL

The theory of shell structures has existed as a well-defined branch of structural mechanics for about a hundred years, and the literature is not only extensive but also rapidly growing. This growth has two main aspects- the first one is the development of shell theories based on various assumptions and approximations, and on different geometrical configurations of the shell meridian, and the second is the development of various exact and approximate analytical and numerical methods for solving these equations.

Use of the nonlinear strain-displacement equations in the development of shell theories is motivated by the need for an accurate prediction of load-deflection curves, analysis of stability and post-buckling behavior, and natural vibration data for the design of shell structures.

Consideration of geometric nonlinearity in shells is originally due to Donnel [22], Von Karman [100, 101], Marguerre [47] and Mushtari [52], among others. Following these pioneering works several generalizations and modifications of the theories appeared in the literature. The geometric nonlinearity in shells is accounted for in three different levels:

- i. The Von Karman type nonlinearity that accounts only for the products and squares of the derivatives of the transverse deflection in the strain displacement equations;

- ii. The moderate rotation theories that account for moderate rotation terms;
- iii. The large rotation theories that account for large rotations.

Full nonlinear theories are those which do not neglect any nonlinear terms in the strain-displacement equations. However, full nonlinear theories are not only complex but not warranted in the analysis of most shell structures. As a result, several authors attempted to present nonlinear shell theories at different stages of approximations.

The earliest work of some generality is Marguerre's nonlinear theory of shallow shells [47]. Donnel [22] developed an approximate theory specially for cylinders and suggested its extension for a general middle surface. The result, a theory for what might be termed "quasi-shallow shells", has been worked out by a number of authors, notably Mushtari and Galimov [52].

The earliest work of a completely general nature appears to be the papers by Synge and Chien [86] followed by a series of paper by Chien [19, 20]. The theory of shells developed by Synge and Chien avoids the use of displacements as unknowns in the equations. The theory is deduced from the three-dimensional theory of elasticity and then, by means of series expansion in powers of small thickness parameter, approximate theories of thin shells are derived.

Another general formulation of the problem is worked out by Ericksen and Truesdell [25]. They developed it as a two dimensional theory instead of attempting to deduce it from three-dimensional theory of elasticity. They were able to account for transverse shear and normal strains and the rotations associated with couple stresses. The two-dimensional approach to shell theory

really evades the question of the approximations involved in the descent from three-dimensional, but this seems to be a virtue rather than a defect. Such questions are effectively isolated and shown to belong to the part of the theory in which constitutive relations are established.

Novozhilov [56] has presented an incomplete treatment of the general large deflection theory of thin shells based on the assumption of small middle surface strains.

F. Jordan Peter [59] presented a quasi-linear approach to the rotationally symmetric deformations of thin elastic shells of revolution. In this approach, the shell strains and rotations are assumed to be small, but, contrary to the approach of linear shell theory, the shell equilibrium conditions are fulfilled on the deformed shell.

Other developments which also employ linear constitutive relations are founded upon the Kirchhoff hypothesis and often contain other approximations. Among these are Reissner's [68, 69] formulation of axisymmetric deformation of shell of revolution and the more general works of Sanders [76] and Leonard [42]. Beginning with the three-dimensional field equations Naghdi and Nordgren deduced an exact, complete, and fully general nonlinear theory of elastic shells founded upon the Kirchhoff hypothesis.

Several nonlinear theories for thin shells have been derived in increasing stages of approximations. In most cases, theories are first approximative theories in the sense that transverse shears and normal strains are neglected. Such approximations and omissions are justified because the exact and general

equations characterizing the deformation of an elastic shell, even under the Kirchhoff hypothesis, are fairly complex and discouraging from the point of view of practical applications. However, as may be seen in the literature, with the advent of high speed computing machines and corresponding development and adaptation of efficient and versatile numerical techniques, some authors [11, 39, 64, 65, 77, 95, 103] are tempted towards the analysis of more comprehensive and general nonlinear shell theories and coming out with useful results.

2.2 SOME ANALYTICAL, NUMERICAL AND EXPERIMENTAL INVESTIGATIONS OF SHELL PROBLEMS

The majority of the large deflection and stability problems of practical structural components cannot be solved in closed form. Therefore, one has to resort to approximate and numerical discretization techniques for their solution, leaving analytical techniques limited to comparatively simpler structural elements.

Ahmed and Noor [1] presented a two-step hybrid analytical technique for predicting the nonlinear response of structural elements. They also discussed in length the potential of the proposed hybrid technique for nonlinear analysis of structures.

The effectiveness of this technique was demonstrated by means of three numerical examples :

- i. nonlinear axisymmetric response of clamped shallow spherical cap;
- ii. large deflection analysis of laminated anisotropic plate subjected to uniform transverse loading;

- iii. nonlinear axisymmetric response of an isotropic circular plate subjected to combined uniform and concentrated load.

Based on extended Sander's shell theory, that accounts for the shear deformation and the Von Karman strains, J. N. Reddy and K Chandrashekhra [65] presented numerical results for the laminated cylindrical and doubly curved shells. George J. Simitses, Dein Shaw and Izhak Sheinman [29] presented a comparison between analytical results (critical loads) and experimental results (buckling loads) for imperfect, laminated cylindrical thin shells. The loading consists of uniform axial compression and torsion, applied individually and in combination. The theoretical results are obtained from solution methodology based on nonlinear kinematic relations, linearly elastic material behavior, and the usual lamination theory.

In Ref. 88 an analytical formulation is made extending Reissner-Naghdi theory and numerical solutions are obtained for the elasto/visco-plastic deformation of multilayered cylindrical shells subjected to asymmetrical loading.

In Ref. 83 a modified mixed variational principle is established for a class of problems with one spatial as the independent variable. The specific applications are on three-dimensional deformations of elastic bodies and the nonsymmetric deformation of shells of revolution. The feature is the elimination in the variational formulation of the stress components which can not be prescribed on the boundaries.

Among the numerical techniques used in nonlinear shell analysis, the finite element method is used rather extensively due to the flexibility in making discrete any unusual irregular domain. J. G. Teng and J. M. Rotter [89] developed

a finite element formulation for elastic-plastic large deflection analysis of shells of revolution. Here, in place of widely used relations of Donnel, Novozhilov or Sanders, more comprehensive nonlinear thin shell strain-displacement relations are used, which account for the nonlinearity caused by in-plane displacements. Unlike most other nonlinear shell formulations, the in-plane shearing is included throughout this treatment. As asserted by the authors, this formulation contains most of the best features of nonlinear finite element analysis currently available in the literature, together with some new numerical schemes to improve the capability, accuracy and speed of the computation.

In Ref. 58 the occurrence of dynamic buckling of thick rings responding to an impulse load is investigated using both analytical and finite element method using the computer code ADINA. The results show that the nonlinear solutions by the finite element method predict a significant reduction in the amplitude of buckling response and an increase in the predominant wavelength response with time in comparison to the linear analytical solution.

S. K. Kwok [71-74] presented a curvilinear finite difference energy approach to the geometrically nonlinear analysis of general thin shells. This approach relaxes the requirement of usual finite difference method of using regular mesh spacings or the requirement that the grid lines must be parallel to the coordinate axes. Irregular meshes can now be employed in the analysis of shell with an irregular boundary geometry without any difficulty. The author developed a software named NAOSIS (Nonlinear Analysis of Shallow Shells) based on this method. As asserted by the author, the main aspects of this present finite difference formulation are firstly, its ability to implement the most general nonlinear strain-displacement relationship directly in a tensor code; secondly, its ability to model

any arbitrary shell geometry; and thirdly, its capability to use irregular computational meshes in a finite difference sense.

Recent efforts include the development of a number of general purpose computer programs [8, 12, 13, 51] for the linear and nonlinear analysis of general shells of revolution. These programs are based either on finite element or on finite difference method of analyses. An overview of the current capabilities of some computer programs that can be used for the solution of nonlinear structural and solid mechanics problems is available in Refs. [2, 10, 80]. A critical review of two such programs, namely, BOSOR4 [13] and BOSOR5 [12], is presented in Ref. [97, 98]. Here the author has discussed precisely the causes of their disagreements with experimental evidences.

Some experimental investigations on the shell analysis are reported in the ref. [14-18, 48].

A few of the latest investigations of the instability of structures are reported in ref [6, 58, 79, 81, 98].

Based on Reissner's [69] large deflection theory of shells of revolution, and using multisegment method of integration, Uddin [95] has developed a computer program for the analysis of composite shells of revolution. He has found extensive numerical results on spherical, ellipsoidal, conical and composite head pressure vessels based on both the linear and nonlinear theories and also obtained buckling pressure of general spherical shells and semi-ellipsoidal shells [93-98]. In all those investigations, he has exposed the conservativeness of linear theory and demonstrated the superiority of nonlinear analysis over linear analysis. Later

on, using the same program, Haque [31,98] has made buckling analysis of ellipsoidal shells of revolution under external pressure and Rahman [63] has extended it to the case of imperfection in geometry.

Later on, Ali [6] carried out the stability and stress analysis of general truncated conical shells to be used as pipe reducers modifying Uddin's original program.

In his research, Ali [6] pointed out that the critical load for a conical reducer decreases almost linearly as the apex angle of the conical frustums are gradually increased keeping all other parameters constant.

Stability analysis which inherently involves complex nonlinear mathematics has been mostly confined to shallow shells or circular plates. This is due to the fact that the nonlinear equations of shells could be solved only when the simplifications pertaining to the shallowness of the shell were made, as pointed out by Uddin [95]. The simplified equations are then solved by different methods mentioned in the introduction.

Also, some of the analyses have been made with the assumptions like the predetermined buckling modes of the structures [23, 24] which may or may not exist at all.

The present analysis, which deals with the stability and stresses of the general truncated parabolic shells to be used as pipe reducers, is however free from those sorts of weaknesses as it is based on large deflection analysis and the used computer program has established reliability.

The present investigation is in fact an extension of Ali's [6] research and to the author's knowledge the stability and stress analysis of general truncated parabolic shells has not been reported so far in an identical way.

CHAPTER 3

GOVERNING EQUATIONS

3.1 GENERAL

As mentioned earlier, the 'Classical' or 'Bifurcation' technique pertaining to a secondary mode of deformation has been used here to calculate the critical pressure. This is possible, because the equilibrium equations in the governing equations of parabolic reducers in the present analysis ensure stationary potential energy ($\delta E_t = 0$). In fact the governing equations consists of three sets of equations, namely the equilibrium equations, the Hook's law equations and the compatibility equations. The equilibrium equations relate the external load with the internally induced stress and bending moment resultants. The Hook's law equations are for linear stress-strain relations of the shell material. And the compatibility equations relate the internal strains with the physical deflections of the shell wall. These three sets of equations, together with the appropriate boundary conditions, constitute the mathematical embodiment of the problem.

3.2 THE SHELL THEORY

The external load applied to a shell is resisted by the membrane stress as well as the internal resisting couples, that is, the shell wall is subjected to the combined action of stretching and bending. In general, the shell wall is a three dimensional body. But, the use of Kirchoff's hypothesis reduces the shell analysis to a two dimensional problem. Further, in the case of axisymmetric deformations of shells of revolution, which comprise the majority of shells in practical use, the

analysis becomes a one dimensional problem. Again, the analysis of the problem of shell structures is dominated by the geometry of the shell surface through the compatibility relations and the equilibrium equations. Therefore, as can be seen from the literature, different authors have attempted to present different shell analyses including the purely stretching 'membrane' theory, linear membrane and bending theory and the finite deflection 'nonlinear' shell analyses for shells of varied configurations. For the present problem the large deflection theory of shells of revolution as presented by Reissner [69] will be used.

3.3 REISSNER'S THEORY OF AXISYMMETRIC DEFORMATIONS OF SHELLS OF REVOLUTION

The basic equations of Reissner's theory of finite axisymmetric deformations of shells of revolution which form the basis of this analysis are presented here for ready reference.

The equation of the meridian of the shell is written in the parametric form as (Fig. 1)

$$r = r(\xi), \quad z = z(\xi) \quad (3.1a)$$

The angle ϕ of the tangent to the meridian curve is given by

$$\cos\phi = r'/\alpha \quad \sin\phi = z'/\alpha \quad (3.1b)$$

where primes denote differentiation with respect to ξ and where α is given by

$$\alpha = [(r')^2 + (z')^2]^{1/2} \quad (3.1c)$$

The principal radii of curvature of the middle surface of the shell are given by

$$R_t = \alpha/\phi', \quad R_\theta = r/\sin\phi \quad (3.1d)$$

With reference to Fig. 2a, the equation of the deformed middle surface is written in the form

$$r = r_o + u, \quad z = z_o + w \quad (3.2a)$$

where the subscript "o" refers to undeformed middle surface and the quantities u and w are, respectively, the radial and axial components of displacements.

The angle enclosed by the tangents to the deformed and undeformed meridian, at the same material point, is given by

$$\beta = \phi_o - \phi \quad (3.2b)$$

With the above definition of displacements and rotation, the strain components and curvature changes of the deformed middle surface are given by the following equations

$$e_t = (\alpha - \alpha_o) / \alpha_o = (\cos\phi_o / \cos\phi) (1 + u'/r_o') - 1 \quad (3.2c)$$

$$e_\theta = \frac{u}{r_o} \quad (3.2d)$$

$$k_t = (\phi' - \phi'_o) / \alpha_o = \beta' / \alpha_o \quad (3.2e)$$

$$k_\theta = - (\sin\phi - \sin\phi_o) / r_o \quad (3.2f)$$

The equation containing the axial displacement component w is introduced as

$$w' = \alpha \sin\phi - z'_0 \quad (3.2g)$$

With the definition of stress resultants and stress couples as shown in Fig. 2a and Fig. 2b, the three equations of equilibrium are written as

$$(rV)' + r\alpha P_v = 0 \quad (3.3a)$$

$$(rH)' - \alpha N_\theta + r\alpha P_H = 0 \quad (3.3b)$$

$$(rM_\xi)' - \alpha \cos\phi M_\theta + r\alpha (H \sin\phi - V \cos\phi) = 0 \quad (3.3c)$$

Equation (3.3a) is the condition of force equilibrium in the axial direction, Eq. (3.3b) is the condition of force equilibrium in the radial direction, while Eq. (3.3c) is the condition of moment equilibrium about circumferential tangent.

With the assumption that the behaviour is elastic, the relations between strains and stress resultants are given by

$$C\epsilon_\xi = N_\xi - \nu N_\theta, \quad C\epsilon_\theta = N_\theta - \nu N_\xi \quad (3.4a)$$

$$M_\xi = D(k_\xi + \nu k_\theta), \quad M_\theta = D(k_\theta + \nu k_\xi) \quad (3.4b)$$

where $C = Eh$, $D = Eh^3/[12(1-\nu^2)]$, and h is the thickness of the shell. The radial stress resultant H and axial stress resultant V are related to N_ξ and transverse shear Q as follows:

$$N_\xi = H \cos\phi + V \sin\phi, \quad Q = -H \sin\phi + V \cos\phi \quad (3.4c)$$

3.4 DERIVATION OF THE FIELD EQUATIONS

The order of the system of equations (3.2-3.4) is six with respect to ξ , and consequently it is possible to reduce Eqs. (3.2-3.4) to six first-order differential equations which involve six unknowns. In the following derivation the six fundamental variables are taken as u , β , w , V , H , M_ξ and the differential equations are expressed in terms of these variables. The independent variable ξ is taken as the distance measured along the meridian of shell so that the differential equation can be used for all possible geometries of the meridian. With this definition of ξ , from equation (3.1c),

$$\alpha_o = [(\mathcal{I}'_o)^2 + (z'_o)^2]^{1/2} = 1$$

from the geometry of the meridian, which is not yet specified,

$$r_o = r_o(\xi) \tag{3.5a}$$

$$\phi_o = \phi_o(\xi) \tag{3.5b}$$

The following equations are written from the previous section in such an order that, when evaluated serially, they are in terms of the fundamental variables. This is done in order to keep the fundamental set of differential equations as simple as possible.

Rewriting Eqs. (3.2d), (3.2a), (3.2b), (3.2f), (3.4c), (3.4b) in that order,

$$\epsilon_\theta = u/r_o \tag{3.5c}$$

$$r = r_o + u \tag{3.5d}$$

$$\phi = \phi_o - \beta \tag{3.5e}$$

$$k_\theta = (\sin\phi_o - \sin\phi)/r_o \tag{3.5f}$$

$$N_{\xi} = H \cos\phi + V \sin\phi \quad (3.5g)$$

$$k_{\xi} = M_{\xi}/D - vk_{\theta} \quad (3.5h)$$

$$M_{\theta} = D(k_{\theta} + vk_{\xi}) \quad (3.5i)$$

Eliminating N_{θ} from Eqs. (3.4a) it follows that

$$\epsilon_{\xi} = (1-v^2)/C. N_{\xi} - v\epsilon_{\theta} \quad (3.5j)$$

Similarly, eliminating N_{ξ} from Eqs. (3.4a) and rearranging,

$$N_{\theta} = \left\{ \frac{C}{(1-v^2)} \right\} (\epsilon_{\theta} + v \epsilon_{\xi}) \quad (3.5k)$$

Rearrangement of Eq. (3.2c) and substitution of $\alpha_0 = 1$ leads to

$$\alpha = 1 + \epsilon_{\xi} \quad (3.5l)$$

Elimination of z_0' from Eq. (3.2g) by means of Eq. (3.1b) gives

$$\frac{dw}{d\xi} = \alpha \sin\phi - \sin\phi_0 \quad (3.5m)$$

Substituting the values of ϵ_{ξ} from Eq. (3.5l) and r_0' from Eq. (3.1b) in the Eq. (3.2c),

$$\frac{du}{d\xi} = \alpha \cos\phi - \sin\phi_0 \quad (3.5n)$$

From Eq. (3.2e) an expression for β' is obtained in the form

$$\frac{d\beta}{d\xi} = k_{\xi} \quad (3.5o)$$

Expansion of the three equations of equilibrium and elimination of P_v , P_H and r' from these equations result in the following expressions for V' , H' and M_{ξ}' .

$$\frac{dV}{d\xi} = -\alpha [(V \cos\phi)/r - P \cos\phi] \quad (3.5p)$$

$$\frac{dH}{d\xi} = -\alpha [(H \cos\phi - N_{\theta})/r + P \sin\phi] \quad (3.5q)$$

$$\frac{dM_{\xi}}{d\xi} = -\alpha \cos\phi (M_{\theta} - M_{\xi})/r - \alpha (H \sin\phi - V \cos\phi) \quad (3.5r)$$

where P is the outward normal pressure.

Eqs. (3.5) are the nonlinear governing equations of the axisymmetric deformations of shells of revolution expressed in terms of the fundamental variables. It should be noted that this fundamental set of differential and algebraic equations are expressed in such a manner that all the quantities of physical importance are evaluated during the process of solution of these equations.

3.5 LINEARIZED EQUATIONS OF AXISYMMETRIC SHELLS

The equations of small-deflection theory follow from the foregoing Eqs. (3.5) by referring the differential equations of equilibrium (3.5p) to (3.5r) together with (3.5g) to the undeformed shell and by omitting all nonlinear terms in the remaining equations of the fundamental set (3.5). The resulting equations are recorded below for ready reference.

$$e_{\theta} = u/r_o \quad (3.6a)$$

$$k_{\theta} = \beta \cos \phi_o / r_o \quad (3.6b)$$

$$N_{\xi} = H \cos \phi_o + V \sin \phi_o \quad (3.6c)$$

$$e_{\xi} = \frac{1-\nu^2}{C} N_{\xi} - \nu e_{\theta} \quad (3.6d)$$

$$k_{\xi} = \frac{M_{\xi}}{D} - \nu k_{\theta} \quad (3.6e)$$

$$N_{\theta} = \left(\frac{C}{1-\nu^2} \right) (e_{\theta} + \nu e_{\xi}) \quad (3.6f)$$

$$M_{\theta} = D(K_{\theta} + \nu K_{\xi}) \quad (3.6g)$$

$$w' = e_z \sin \phi_o - \beta \cos \phi_o \quad (3.6h)$$

$$u' = e_z \cos \phi_o - \beta \sin \phi_o \quad (3.6i)$$

$$\beta' = k_z \quad (3.6j)$$

$$v' = - \left(\frac{V \cos \phi_o}{I_o} - P \cos \phi_o \right) \quad (3.6k)$$

$$H' = - \left[\frac{H \cos \phi_o - N_\theta}{I_o} + P \sin \phi_o \right] \quad (3.6l)$$

$$M'_z = - \cos \phi_o \frac{(M_z - M_\theta)}{I_o} - (H \sin \phi_o - V \cos \phi_o) \quad (3.6m)$$

3.6 BOUNDARY CONDITIONS OF AXISYMMETRIC SHELLS

The general boundary conditions of a shell on an edge $\xi_1 = \text{constant}$ are to prescribe, in Sander's [76] notations,

N_{11} or U_1 ,

$$N_{12} + \frac{1}{2} (3R_2^{-1} - R_1^{-1}) M_{12} + \frac{1}{2} (M_{11} + N_{22}) \phi \text{ or } U_2 ,$$

$$Q_1 + \alpha_2^{-1} \frac{\partial M_{12}}{\partial \xi_2} - \phi_1 N_{11} - \phi_2 N_{12} \text{ or } w, \quad (3.7a)$$

and M_{11} or ϕ_1 ,

where ξ_1 and ξ_2 are the shell coordinates along the principal lines of curvature; N and M are the stress and couple resultants; ϕ 's are the rotations about respective axes; u and w are tangential and normal displacement components.

When the quantities in (3.7a) are specialized for axisymmetric deformations of shells of revolution they reduce to prescribing

$$N_{11} \text{ or } u_1,$$

$$Q_1 - \phi_1 N_{11} \text{ or } w, \quad (3.7b)$$

and M_{11} or ϕ_1 ,

on an edge $\xi_1 = \text{constant}$. From (3.7b) it is seen that the boundary conditions consists of the specification of rotational, tangential and normal restraints at the edge. But in most of the practical cases of shell problems the conditions of the horizontal and vertical restraints are known rather than those of the normal and tangential restraints. So it is concluded that it will be preferable to specify the boundary conditions in terms of the horizontal and vertical restraints from the

point of view of practical application. When this is done, the boundary conditions in terms of the notations used in the body of this thesis will be to prescribe

$$\begin{aligned} & H \quad \text{or} \quad u \quad , \\ & M_{\xi} \quad \text{or} \quad \beta \quad , \\ \text{and} \quad & V \quad \text{or} \quad w \quad . \end{aligned} \tag{3.7c}$$

on the edge $\xi = \text{constant}$.

3.7 EQUATIONS IN NON-DIMENSIONAL FORMS

It is always desirable to solve any engineering problem in terms of non-dimensional quantities in order to decrease the number of input physical parameters as well as to increase the applicability of the solution. With this in mind and also to make the variables more or less of the same order of magnitude the displacement components and stress resultants are expressed as ratios of their actual values to those of the circumferential displacement and stress resultant of an unrestrained thin cylindrical shell. The independent variable ξ is normalized in such a manner that ξ_e , the total length of the shell meridian corresponds to unity (Fig. 3b). The normalized quantities are defined mathematically by the following equations:

$$\bar{w} = \frac{wEh}{PR^2}, \quad \bar{u} = \frac{uEh}{PR^2}, \quad \bar{H} = \frac{H}{PR}, \quad \bar{V} = \frac{V}{PR}, \quad \bar{\beta} = \beta$$

$$\bar{M}_{\xi} = \frac{M_{\xi}}{PRh}, \quad \bar{M}_{\theta} = \frac{M_{\theta}}{PRh}, \quad \bar{N}_{\xi} = \frac{N_{\xi}}{PR}, \quad \bar{N}_{\theta} = \frac{N_{\theta}}{PR}$$

$$\bar{e}_\theta = e_\theta E h \xi_o / (PR^2), \bar{e}_\xi = e_\xi E h \xi_o / (PR^2), \bar{K}_\theta = k_\theta \cdot \xi_o \quad (3.8)$$

$$\bar{k}_\xi = k_\xi \cdot \xi_o, \bar{\xi} = \xi / \xi_o, \bar{C} = (1-v^2) \xi_o / R, \bar{P} = \frac{P}{E}, \bar{T} = \frac{R}{h}$$

$$\bar{R} = \xi_o / R, \bar{D} = 1 / [12 (1-v^2) \bar{P} \bar{T}^2 \bar{R}], \bar{L} = \bar{R} / (\bar{P} \cdot \bar{T}), \bar{I}_o = I_o / \xi_o$$

where R is the larger radius, or the base radius of the truncated parabolic shells. With the help of the normalized quantities defined in Eqs. (3.8) the fundamental set of differential Eqs. (3.6) (linear theory) becomes

$$\bar{e}_\theta = \bar{u} / \bar{r}_o \quad (3.9a)$$

$$\bar{k}_\theta = \bar{\beta} \cos \phi_o / \bar{r}_o \quad (3.9b)$$

$$\bar{N}_\xi = \bar{H} \cos \phi_o + \bar{V} \sin \phi_o \quad (3.9c)$$

$$\bar{e}_\xi = \bar{C} \bar{N}_\xi - v \bar{e}_\theta \quad (3.9d)$$

$$\bar{k}_\xi = \bar{M}_\xi / \bar{D} - v \bar{k}_\theta \quad (3.9e)$$

$$\bar{N}_\theta = (\bar{e}_\theta + v \bar{e}_\xi) / \bar{C} \quad (3.9f)$$

$$\bar{M}_\theta = \bar{D} (\bar{k}_\theta + v \bar{k}_\xi) \quad (3.9g)$$

$$\bar{w}' = \bar{e}_\xi \sin\phi_o - \bar{\beta} \cos\phi_o \cdot \bar{L} \quad (3.9h)$$

$$\bar{u}' = \bar{e}_\xi \cos\phi_o + \bar{\beta} \sin\phi_o \cdot \bar{L} \quad (3.9i)$$

$$\bar{\beta}' = \bar{k}_\xi \quad (3.9j)$$

$$\bar{v}' = - (\bar{V} \cos\phi_o / \bar{r}_o - \bar{R} \cos\phi_o) \quad (3.9k)$$

$$\bar{h}' = \{ (\bar{H} \cos\phi_o - \bar{N}_o) / \bar{r}_o + \bar{R} \sin\phi_o \} \quad (3.9l)$$

$$\bar{m}_\xi = - \cos\phi_o (\bar{M}_o - \bar{M}_\xi) / \bar{r}_o - \bar{R} \cdot \bar{T} (\bar{H} \sin\phi_o - \bar{V} \cos\phi_o) \quad (3.9m)$$

where $(\dots)' = \frac{d}{d\xi} (\dots)$

The corresponding nonlinear Equations of the fundamental set in non-dimensional form are as follows:

$$\bar{e}_o = \bar{u} / \bar{r}_o \quad (3.10a)$$

$$\phi = \phi_o - \bar{\beta} \quad (3.10b)$$

$$\bar{k}_o = (\sin\phi_o - \sin\phi) / \bar{r}_o \quad (3.10c)$$

$$\bar{N}_\xi = \bar{H}\cos\phi + \bar{V}\sin\phi \quad (3.10d)$$

$$\bar{e}_\xi = \bar{C} \bar{N}_\xi - v\bar{e}_0 \quad (3.10e)$$

$$\bar{k}_\xi = \bar{M}_\xi/\bar{D} - v\bar{k}_0 \quad (3.10f)$$

$$\bar{N}_0 = (\bar{e}_0 + v\bar{e}_\xi)/\bar{C} \quad (3.10g)$$

$$\bar{M}_0 = \bar{D}(\bar{k}_0 + v\bar{k}_\xi) \quad (3.10h)$$

$$\bar{\alpha} = \bar{L} + \bar{e}_\xi \quad (3.10i)$$

$$\bar{r} = \bar{L} \cdot \bar{r}_0 + \bar{u} \quad (3.10j)$$

$$\bar{w}' = \bar{\alpha}\sin\phi - \bar{L}\sin\phi_0 \quad (3.10k)$$

$$\bar{u}' = \bar{\alpha}\cos\phi - \bar{L}\cos\phi_0 \quad (3.10l)$$

$$\bar{\beta}' = \bar{k}_\xi \quad (3.10m)$$

$$\bar{v}' = -\bar{\alpha}\cos\phi(\bar{v}/\bar{r} - \bar{p} \bar{T}) \quad (3.10n)$$

$$\bar{H}' = - \bar{\alpha} (\bar{H} \cos \phi - \bar{N}_o) / \bar{r} + \bar{P} \bar{T} \sin \phi \quad (3.10o)$$

$$\begin{aligned} \bar{M}_\xi &= \bar{\alpha} \cos \phi (\bar{M}_o - \bar{M}_\xi) / \bar{r} \\ &- \bar{\alpha} \bar{P} \bar{T}^2 (\bar{H} \sin \phi - \bar{V} \cos \phi) \end{aligned} \quad (3.10p)$$

It should be noted that some of the nondimensional shell parameters in Eqs. (3.8) are defined in terms of ξ_e which will depend on the geometry of the meridian and thus should be derived for each individual case. In some cases there is no closed form expression for ξ_e and, therefore, ξ_e has to be evaluated either from a series expression or by numerical integration. The same is true for the expressions of \bar{r}_o and ϕ_o in terms of $\bar{\xi}$. There may not be any closed form expression for \bar{r}_o and ϕ_o and thus numerical integration has to be applied. For the case of a parabolic reducer, there is no closed form expressions for the parameters \bar{r}_o and ϕ_o . Thus numerical integration of the differential equation, given below is essential,

$$\frac{d\phi}{d\xi} = \frac{\bar{R}}{2F(1-xI)} \sin^3 \phi$$

Once ϕ is known, \bar{r}_o is given by

$$\bar{r}_o = \frac{1}{R} \{1 - F(1-xI) \cot^2 \phi\}$$

where

$$F = \frac{a}{R(1-x_1)}$$

a = distance between the vertex and the focus of the parabola,

R = larger radius of the reducer,

x₁ = diameter ratio, R₁/R.

CHAPTER 4

METHOD OF SOLUTION

4.1 INTRODUCTION TO MULTISEGMENT INTEGRATION

The fundamental set of linear Eqs. (3.9) and nonlinear Eqs. (3.10) together with the boundary conditions (3.7c) have to be integrated over a finite range of the independent variable $\bar{\xi}$. But numerical integration of these equations is not possible beyond a very limited range of $\bar{\xi}$ due to the loss of accuracy in solving for the unknown boundary values, as pointed out by Kalnins [36], and thus the multisegment method of integration developed by Kalnins and Lestingi [37] will be used for the present analysis.

The multisegment method of integration of a system of m first order ordinary differential equations

$$\frac{dy(x)}{dx} = F(x, y^1(x), y^2(x), \dots, y^m(x)) \quad (4.11a)$$

in the interval $(x_1 \leq x \leq x_{M+1})$ consists of (see Fig. 3d)

- a. the division of the given interval into M segments.
- b. $(m+1)$ initial-value integrations over each segment.
- c. solution of a system of matrix equations which ensures continuity of the dependent variables at the nodal points.
- d. repetition of (b) and (c) until continuity of the dependent variables at the nodal points is achieved.

In Eqs. (4.11a) the symbol $y(x)$ denotes a column matrix whose elements are m dependent variables, denoted by $y^j(x)$ ($j = 1, 2, \dots, m$); F represents m functions arranged in a column matrix form; and x is the independent variable. It is assumed here for convenience that the first $m/2$ elements of $y(x_1)$ and the last $m/2$ elements of $y(x_{m+1})$ are prescribed by the boundary conditions.

If at the initial point x_i of the segment S_i (see Fig. 3d) a set of values $y(x_i)$ is prescribed for the variables of Eqs. (4.11a) then the variables at any x within S_i can be expressed as

$$y(x) = f[y^1(x_i), y^2(x_i), \dots, y^m(x_i)] \quad (4.11b)$$

where the function f is uniquely dependent on x and the system of equations (4.11a). From Eqs. (4.11b) the expressions for the small changes $\delta y(x)$ can be expressed to a first approximation by the following linear equations:

$$\delta y(x) = Y_i(x) \delta y(x_i) \quad (4.11c)$$

where

$$Y_i(x) = \begin{bmatrix} \frac{\partial y^1(x)}{\partial y^1(x_i)} & \frac{\partial y^1(x)}{\partial y^2(x_i)} & \dots & \frac{\partial y^1(x)}{\partial y^m(x_i)} \\ \frac{\partial y^2(x)}{\partial y^1(x_i)} & \dots & \dots & \frac{\partial y^2(x)}{\partial y^m(x_i)} \\ \vdots & & & \\ \frac{\partial y^m(x)}{\partial y^1(x_i)} & \dots & \dots & \frac{\partial y^m(x)}{\partial y^m(x_i)} \end{bmatrix} \quad (4.11d)$$

Expressing Eqs. (4.11c) in finite difference form and evaluating them at

$$x = x_{i+1},$$

$$y^t(x_{i+1}) - y(x_{i+1}) = Y_i(x_{i+1}) [y^t(x_i) - y(x_i)] \quad (4.11e)$$

where y^t denotes a trial solution state and y denotes an iterated solution state based on the condition of continuity of the variables at the nodal points. Eqs. (4.11e) is rearranged as

$$Y_i(x_{i+1}) y(x_i) - y(x_{i+1}) = -Z_i(x_{i+1}) \quad (4.11f)$$

where $Z_i(x_{i+1}) = y^t(x_{i+1}) - Y_i(x_{i+1}) y^t(x_i)$

In order to determine the coefficients $Y_i(x)$ in Eqs. (4.11f) the j th column of $Y_i(x)$ can be regarded as a set of new variables, which is a solution of an initial value problem governed within each segment by a linear system of first order differential equations, which is obtained from Eqs. (4.11a) by differentiation with respect to $y^j(x_i)$ in the form

$$\frac{d}{dx} \left[\frac{\partial y(x)}{\partial y^j(x_i)} \right] = \frac{\partial}{\partial y^j(x_i)} \{F[x, y^1(x), y^2(x), \dots, y^m(x)]\} \quad (4.11g)$$

Thus the columns of the matrix $Y_i(x)$ are defined as the solutions of m initial value problems governed in S_i by (4.11g) (with $j = 1, 2, \dots, m$) with the initial values, in view of Eqs. (4.11c), specified by

$$Y_i(x_i) = I \quad (4.11h)$$

where I denotes the (m,m) unit matrix. To obtain the iterated solution $y(x_i)$ Eqs. (4.11f) are rewritten as a partitioned matrix product of the form

$$\begin{bmatrix} y_1(x_{i+1}) \\ y_2(x_{i+1}) \end{bmatrix} = \begin{bmatrix} Y_i^1(x_{i+1}) & \vdots & Y_i^2(x_{i+1}) \\ Y_i^3(x_{i+1}) & \vdots & Y_i^4(x_{i+1}) \end{bmatrix} \begin{bmatrix} y_1(x_i) \\ y_2(x_i) \end{bmatrix} + \begin{bmatrix} Z_i^1(x_{i+1}) \\ Z_i^2(x_{i+1}) \end{bmatrix}$$

so that the known boundary conditions are separated from the unknowns and, therefore, turns into a pair of equations given by

$$Y_i^1(x_{i+1})y_1(x_i) + Y_i^2(x_{i+1})y_2(x_i) - y_1(x_{i+1}) = -Z_i^1(x_{i+1})$$

$$Y_i^3(x_{i+1})y_1(x_i) + Y_i^4(x_{i+1})y_2(x_i) - y_1(x_{i+1}) = -Z_i^2(x_{i+1}) \quad (4.11i)$$

The result is a simultaneous system of 2M linear matrix equations, in which the known coefficients $Y_i^j(x_{i+1})$ and $Z_i^j(x_{i+1})$ are (m/2, m/2) and (m/2, 1) matrices, respectively, and the unknown, $y_j(x_i)$ are (m/2,1) matrices. Since $y_1(x_1)$ and $y_2(x_{M+1})$ are known, there are exactly 2M unknowns: $y_1(x_i)$, with $i = 2, 3, \dots, M + 1$, and $y_2(x_i)$, with $i = 1, 2, \dots, M$.

By means of Gaussian elimination, the system of equations (4.11i) is first brought to the form

$$E_i y_2(x_i) - y_1(x_{i+1}) = A_i$$

$$C_i y_1(x_{i+1}) - y_2(x_{i+1}) = B_i \quad (4.11j)$$

for $i = 1, 2, \dots, M$. Using the notations Z_i^j and Y_i^j in place of the symbols $Z_i^j(x_{i+1})$ and $Y_i^j(x_{i+1})$, the $m/2, m/2$ matrices E_i and C_i in the Eqs. (4.11j) are defined by

$$E_1 = Y_1^2, \quad C_1 = Y_1^4 (Y_1^2)^{-1}$$

and
$$E_i = Y_i^2 + Y_i^1 C_{i-1}^{-1}$$

$$C_i = (Y_i^4 + Y_i^3 C_{i-1}^{-1}) E_i^{-1}$$

for $i = 2, 3, \dots, M$.

The $(m/2, 1)$ matrices A_i and B_i are given by

$$A_1 = -Z_1^1 - Y_1^1 y_1(x_1)$$

$$B_1 = -Z_1^2 - Y_1^2 y_1(x_1) - Y_1^4 E_1^{-1} A_1$$

and
$$A_i = -Z_i^1 - Y_i^1 C_{i-1}^{-1} B_{i-1}$$

$$B_i = -Z_i^2 - Y_i^3 C_{i-1}^{-1} B_{i-1} - (Y_i^4 + Y_i^3 C_{i-1}^{-1}) E_i^{-1} A_i$$

for $i = 2, 3, \dots, M$.

Then the unknowns of (4.11i) are obtained by

$$y_1(x_{M+1}) = C_M^{-1} [B_M - y_2(x_{M+1})]$$

$$y_2(x_M) = E_M^{-1} [y_1(x_{M+1}) + A_M]$$

and $y_1(x_{M-i+1}) = C_{M-i}^{-1} [y_2(x_{M-i+1}) + B_{M-i}]$

$$y_2(x_{M-i}) = E_{M-i}^{-1} [y_1(x_{M-i+1}) + A_{M-i}]$$

for $i = 1, 2, \dots, M-1$.

Assuming $y(x_i)$ as the next trial solution $y^t(x_i)$ the process is repeated until the integration results of Eqs. (4.11a) at x_{i+1} , as obtained from the integrations in segment S_i with the initial values $y(x_i)$, match with the elements of $y(x_{i+1})$ as obtained from (4.11f) and also with the boundary conditions at x_{M+1} .

4.2 DERIVATION OF ADDITIONAL EQUATIONS

In the multisegment integration technique for a set of ordinary differential equations it has already been noted that in addition to the integration of the given set of equations another m sets of equations represented by (4.11g) has to be integrated. Thus, in order to apply the method of multisegment integration, differential equations corresponding to Eqs. (4.11g) for the m^2 additional variables as represented in Eqs. (4.11d) have to be derived. These differential equations are obtained by differentiating Eqs. (3.9) for the linear case and Eqs. (3.10) for the nonlinear case with respect to each of the fundamental variables. As the variables in any column of (4.11d) have the same form, the system of equations (4.11g) is derived here for the variables of any one column of (4.11d)

where the new variables are identified from the fundamental variables by the subscript a.

From the nonlinear equations (3.10), by differentiation in succession,

$$\bar{e}_{\theta a} = \bar{u}_a / \bar{r}_o \quad (4.12a)$$

$$\phi_a = -\bar{\beta}_a \quad (4.12b)$$

$$\bar{k}_{\theta a} = \beta_a \cos \phi / \bar{r}_o \quad (4.12c)$$

$$\bar{N}_{\xi a} = (\bar{H}_a - \bar{V} \bar{\beta}_a) \cos \phi + (\bar{H} \bar{\beta}_a + \bar{V}_a) \sin \phi \quad (4.12d)$$

$$\bar{e}_{\xi a} = \bar{C} \bar{N}_{\xi a} - v \bar{e}_{\theta a} \quad (4.12e)$$

$$\bar{k}_{\xi a} = \bar{M}_{\xi a} / \bar{D} - v \bar{k}_{\theta a} \quad (4.12f)$$

$$\bar{N}_{\theta a} = (\bar{e}_{\theta a} + v \bar{e}_{\xi a}) / \bar{C} \quad (4.12g)$$

$$\bar{M}_{\theta a} = \bar{D} (\bar{k}_{\theta a} + v \bar{k}_{\xi a}) \quad (4.12h)$$

$$\bar{\alpha}_a = \bar{e}_{\xi a} \quad (4.12i)$$

$$\bar{r}_a = \bar{u}_a \quad (4.12j)$$

$$\bar{u}'_a = \bar{\alpha}_a \cos \phi + \bar{\beta}_a \bar{\alpha}_a \sin \phi \quad (4.12k)$$

$$\bar{w}'_a = \bar{\alpha}_a \sin \phi - \bar{\alpha}_a \bar{\beta}_a \cos \phi \quad (4.12l)$$

$$\bar{\beta}'_a = \bar{k}_{\xi a} \quad (4.12m)$$

$$\begin{aligned} \bar{V}'_a = & - (\bar{\alpha}_a \cos \phi + \bar{\alpha}_a \bar{\beta}_a \sin \phi) (\bar{V} / \bar{r} - \bar{P} \bar{T}) \\ & - \bar{\alpha}_a \cos \phi (\bar{V}_a / \bar{r} - \bar{V} \bar{r}_a / \bar{r}^2) \end{aligned} \quad (4.12n)$$

$$\begin{aligned} \bar{H}'_a = & - \bar{\alpha}_a \{ (\bar{H} \cos \phi - \bar{N}_\theta) / \bar{r} + \bar{P} \bar{T} \sin \phi \} - \bar{\alpha}_a \{ [\bar{H}_a \cos \phi \\ & + \beta_a \bar{H} \sin \phi - \bar{N}_{\theta a} - \bar{u}_a (\bar{H} \cos \phi - \bar{N}_\theta) / \bar{r}] / \bar{r} - \bar{P} \bar{T} \bar{\beta}_a \cos \phi \} \end{aligned} \quad (4.12o)$$

$$\bar{M}'_{\xi a} = (\bar{\alpha}_a \cos \phi + \bar{\beta}_a \bar{\alpha}_a \sin \phi) \{ (\bar{M}_\theta - \bar{M}'_\xi) / \bar{r} + \bar{P} \bar{T}^2 \bar{V} \}$$

$$\begin{aligned}
& + \bar{\alpha} (\cos\phi [\bar{P} \bar{T}^2 \bar{V}_a + (\bar{M}_{\theta a} - \bar{M}_{\zeta a} - \bar{u}_a (\bar{M}_\theta - \bar{M}_\zeta) / \bar{r}] \\
& - \bar{P} \bar{T}^2 \bar{H}_a \sin\phi) - \bar{P} \bar{T}^2 \bar{H} (\bar{\alpha}_a \sin\phi - \bar{\alpha} \bar{\beta}_a \cos\phi)
\end{aligned} \tag{4.12p}$$

Equations (4.12a - 4.12p) have to be integrated as initial value problems m times in each segment with the initial values given by (4.11h). It should be noted that the equations (4.12) contain not only the variables (4.11d) but also the variables of the fundamental set. Thus, Eqs. (4.12) can not be integrated unless the fundamental set of equations is integrated first and the values of the fundamental variables are stored for use in Eqs. (4.12). It should be further pointed out that one point integration formula can not be used for the integration of Eqs. (4.12) since this formula needs evaluation of the derivatives at intermediate points where the variables are never evaluated.

The corresponding equations for the linear theory are given by the homogeneous form of Eqs. (3.9) and thus readily obtainable by dropping the load terms in Eqs. (3.9).

4.3 TREATMENT OF BOUNDARY CONDITIONS

In the introduction of the multisegment method of integration it was assumed that the first $m/2$ elements of $y(x)$ at x_1 and the last $m/2$ elements of $y(x)$ at x_{M+1} were prescribed as boundary conditions. But, in general, the boundary conditions are given as

$$T_1 y(x_1) = b_1 \quad \text{at } x_1$$

and
$$T_{M+1} y(x_{M+1}) = b_{M+1} \quad \text{at } x_{M+1} \tag{4.13a}$$

in which any $m/2$ elements of b_1 and any $m/2$ elements of b_{M+1} may be specified as boundary conditions. The symbols T_1 and T_{M+1} represent nonsingular (m,m) matrices which are known from the specification of the boundary conditions at the ends of the interval.

By rearranging the rows of T_1 and T_{M+1} in a special order, equations (4.13a) can always be stated in a manner such that the prescribed elements of b_1 and b_{M+1} become respectively the first and the last $m/2$ elements of b_1 and b_{M+1} . When this is achieved, evaluation of (4.11f) at $i = 1$ and $i = M$, and then elimination of $y(x_1)$ and $y(x_{M+1})$ by means of (4.13a) yield

$$Y_1(x_2) T_1^{-1} b_1 - y(x_2) = - Z_1(x_2) \quad (4.13b)$$

$$T_{M+1} Y_M(x_{M+1}) y(x_M) - b_{M+1} = - T_{M+1} Z_M(x_{M+1}) \quad (4.13c)$$

The form and notation of (4.11f) can now be retained if the coefficient matrices $Y_1(x_2)$, $Y_M(x_{M+1})$, $Z_M(x_{M+1})$, occurring in (4.11f), represent $Y_1(x_2) T_1^{-1}$, $T_{M+1} Y_M(x_{M+1})$, and $T_{M+1} Z_M(x_{M+1})$ respectively. In doing so, the solution of (4.11f) will not yield $y(x_1)$ and $y(x_{M+1})$ but rather the transformed variables b_1 and b_{M+1} . When $y(x_1)$ and $y(x_{M+1})$ are desired they can be obtained by the inversion of the matrix equations (4.13a).

It should be noted here that with reference to the boundary conditions (3.7c) stated in terms of the fundamental variables the matrices T_1 and T_{M+1} are both unit matrices of order 6. The construction of T_1 and T_{M+1} , in accordance with any possible statement of (3.7c) so that equations (4.13a) are in order, is treated in Appendix A.

4.4 DETERMINATION OF CRITICAL LOAD

It is obvious that a shell structure is at equilibrium condition when its total potential energy, at that level of loading, is stationary and that equilibrium condition is stable when this potential energy has got a relatively larger value in the neighboring disturbed conditions. The governing differential equations which are solved here always seek for the state of deformation of the shell at which, for given external pressure, the potential energy in the deformed shape of the shell is stationary. The critical pressure for a particular shell is interpreted from the fact that any further increase in pressure above its critical value, no matter how small, will cause the shell to undergo enormous deformation (linear and rotational) indicating that the state of deformation of the shell which corresponds to the lowest potential energy is far off from that at the critical pressure. Uddin [95] has also pointed out that the method of solution of the nonlinear governing equations for any value of loading parameter will fail when the load exceeds its critical value in the sense that the shell must deform enormously to assume the configuration which corresponds to this load or that the shell passes on to a secondary mode of deformation. In both these cases, the shell is in a state of instability which leads to its buckling.

The steps followed in finding the critical pressure are as follows:

- i. First the linear governing equations of the shell are solved by the multisegment method of integration as described earlier. With the linear solution providing initial values to the dependent variables, the nonlinear equations are solved by the process of iteration at the initially assigned load.

- ii. The nonlinear equations are then repeatedly solved for increasing values of the load parameter while the initial values for iteration process at any step of load parameter are provided by the solution for immediate previous step of loading.
- iii. If at any step of the scheme of increasing loading steps, the iteration process fails to converge, it first subtracts previous loading increment from the normalized loading, then halves the load increment and adds it to previous loading to arrive at the new normalized loading. In this way the equilibrium configuration path is traced against increased loading.
- iv. The critical pressure is anticipated from the load-displacement curves, where the equilibrium configuration path is traced against increasing loading and the appearance of a secondary mode of deformation is searched. This appearance of a second solution always corresponds to the bifurcation point as pointed out by Thompson [90] and consequently, it is always the bifurcation point where the numerical solutions fail to converge as the shell structures become unstable as pointed out by Uddin [95].

It should be mentioned here that the term 'Bifurcation point' is used here to refer to the point of initiation of a secondary mode of deformation, be a limit point or branching point.

CHAPTER 5

RESULTS AND DISCUSSIONS

5.1 ACCURACY AND RELIABILITY OF THE ANALYSIS

It is always desirable that the solutions obtained by a numerical technique be compared with the corresponding results in the literature, if available, in order to check the accuracy and reliability of the numerical method employed. It also helps to ascertain that no error in logic is committed in formulating the problem and no mistake has been made in the computer programming.

Actually the accuracy of the multisegment method of integration is self-ascertaining. Once the values of the fundamental variables at the nodal points are known from the multisegment method of integration, the fundamental set of differential equations is integrated over each segment of the meridian as initial-value integration of the fundamental set of different equations. If the values of the fundamental variables at the end of the segment S_i , as obtained from the initial-value integration, match up to a certain number of digits with their respective initial values for the segment S_{i+1} for $i = 1, 2, 3 \dots M$ and also with the given boundary conditions, only then the solution scheme accepts the results.

As regard to the reliability of the problem formulation and computer programming, Ref. 95 can be referred. In Ref. 95 solutions were found for uniformly loaded circular plate with clamped edge by the present methodology and it was found that the results are correct up to eight digits when compared with the results of the corresponding analytical solution. In Ref. 95, results were

also obtained on the variation of meridional stress and circumferential stress along the meridian of ellipsoidal head pressure vessel based on both linear and nonlinear theories by the present method of solution and were compared with previously established results. It was found that there was hardly any difference between these results. That the used computer program can accurately calculate the critical pressure for axisymmetric shells of revolution of any geometry have been demonstrated by Uddin [95, 97, 98], Haque [31,98], Rahman [63] and Ali [6].

5.2 GENERAL DISCUSSION ON RESULTS

The nonlinear differential equations of shells, which embody the principle of minimum potential energy, are solved for increasing values of load parameter till the first unstable state of equilibrium is reached. The onset of the first bifurcation point is hinted by a substantial increase in the displacements and stresses of the shell for very small increase in the load parameter. Right at the bifurcation point, in the case of limit-point buckling, any increase of load parameter, however small, produces enormous deformations and, thus, the numerical technique used here fails to converge to any solution.

That the present analysis based on axisymmetric deformations can predict the critical condition is justified by the following two theorems, delineated by Thompson [90].

Theorem 1: An initially-stable (Primary) equilibrium path rising monotonically with the loading parameter can not become unstable without intersecting a further distinct (secondary) equilibrium path [90].

Theorem 2: An initially-stable equilibrium path rising with the loading parameter cannot approach an unstable equilibrium state from which the system would exhibit a finite dynamic snap without the approach of an equilibrium path (which may or may not be an extension of the original path) at values of the loading parameter less than that of the unstable state [90].

Therefore, it is the initiation of the secondary path which the scheme of solution predicts, and up to this point, it is quite fair to assume that the deformations were axisymmetric. After the initiation of the secondary path the system assumes its buckled mode which can be non-axisymmetric.

The critical pressure for a parabolic reducer was calculated for different diameter ratios (R_1/R) and thickness ratios (R/h). It should be mentioned here, that stability analysis is justified for thin shells with large diameters. This is why the presented results are for thinner parabolic reducers with larger diameters only. The investigated values of R/h and R_1/R are: $R/h = 500, 750, 1000, 1250, 1500, 1750, 2000$ and $R_1/R = 0.5, 0.6, 0.7, 0.8, 0.9$. Results beyond this range of values of R_1/R and R/h can be readily obtained by using the computer program presented in Appendix B of this thesis, if they are of any importance to the practicing engineers.

The summary of the analysis is presented in Figs.4, 5, 6, 7 and 8 and in Table-1. Thompson's theorem [90] is used to find out the limit point or the branching point which corresponds to the critical load.

Table-1 gives a comparison of critical pressures between a parabolic and a conical reducer with identical parameters (that is, with the same diameter ratio

and thickness ratio). It should be mentioned here that same boundary conditions, that is, clamped edges are assumed for the comparison. It is seen that the critical load is always higher for a parabolic reducer. For a diameter ratio of 0.5 and thickness ratio of 500, the critical load for a parabolic reducer is 1.8 times greater than that of a conical reducer with an apex angle of 60° , 2 times for an apex angle of 90° and 3.5 times for an apex angle of 120° . This superiority of the parabolic reducer regarding stability becomes more prominent with increasing thinness and decreasing diameter ratio as can be seen from Table-1. For $R_1/R = 0.3$ and $R/h = 1500$, the critical load for a parabolic reducer is 2.2 times greater than that for an identical conical reducer of an apex angle of 60° , 3.3 times greater for an apex angle of 90° and 6 times greater for an apex angle of 120° . It was shown in ref. [6] that the critical pressure for a conical reducer decreases almost linearly if the apex angle is increased. The highest critical load is thus for the minimum apex angle which was 60° in ref. [6]. But it is seen in Table-1 that the critical pressure for a parabolic reducer is almost double of the critical pressure for the conical reducer with an apex angle of 60° for the same diameter ratio and thickness ratio.

The stresses developed under uniform external pressure for a parabolic reducer and an identical conical reducer (that is, with the same thickness ratio and diameter ratio) are presented in the figures 6, 7 and 8. It should be mentioned here that same boundary conditions, that is, clamped edges are considered for the comparison. From the above mentioned figures it is obvious that at the same level of external loading, parabolic reducers develop uniform stresses of much lower magnitude than compared to its counter parts. Fig. 6b, 7b and 8b show that for a parabolic reducer there is no perturbations in the membrane solutions except near the two ends. Whereas, at the same level of loadings, the conical

reducers show perturbations all along the shell meridian, the severe ones being near the larger end as depicted in the figures 6a, 7a and 8a. It is because of the fact that a parabolic reducer having sufficient membrane stiffness can sustain the external loading without the action of the bending moments except near the two ends at such a low level of loading. For the same reason, the solutions predicted by the linear and the nonlinear theories are identical for a parabolic reducer if the loading is very low (Figures 6b, 7b and 8b). It has been found that under external pressure the meridional stress at the inner fibre (σ_{ai}) is of the highest magnitude among the four components of stresses (σ_{ci} , σ_{co} , σ_{ai} , σ_{ao}) for both the reducers. It is seen from figure 6a that at a load of $(P/E) = 4.21 \times 10^{-7}$, which is the buckling load for that particular conical reducer the maximum meridional stress at the inner fibre (σ_{ai}/E) is - 0.0015 which occurs at the larger end. But for an identical parabolic reducer the same stress (σ_{ai}/E) at the same load is only - 0.000262 (almost six times lower than that developed in a conical reducer) at the smaller end. That parabolic reducers are far superior to conical ones in developing uniform stresses of much lower magnitude is also true for the case of circumferential stresses (σ_{ci} , σ_{co}) as seen from the Figures 6c and 6d. Figures 7a to 7d show the stresses developed in three times thinner reducers ($R/h = 1500$) than the previously discussed ones. Here also the parabolic reducers are found to develop much more uniform stresses of lower magnitude (almost six times lower) than by its counter parts.

Ali [6] showed that the load carrying capacity of a conical reducer decreases almost linearly with the increase of the apex angle keeping all other parameters constant. Thus the reducer with the least apex angle (which was 60° in Ali's research) has the highest load carrying capacity. But as depicted in the Figures 8a to 8d, the stresses developed in a conical reducer with an apex angle of 60°

is always higher than those developed in a parabolic reducer. The highest meridional stress (σ_{ai}/E) for a parabolic reducer is 1.5 times lower than that developed in an identical conical reducer with an apex angle of 60° .

Thus it is seen that under the same level of external loading, stresses are more uniform and of much lower magnitudes in a parabolic reducer than in an identical conical reducer in all the cases. Consequently, it is quite logical that the buckling loads will be always higher for a parabolic reducer, that is, a parabolic reducer will be much more stable than a conical reducer under uniform external pressure.

Figures 4 and 5 show the effect of thickness ratio (R/h) and diameter ratio (R_1/R) on the critical load, respectively. Figure 4 is the evidence of the common truth that, 'thinner the structure, lower the critical load', while figure 5 shows that, 'higher the diameter ratio, higher the critical load'. Figure 5 shows that the critical load increases slowly upto diameter ratio of 0.8 but increases at a faster rate if the diameter ratio is further increased. Of course, the effect of the diameter ratio on the critical load diminishes as the structures are made thinner.

5.3 DISCUSSIONS ON THE PATTERN OF STRESSES

The non-dimensional stresses, stress resultants and the bending moments for parabolic reducers with different diameter ratio and thickness ratio are presented in the Figures 9-12, 13d-13f, 14d-14f, 15d-15f, 16d-16f, 17d-17f and 18d-18f considering both the linear and the non-linear theories.

It should be mentioned here that the above mentioned parameters are normalized in terms of the loading parameter. As a result, there is no variation of the normalized parameters with the loading for linear theory. It should also be pointed out that because of normalizing, the actual signs (positive or negative) of the normalized parameter will be the opposite of those in the graphs.

Figures 9a-9f and 10a-10f show the variation of the bending moments along the shell meridian. The presence of bending moment in effect shows perturbations in the membrane solutions as seen in the Figures 13d, 14d, 15d, 16d, 17d and 18d. The presence of positive bending moments causes inward convex bending of the shell meridian and vice versa. This will be evident from the buckled configurations of the reducer, presented in the Figures 13c, 14c, 15c, 16c, 17c and 18c . The discrepancy between the linear and the nonlinear theories in predicting the solutions increases with increasing loading and decreasing thickness. At higher loading, the linear solutions fail to predict the perturbations in the bending moments. It is also seen in Figures 9e and 9f, 10e and 10f that for long reducers (lower diameter ratios) there is hardly any difference between the solutions predicted by the two theories except in a narrow zone near the larger end of the reducer, where the nonlinear solutions show sharp perturbations in the bending moments.

The meridional stress resultants are presented in the Figures 11a-11f. That linear theory fails to provide necessary information especially at higher loadings are evident from the above mentioned figures. The nonlinear theory on the other hand, can measure the profound change in curvature and predicts stress resultants with perturbations. It is also seen that the perturbations increases with increasing loading and decreasing thickness. It is also notable that

perturbations become sharper with decreasing diameter ratio and for very long reducer it is prominent only near the larger end of the reducers as seen in the Figures 11e and 11f.

The circumferential stress resultants are presented in the Figures 12a to 12f. Here, the effect of change in radii outweighs the effect of change in curvature. As a result the nonlinear theory predicts lower values of the stress resultants than that predicted by the linear theory. That long reducers fail due to meridional buckling without appreciable change in radii is evident from the Figures 12e and 12f. For these particular reducers the solutions predicted by the two theories merge together as there is no change in radii.

The membrane solutions are predominant in the long reducers as seen in the Figures 17d and 18d of meridional stresses at the inner and the outer fibres. Of course, the presence of bending moments at the two ends, specially near the larger end of the reducer causes sharp perturbations in the membrane solutions resulting in crooked deformation of the shell meridian near the larger end (Figures 17c and 18c).

An interesting observation from the Figures 17d-17f, 18d-18f is that long parabolic reducers are critically stressed near the larger end due to the combined action of meridional and circumferential stresses but for short reducers, this critical zone shifts towards the smaller end of the reducer (Figures 13d-13f, 14d-14f). This results in local instability near the larger end for long reducer and near the smaller end for a shorter one, as evident from the load-displacement curves and the buckled states of the reducers are discussed later.

5.4 DISCUSSIONS ON THE MODES OF BUCKLING

An interesting observation from the present investigation is that long parabolic reducers (lower diameter ratios) are prone to local instability at the larger end as shown in the buckled configurations of the reducers in the Figures 17c and 18c where the adjacent material points on the shell meridian are severely displaced in opposite directions resulting in crooked deformation of the reducers near the larger end. On the other hand, short parabolic reducers (higher diameter ratios) are most critically stressed near the smaller end and thus short reducers are prone to local instability away from the larger end. For ready reference Figures 13c, 14c are presented, where the waviness in the buckled shell meridian are seen near the smaller end. It should be mentioned here that waviness in the shell meridian, whether sharper (in long reducer near the larger end) or flatter (in short reducer near the smaller end), is produced by sinusoidal variation of bending moments which weaken the reducers.

The critical load which corresponds to the first bifurcation point is anticipated from the load-displacement curve (equilibrium path) by noting the initiation of a distinct secondary mode of deformation, whether the bifurcation point is a limit point or a branching point. The critical pressure of the shell is interpreted from the fact that the mode of primary deformation along the fundamental equilibrium path of a structure can not change without a change in its status of stability as pointed out by Thompson [90]. The load-displacement curves are presented in the Figures 13 to 18. The total meridional distance in between the two ends of the reducer is equally divided into four parts and the load-displacement curves are plotted for three equidistant material points along the shell meridian. Thus the points are at a distance of 25%, 50% and 75% of the

meridional length of the reducer from either of the two ends. This is done to anticipate which portion of the shell meridian is most severely displaced under loading. As for example, it has been observed that for long parabolic reducers (lower diameter ratios) the material points at a distance of 25% from the larger end ($\bar{\xi} = 0.83$) are most severely displaced both radially and axially, during buckling (Figures 17a, 17b, 18a, 18b), indicating local instability near the larger end. On the other hand, a short parabolic reducer (higher diameter ratios) is prone to local instability near the smaller end, as the material points at a distance of 25% from the smaller end ($\bar{\xi} = 0.85$) are most severely displaced during buckling (Figs. 13a, 13b, 14a, 14b).

The stress variations along the shell meridian (Figs. 13d-13f, 14d-14f, 15d-15f, 16d-16f, 17d-17f, 18d-18f) are in complete harmony with the failure pattern of the particular type of reducer as indicated by the load-displacement curves. It has been observed that for a long reducer, the material points along the shell meridian near the larger end are most critically stressed by the combined effect of the meridional and the circumferential stresses (Figs. 17d-17f, 18d-18f) which in turn causes the severe displacements of those points near the larger end. Conversely, for a short parabolic reducer the portion near the smaller end is most critically stressed (Figs. 13d-13f, 14d-14f) indicating that local instability is likely near the smaller end.

Thus from the above discussions it can be concluded that longer the reducer (that is lower the diameter ratio) higher is the buckling tendency near the larger end and vice versa. However, we have already seen that increasing the diameter ratio increases the buckling load (Figs. 4 and 5).

It should be mentioned here that the present analysis is based on the elastic deformations of the shell material. The following discussions, therefore, point out whether or not the maximum stress in the shell material remains within the elastic limit of the material at the critical load.

For ready identification, each parabolic reducer has been given a four digit number. The first two digits represent the radius thickness ratio (R/h) in hundreds and the last two digits represent diameter ratio (R_1/R) in hundredths.

To show the effect of diameter ratio and thickness ratio on the stress distributions and critical loads, two sets of representative shell elements are chosen. The chosen diameter ratios (R_1/R) are 0.5, 0.7 and 0.9 for each of the thickness ratios (R/h) 1000 and 1500.

SHELL-1090: Shell parameters are radius thickness ratio (R/h) = 1000, diameter ratio (R_1/R) = 0.90. The critical pressure (P_{cr}/E) for this shell element was found to be -1.93×10^{-6} .

From the detail output of the results, for this very short reducer, it is found that the maximum non-dimensional stress [$\sigma/(PR/h)$] is the meridional stress of the inner fibre at the smaller end ($\bar{\xi} = 0.796$) and its value is 1.43. Assuming the shell material to be steel, the actual value of this stress comes out to be -580 MPa. The yield strength of high quality steel is as high as 1800 MPa. Therefore, the induced maximum stress is well below the yield strength and it is concluded that the deformations are elastic. The bifurcation point (which may be a limit point or a branching point) is anticipated from the load-displacement curves by noting the initiation of a distinct secondary mode of deformation.

Figures 13a and 13b show the load-displacement curves for this short reducer. It is seen that the material points at a meridional distance of 25% ($\bar{\xi} = 0.85$) from the smaller end are most severely displaced during buckling as buckling initiates in that region. It is also seen from Figures 13d-13f that this particular region is most critically stressed prior to buckling. So we can conclude that this very short parabolic reducer ($R_1/R = 0.90$) is prone to local instability near the smaller end.

SHELL-1590: Shell parameters are radius thickness ratio (R/h) = 1500, diameter ratio (R_1/R) = 0.90. This shell element is 1.5 times thinner than the previously discussed shell element (SHELL-1090). The critical pressure (P_{cr}/E) for this shell element was found to be -9.6×10^{-7} .

From the detail output of the results, for this very short reducer, it is found that the maximum non-dimensional stress [$\sigma/(PR/h)$] is the meridional stress of the inner fibre at the smaller end ($\bar{\xi} = 0.796$) and its value is 1.56. Assuming the shell material to be steel, the actual value of this stress comes out to be -472 MPa. The yield strength of high quality steel is as high as 1800 MPa. Therefore, the induced maximum stress is well below the yield strength and it is concluded that the deformations are elastic. The bifurcation point (which may be a limit point or a branching point) is anticipated from the load-displacement curves, indicated by the initiation of a distinct secondary mode of deformation.

Figures 14a and 14b show the load-displacement curves for this short reducer. It is seen that the material points at a meridional distance of 25% ($\xi = 0.85$) from the smaller end are most severely displaced during buckling as buckling initiates in that region. It is also seen from Figures 14d-14f that this particular region is most critically stressed prior to buckling. So we can conclude that this short parabolic reducer ($R_1/R = 0.90$) like SHELL-1090 is prone to local instability near the smaller end.

SHELL-1070: Shell parameters are radius thickness ratio (R/h) = 1000, diameter ratio (R_1/R) = 0.70. The critical pressure (P_{cr}/E) for this shell element was found to be -1.23×10^{-6} .

From the detail output of the results, for this short reducer, it is found that the maximum non-dimensional stress [$\sigma/(PR/h)$] is the meridional stress of the inner fibre at the smaller end ($\bar{\xi} = 0.50$) and its value is 1.53. Assuming the shell material to be steel, the actual value of this stress comes out to be -395 MPa, well below the yield strength of good quality steel. So it is concluded that the deformations are elastic.

The load-displacement curves for this short reducer show that the material points from the smaller end up to half of the meridional distance are most severely displaced during buckling (Figures 15a and 15b). The stress curves (Figures 15d-15f) show that the above mentioned portion is critically stressed prior to buckling, indicating that buckling initiates in this region for this particular reducer.

SHELL-1570: Shell parameters are radius thickness ratio $(R/h) = 1500$, diameter ratio $(R_1/R) = 0.70$. The critical pressure (P_{cr}/E) for this shell element was found to be -5.63×10^{-7} .

This shell element is 1.5 times thinner than SHELL-1070. From the detail output of the results, for this short reducer, it is found that the maximum non-dimensional stress $[\sigma/(PR/h)]$ is the meridional stress of the inner fibre at the smaller end ($\bar{\xi} = 0.50$) and its value is 1.21. Assuming the shell material to be steel, the actual value of this stress comes out to be -218 MPa, well below the yield strength of steel. So it is concluded that the deformations are elastic.

875-38
The load-displacement curves for this short reducer show that the material points from the smaller end up to half of the meridional distance are most severely displaced during buckling (Figures 16a and 16b). The stress curves (Figures 16d-16f) show that the above mentioned portion is critically stressed prior to buckling, indicating that buckling initiates in this region for this particular reducer.

SHELL-1050: Shell parameters are radius thickness ratio $(R/h) = 1000$, diameter ratio $(R_1/R) = 0.50$. The critical pressure (P_{cr}/E) for this shell element was found to be -1.14×10^{-6} .

This shell element represents a long parabolic reducer. From the detail output of the results, for this long reducer, it is found that the maximum non-dimensional stress $[\sigma/(PR/h)]$ is the meridional stress of the inner fibre at the smaller end ($\bar{\xi} = 0.30$) and its value is 1.32. Assuming the shell material to be steel, the actual value of this stress comes out to be -316 MPa. Therefore, this

induced maximum stress is well below the yield strength and it is concluded that the deformations are elastic.

That long parabolic reducers are prone to local instability near the larger end (unlike the shorter reducers) are verified from the load-displacement curves (Figures 17a and 17b) and the stress distribution along the shell meridian (Figures 17d-17f). The load displacement curves show how sharply the rate of deformation of the material points at a distance of 25% of its length from the larger end ($\bar{\xi} = 0.83$) are changed just after the bifurcation point is exceeded. The stress curves (Figures 17d-17f) show that this particular portion of the shell meridian ($\bar{\xi} = 0.80 - 1$) is under high meridional and circumferential stresses. The buckled configuration of the reducer (Figure 17c) is also the evidence of the fact that longer the reducer (lower the diameter ratio) the higher is the buckling tendency near the larger end.

SHELL-1550: Shell parameters are radius thickness ratio (R/h) = 1500, diameter ratio (R_1/R) = 0.50. This shell element is 1.5 times thinner than the previously discussed shell element (SHELL-1050). The critical pressure (P_{cr}/E) for this shell element was found to be -5.30×10^{-7} .

This shell element show the same behavior as shown by shell element 1050 under load. But the perturbations in the stress curves are sharper resulting in much lower critical load, obviously because of the increasing thinness.

From the detail output of the results, for this long reducer, it is found that the maximum non-dimensional stress [$\sigma/(PR/h)$] is the meridional stress of the inner fibre at the smaller end ($\bar{\xi} = 0.30$) and its value is 1.3. Assuming the shell

material to be steel, the actual value of this stress comes out to be -217 MPa. Therefore this induced maximum stress is well below the yield strength and it is concluded that the deformations are elastic.

That long parabolic reducers are prone to local instability near the larger end (unlike the shorter reducers) are verified from the load-displacement curves (Figures 18a and 18b) and the stress distribution along the shell meridian (Figures 18d-18f). The load displacement curves show how sharply the rate of deformation of the material points at a distance of 25% of its length from the larger end ($\bar{\xi} = 0.83$) are changed just after the bifurcation point is exceeded. The stress curves (Figures 18d-18f) show that this particular portion of the shell meridian ($\bar{\xi} = 0.80 - 1$) is under high meridional and circumferential stresses. From the above discussions and observing the buckled configuration of the reducer (Figure 18c), we can conclude that unlike shorter parabolic reducers, the longer ones are prone to local instability near the larger end.

CHAPTER 6

CONCLUSIONS AND RECOMMENDATIONS

6.1 CONCLUSIONS

The following has been achieved from the present analysis:

1. Starting with the Reissner's equations for axisymmetric deformations of shells of revolution, critical pressures and stress distributions for parabolic reducers are obtained.
2. The parabolic pipe reducers are far superior to conical reducers in developing uniform stresses of lower magnitude under the same level of external loading. From the stress distribution along the meridional length, it has been found that the regions near the fixed edges are most critically stressed. It has also been observed that long parabolic reducers (lower diameter ratios) are critically stressed near the larger end of the reducer but this critical zone shifts away from the larger end as the diameter ratio is gradually increased.
3. It has been observed that parabolic reducers are much more stable than the conical reducers under uniform external pressure. The ratio of the critical pressure of a parabolic reducer to that of a conical reducer (with the same diameter ratio and thickness ratio) increases with increasing thickness ratio and decreasing diameter ratio.

4. For a parabolic reducer, the critical load increases with the increasing diameter ratio but the effect of the diameter ratio diminishes as the reducers are made thinner.
5. For practical uses, specific reducers can be designed using the presented results.

6.2 RECOMMENDATIONS FOR FUTURE WORK

In the light of the experience gained while achieving the set objectives of this thesis, the author feels that the following further investigations will enrich the field of the present work:

1. In the present analysis the edges of the parabolic reducer are taken to be completely restrained. But, in practice, even with thick-flanged-edges, there will always be some degree of axial and rotational flexibility. It is thus felt that the present investigation should be extended to include various degrees of edge-flexibility of this kind of reducers.
2. It is assumed in this analysis that the parabolic reducers are perfectly axisymmetric and the thickness of the reducer-wall does not vary either axially or circumferentially. This kind of idealization can hardly be attained, no matter how good is the fabrication process. It is thus felt that the present analysis should be extended to include the investigation of the effects of different degrees of deviations from axisymmetry and also the effects of variations in thickness, axially and circumferentially, separately as well as combinedly.

3. The present investigation has revealed the fact that the proposed parabolic reducers are far superior to the traditional conical reducers as far as uniform distribution of stresses and the buckling loads are concerned. The author feels that analysis with other geometrical shapes of the pipe reducers may yield better results. It is thus recommended that the present investigation can be extended to include reducers of other geometrical shapes.

REFERENCES

1. Ahmed, K. Noor, Hybrid Analytical Technique for Nonlinear Analysis of Structures. *AIAA Journal*, 23, (1985).
2. Ahmed K. Noor, Survey of Computer Programs for Solution of Nonlinear Structural and Solid Mechanics Problems. *Comp. & Struct.*, 13, 425-465, (1981).
3. Akkas, N. and Bauld, N. R. Jr., Axisymmetric Dynamic Buckling of Clamped Shallow Spherical and Conical Shells Under Step Load. *AIAA Journal*, 8, 2276-2277, (1970).
4. Akkas, N. and Bauld, N. R. Jr., Static and Dynamic Buckling Behavior of Clamped Shallow Conical Shells. *Int. J. Mech. Sc.*, 8, 689-706, (1971).
5. Alfutov, N. A., Stability of a Cylindrical Shell Reinforced with Transverse Stiffening Rings and Subject to Uniform External Pressure, *Inzb. Sbornik Akad. Nauk SSSR* 23, 36-46, 1956.
6. Ali, G. M. Zulfikar, Stability and Stress Analysis of Conical Reducers, M. Sc. Engineering Thesis, *Bangladesh University of Engineering and Technology*, 1991.
7. Archer, R. R., Stability Limits for a Clamped Spherical Shell Segment Under Uniform Pressure. *Quarterly of Applied Mathematics*, 15, (1958).
8. Almroth, B. O., Brogan, F. A. and Stanley, G. M., Structural Analysis of General Shells, Vol. 11: *User Instruction for STAGSC*. Lockheed Missiles & Space Co., Report LMSC-D633873 (1979).
9. Ball, R.E., A geometrically Nonlinear Analysis of Arbitrarily Loaded Shells of Revolution. *NASA CR-909*, January (1968).
10. Brebbia, C. and Connor, J.J., Geometrical Nonlinear Finite Element Analysis. *Proc. J. Eng. Mech. Div.*, ASCE 95 (EM2), 463-483, (1969).

11. Broadland, G.W. and Cohen, H., Large-Strain axisymmetric Deformation of Cylindrical Shells. *Journal of Applied Mechanics*, 54, 287-291, (1987).
12. Bushnell, D., BOSOR5, Program for Buckling of Elastic-Plastic Complex Shells of Revolution Including Large Deflection and Creep, *Comput. Struct.* 6 (1976) 221.
13. Bushnell, D., BOSOR4, Program for Stress, Buckling and Vibration of Complex Shells of Revolution, *Structural Mechanics Software Series (Edited by N. Perrone and W. Pilkey)*, pp. 11-143. University Press of Virginia (1977).
14. Bushnell, D., Nonsymmetric Buckling of Internally Pressurized Ellipsoidal and Torispherical Elastic-Plastic Pressure Vessel Heads, *J. Press. Vessel Technol.* 99 (1977) 54.
15. Bushnell, D., Elastic-Plastic Buckling of Internally Pressurized Torispherical Vessel Heads, *Nuclear Engg. Des.* 48 (1978) 405.
16. Bushnell, D. and Galletly, G. D., Stress and Buckling of Internally Pressurized Elastic-Plastic Torispherical Vessel Heads, *Comparison of Tests and Theory*, *J. Press. Vessel Technol.* 99 (1977) 39.
17. Bushnell, D., Elastic-Plastic Buckling of Internally Pressurized Ellipsoidal Pressure Vessel Heads, *Welding Research Council Bulletin 267*, United Engineering Centre, New York (1981).
18. Bushnell, D., Plastic Buckling of Various Shells, *J. Press. Vessel Technol.* 104 (1982) 51.
19. Chien, W.Z., The Intrinsic Theory of Thin Plate and Shells; Part-I General Theory. *Q. Appl. Math.*, 1, 297-327, (1944).
20. Chien, W.Z., The Intrinsic Theory of Thin Plate and Shells; Part-III Application to Thin Shells. *Q. Appl. Math.*, 2, 120-135, (1944).

21. Cunnigham, W.J., Introduction to Nonlinear Analysis. McGraw-Hill Book Company Inc., 1958.
22. Donnel, L. H., A New Theory for The Buckling of Thin cylinders Under Axial Compression and Bending. Trans. ASME 56, 795-806, (1934).
23. Dumir, P. C. and Khatri, K. N., Axisymmetric Static and Dynamic Buckling of Orthotropic Shallow Conical Caps, *AIAA Journal*, Vol. 23 (1985) pp. 1762-1767.
24. Dumir, P. C. and Khatri, K. N., Axisymmetric Static and Dynamic Buckling of Orthotropic Truncated Shallow Conical Caps, *Comp. & Struct.*, 22 (1986) pp. 335-342.
25. Ericksen, J. L., and Truesdell, C., Exact Theory of Stress and Strain in Rods and Shells. *Archive for Rational Mech. and Anal.*, 1, 295-323, (1959).
26. Euler, L., *Methods Inveniendi Lineas Curvas Maximi Minimive Proprietate Gaudents (Appendix, De Curvis Elasticis)*, Marcum Michaellem Bousquet, Lausane and geneva, (1744).
27. Famili, J., Archer, R.R., Finite Asymmetric Deformation of Shallow Spherical Shells. *AIAA Journal*, 3, 506-570, (1965).
28. Galletly, G.D., Kyner, W.T., Moller, C.E., Numerical Methods and Bending of Elliptical Shells. *Journal of the Society of Industrial and Applied Mathematics*, 9, 489-513, (1961).
29. George, J. Simitses, Dein Shaw and Izhak Shienman, Stability of Imperfect Laminated Cylinders: A Comparison Between Theory and Experiment. *AIAA Journal*, 23, (1985).
30. Grigoliuk, E.I., On the Instability with Large Deflections of a Closed Laminated Conical Shell Subject to Uniform Normal Surface Pressure. *Inzb, Sbornik, Akad. Nauk SSSR* 22, 111-119, (1955).

31. Haque, Md. Monzurul, Axisymmetric Buckling of Ellipsoidal Shells Under External Pressure. M.Sc. Engg. Thesis, Bangladesh University of Engineering and Technology, Dhaka, Bangladesh, (1984).
32. Holston, A., Jr., Approximate Analytical Solution of the Finite Difference Equations for a Shallow Spherical Shell. *Journal of Applied Mechanics*. 34, 65-72, (1967).
33. Huang, N.C., Unsymmetrical Buckling of Thin Shallow Spherical Shells, *J. Appl. Mech.*, Series E, No. 3, (1964).
34. Hubner, W., Deformation and Spunnungen bei Tellerfedern. *Konstruktion*, 34, 387-392, (1982).
35. Hubner, W. and Emerling, F.A., Axisymmetrische grobe Deformation einer Elastischen Kegelschale. *Zeitschrift Fuer Angewandte Mathematik und Mechanik*, 62, 408-411, (1982).
36. Kalnins, A., Analysis of Shells of Revolution Subject to Symmetrical and Nonsymmetrical Loads. *Journal of Applied Mechanics*, 31, 467-478, (1954).
37. Kalnins, A., and Lestingi, J.E., On Nonlinear Analysis of Elastic Shells of Revolution. *J. Appl. Mech.*, 34, 59-64,(1967).
38. Kaplan, A., Fung, Y.C., A Nonlinear Theory for Bending and Buckling of Thin Elastic Shallow Spherical Shells. NACA TN 3212, (1954).
39. Kempiski, M.H., Taber, L.A. and Wing-Chen Su, Large Elastic Deformation Results. *Journal of Applied Mechanics*, 55, 629-632, (1988).
40. Kendrick, S., The Buckling Under External Pressure of Circular Cylindrical Shells with Evenly Spaced, Equal Strength, Circular Ring Frames. Part III, Naval Construction Research Establishment, Great Britain, Rep. N. 244, (1953).
41. Langrange, J.L., *Mecanique Analytique*, Courcier, Paris, (1788).

42. Leonard, R.W., Nonlinear First Approximation Thin Shells and Membrane Theory. Thesis, Virginia Polytechnic Institute, June, (1961).
43. Liapunov, A., Probleme General de la Stabilite du Mouvement, Kharkov, 1982. French Translation in Ann. Fac. Sci. Univ. Toulouse, 9, 1907; Reproduced in Ann. Math. Studies, 17, Princeton Univ. Press, Princeton, N.J., (1949).
44. Lohmann, W., Beitrag Zur Integration der Reissner-Meissnerschen Schalengleichung fur Behalter unter Konstantem Innerdruck. Ingenieur Archiv, 6, 338-346, (1935).
45. Mansfield, E.H., The Bending and Stretching of Plates. The Macmilan Company, New York, 1964.
46. March, H.W. and Kuenzi, E.W., Buckling of Cylinders of Sandwich Construction in Axial Compression. For Prod. Lab., U.S. Dept. Agric., Bull. No. 1830, 1952, AMR 6, Rev. 811, (1953).
47. Marguerre, K., Zur Theorie der Gekrummten Platte Grosser Formanderung. Proc. of Fifth International Congress of Appl. Mech., wiley and Sons, 1938, pp. 93-101.
48. McCoy, J.C., An Experimental Investigation of the General Instability of Ring stiffened, Unpressurized, Thin Walled Cylinders under Axial compression. California Institute of Technology, Ph.D. Thesis., (1958).
49. Milne, W.E., Numerical Solutions of Differential Equations. Jhon Willey and Sons Inc., p. 49, (1962).
50. Mitrperskii, Yu.A., Problem of the Asymptotic Theory of Nonstationary Vibration. Israel Program for Scientific Translations, Jerusalem, (1965).
51. Mondkar, D. P. and Pawell, G. H., ANSR, A General Purpose Computer Program for Analysis of Nonlinear Structural Response, 4th SMiRT Conf., Paper M1/4, San Francisco (1977).

52. Mushtari, Kh.M., Some Generalization of the Theory of Thin Shells with Application to the Stability of Elastic Equilibrium (in Russian). *Izvestiia fiz.-mat ob-va pri kazaunte*, 11, p.71-150, (1938).
53. Mushtari, Kh.M. and Galimov, K.Z., *Nonlinear Theory of Thin Elastic Shells*. Israel Program for Scientific Translation, (1961).
54. Nash, W.A., Cooley, I.D., Large Deflection of a Clamped Elliptical Plate Subjected to Uniform Pressure. *Journal of Applied Mechanics*, vol. 26, Series E, No. 2, June, (1959).
55. Nayfeh, A.H., *Introduction to Perturbation Techniques*. John Willey and Sons, New York, 1981.
56. Novozhilov, V.V., *Theory of Thin Shells*. P. Noordhoff Ltd., 1959.
57. Pansford, H.T., The Effect of Stiffeners on the Buckling of Cylinders With Moderate Wall Thickness. California Institute of Technology, Ph.D. Thesis, (1953).
58. Pegg, N.G., An Investigation of Dynamic Pulse Buckling of Thick Rings, *Trans. ASME*, September, Vol.59/615 (1992)
59. Peter F. Jordan, Stiffness of Thin Pressurized Shells of Revolution. *AIAA Journal*, 3, (1965).
60. Pipes, L.A., Solution of Nonlinear Differential Equations by the Reversion Method. *J. Appl. Physic.*, 24, 180-186, (1953).
61. Poincare, H., Sur l'Equilibre d'Une Masse Fluide An'Imme d'Un Mouvement de Rotation, *Acta Math.*, 7, 259 (1885).
62. Radkowski, P.P., Buckling of Thin Single and Multi-layer Conical and Cylindrical Shells with Rotationally Symmetric Stresses. AVCO Report RAD-TR-2-57-32, (1957).

63. Rahman, N.M. Anisur, Axisymmetric Buckling of Imperfect Ellipsoidal Shells Under External Pressure. M.Sc. Engg. Thesis, Bangladesh University of Engineering and Technology, Dhaka, Bangladesh, (1986).
64. Raville, M.E., Buckling of Sandwich Cylinders of Finite Length Under Uniform External Lateral Pressure. For Prod. Lab., U.S. Dept. Agric., Bull. No. 1844-B 1955; AMR 9 (1956) Rev. 719.
65. Reddy, J.N. and K. Chandrashekhara, Nonlinear Analysis of Laminated Shells Including Transverse Shear. *AIAA Journal*, 23, (1985).
66. Reiss, Edward L., Axially Symmetric Buckling of Shallow Spherical Shells Under External Pressure. *Journal of Applied Mechanics*, 25, 556-560, (1958).
67. Reiss, E.L., Greenberg, H.J., Kelley, H.B., Nonlinear Deflections of Shallow Spherical Shells Under External Pressure. *J. Aero. Sci., Series 24*, 1951, pp. 533-543.
68. Reissner, E., On Axisymmetric Deformations of Thin Shells of Revolution. *Proc. Symposia Appl. Math.*, Vol. 3, McGraw-Hill, pp. 27-52, 1950.
69. Reissner, E., On the Theory of Thin Elastic Shells, H. Reissner Anniversary Volume, *J. W. Edwards, Ann Arbor, Michigan*. 231 (1949).
70. Rossettos, J.N., Sanders, J.L., Jr., Torodial Shells Under Internal Pressure in Transitive Range. *AIAA Journal*, 3, 1901-1909 (1965).
71. Kwok, S.K., Numerical Computations of Tensor Quantities on a Curved Surface by the CFD Method. *Comp. & Struct.*, 18, 1087-1097 (1984).
72. Kwok, S.K., Linear and Nonlinear Analysis of General Thin Shells Using a Curvilinear Finite Difference Energy Approach. Ph.D. Thesis, Univ. of Western Australia, Medlands, Australia (1984).
73. Kwok, S.K., An Improved CFD Method for Arbitrary Mesh Systems. *Comp. & Struct.*, 18, 719-731, (1984).

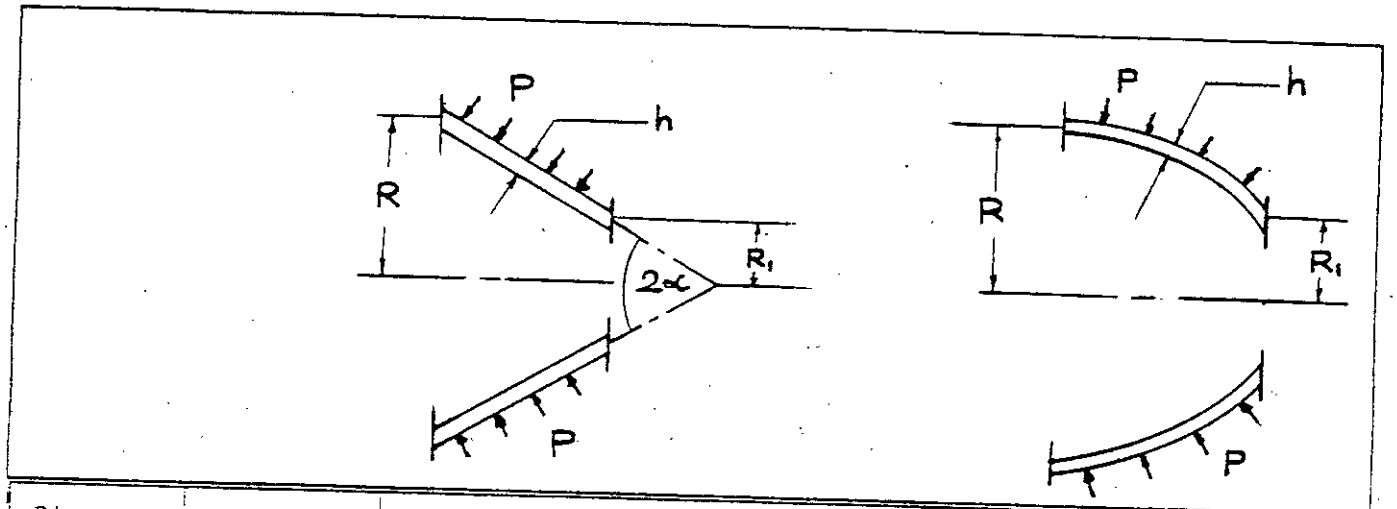
74. Kwok, S.K., Geometrically Nonlinear Analysis of General Thin Shells Using a Curvilinear Finite Difference Energy Approach. *Comp. & Struct.*, 20, 683-697, (1985).
75. Salerno, V.L., Levine, B., General Stability of Reinforced Shells Under Hydrostatic Pressure. Polytech. Inst. Brooklyn, PIBAL Rep. No. 189, 1951.
76. Sanders, J.L., Jr., Nonlinear Theories for Thin Shells. *Q. Appl. Math.*, 21, 21-36, (1963).
77. Schmidt, R. and Reddy, J.N., A Refined Small Strain and Moderate Rotation Theory of Elastic Anisotropic Shells. *Journal of Applied Mechanics*, 55, 611-617, (1988).
78. Schnel, Von W., Zur Stabilitat Dunnwandiger Langsgedruelter Kreiszyinderschalen bei Zusatzlichen Innerdruck. Symposium on the Theory of Thin Elastic Shells, I.U.T.A.M., Delft, 1959.
79. Seah, L. K. and Rhodes, J., Simplified Buckling Analysis of Plates with Compound Edge Stiffeners, *ASCE Journal of Engineering Mechanics*, Vol. 119 No. 1, p-19 (1993)
80. Sepetoski, W.K., Pearson, C.E., Dingwell, I.W., and Adkins, A.W., A Digital computer Program for the General Axially symmetric Thin Shell Problem. *Journal of Applied Mechanics*, 29, 655-661, (1962).
81. Shen-Hui and Williams, F.W., Postbuckling Analysis of Stiffened Laminated Box Columns., *ASCE Journal of Engineering Mechanics*, Vol 119 No. 1, p-39 (1993)
82. Soper, W.G., Large Deflection of Stiffened Plates. *Journal of Applied Mechanics*, 25, 444-448, (1958).
83. Steele, Charles R. and Kim, Yoon Young, Modified Mixed Variational Principle and The State-Vector Equation for Elastic Bodies and Shells of Revolution. *Trans. ASME*, Vol.59/587 (1992).

84. Stricklin, J.A., Haisler, W.E., and Von Reisseman, W.A., Geometrically Nonlinear Structural Analysis by Direct Stiffness Method. J. Structural Div., ASCE, 97, 2299-2314, (1971).
85. Svriski, I.V., Methods of the Type of Bubnov-Galerkin and Successive Approximations. Nauka, Moscow, 1968 (in Russian).
86. Synge, J.L., and Chien, W.Z., The Intrinsic Theory of Thin Shells and Plates. Th. Von Karman Anniverssry Volume, Cal. Inst. of Tech., 1941, p. 103.
87. Tabler, L.A., Large Elastic Deformation of Shear Deformable Shells of Revolution: Theory and Analysis. Trans. of ASME, 54, 578-584, (1987).
88. TAKEZONO, Shigeo, TAO, Katsumi and Tani, Kiyoyuki, Elasto/Visco Plastic Deformation of Multi Layered Moderately Thick Shells of Revolution, *JSME International Journal Series I*, Vol 34, 1 (1991).
89. Teng, J.G. and Rotter, J.M., Elastic-Plastic Large Deflection Analysis of Axisymmetric Shells. *Comp. & Struct.*, 31, 211-233, (1989).
90. Thompson, J. M. T. and Hunt, G. W., A General theory of Elastic Stability, *Jhon Wiley and Sons*, London, U.K. (1973).
91. Thurston, G. A., Newton's Method Applied to Problems in Nonlinear Mechanics. *Journal of Applied Mechanics*, June 1965, pp. 383-388.
92. Thurston, G. A., A Numerical Solution of the Non-linear Equations for Axisymmetric Bending of Shallow Spherical Shells, *Journal of Applied Mechanics*, *Trans. ASME* 28 (1965) pp. 557-562.
93. Uddin, Md. W., A Computer Program for Nonlinear Analysis of Pressure Vessels, *Int. J. Press. Ves. & Piping* 22 (1986) 271-309.

94. Uddin, Md. W., Large Deformation Analysis of Ellipsoidal Head Pressure Vessels. *Comp. & Struct.*, 23, 487-495, (1986).
95. Uddin, Md. W., Large Deflection Analysis of Composite Shells of Revolution, Ph. D. Thesis, *Carleton University, Canada* (1969).
96. Uddin, Md. W., Large Deformation Analysis of Plate-end Pressure Vessels., *Int. J. Pres. Ves. & Piping*, 29, 47-65, (1987).
97. Uddin, Md. W., Buckling of General Spherical Shells Under External Pressure. *Int. J. Mech. Sci.*, 29, 469-481, (1987).
98. Uddin, Md. W. and Haque, Md. M., Instability of Semi-ellipsoidal Shells, *Int. J. Pres. Ves. & Piping*, 58, p 47-65, (1994).
99. Van Dyke, M., *Perturbation Methods in Fluid Mechanics*. Parabolic Press, Stanford, Calif, 1975.
100. Von Karman, T., *Festigkeit Lehre in Maschinenbau*. Math. Niss., Vol. IV/4, Teubner, Leipzig, pp. 311-385, (1910).
101. Von Karman, T. and Kerr, A.D., Instability of Spherical Shells Subjected to External Pressure. *topics in Applied Mechanics, Memorial Volume to the Late Professor E. Schwerin*, pp. 1-22, (1965).
102. Wang, G.T. and De Sant, D.F., Bucking of Sandwich Cylinders Under Axial Compression, Bending and Combined Loads. NYU Report to Office of Naval Research, Contr. No. N6-onr-279, 1953.
103. Wempner, G., A General Theory of Shells and the Complementary Potentials. *Journal of Applied Mechanics*, 53, 881-885, (1986).

104. Wilson, P.E., Boresi, A.P., Large Deflection of a Clamped Circular Plate Including Effects of Transverse Shear. *Journal of Applied Mechanics*, 31, 540-541, (1964).
105. Wilson, P.E., Spier, E.E., Numerical Analysis of Large Axisymmetric Deformations of Thin Spherical Shells. *AIAA Journal*, 3, 1716-1725 (1965).
106. Wood, J.D., The Flexure of a Uniformly Pressurized Circular Cylindrical Shell. *Journal of Applied Mechanics*, 25, 453-458 (1958).

Table-1: Comparison of Critical Pressure Between a Parabolic Reducer and a Conical Reducer with Clamped Ends.



Diameter Ratio (R_1/R)	Thickness Ratio (R/h)	Critical Pressure (P_{cr}/E) for Conical Reducer [Ref. 6.]			Critical Pressure (P_{cr}/E) for Parabolic reducer [Present Analysis]
		Apex Angle (2α)			
		60°	90°	120°	
0.5	500	30×10^{-7}	24×10^{-7}	13×10^{-7}	51×10^{-7}
	1000	7×10^{-7}	5×10^{-7}	2.8×10^{-7}	11.4×10^{-7}
	1500	3×10^{-7}	2.1×10^{-7}	1×10^{-7}	5.3×10^{-7}
0.3	500	25×10^{-7}	17×10^{-7}	9×10^{-7}	50×10^{-7}
	1000	6×10^{-7}	3.9×10^{-7}	2×10^{-7}	11.3×10^{-7}
	1500	2.65×10^{-7}	1.60×10^{-7}	0.85×10^{-7}	5.02×10^{-7}

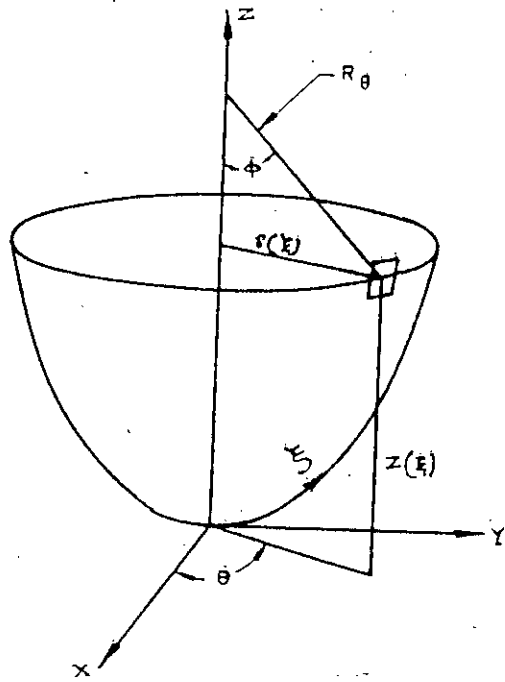


Fig. 1 Middle surface of shell

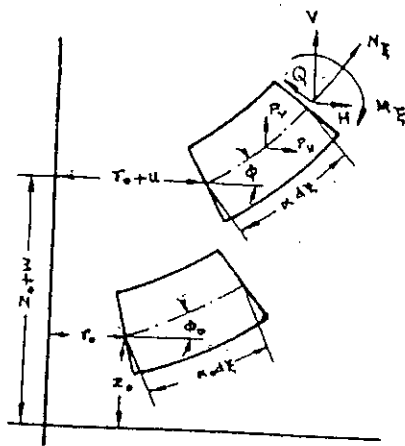


Fig. 2a Side view of element of shell in deformed and undeformed states

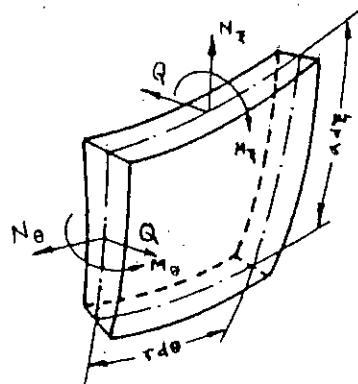


Fig. 2b Element of shell showing stress resultants and couples

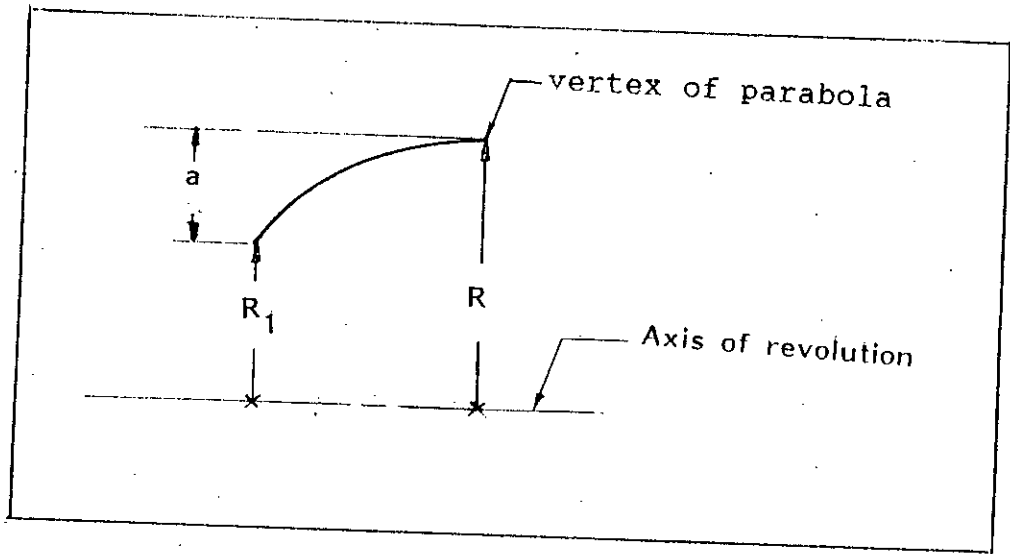


Fig.3a Geometry of the parabolic reducer

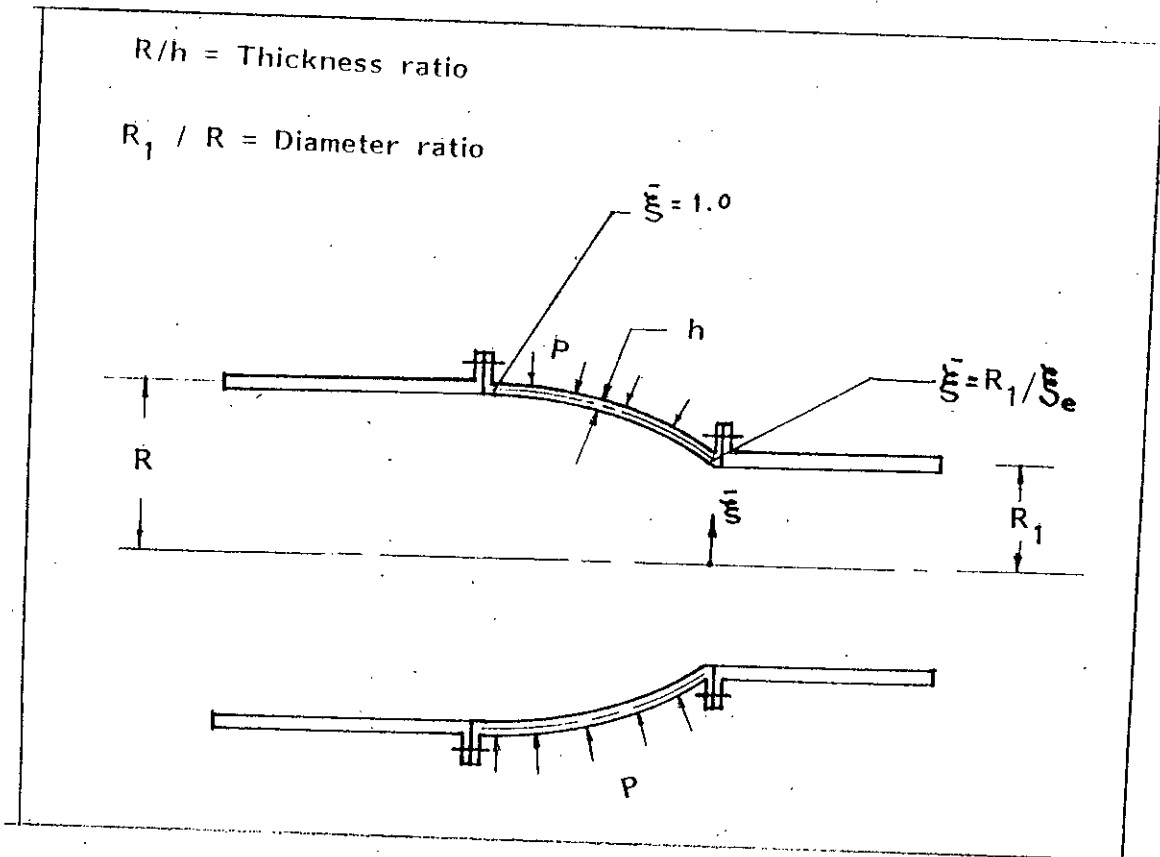


Fig. 3b Parabolic reducer

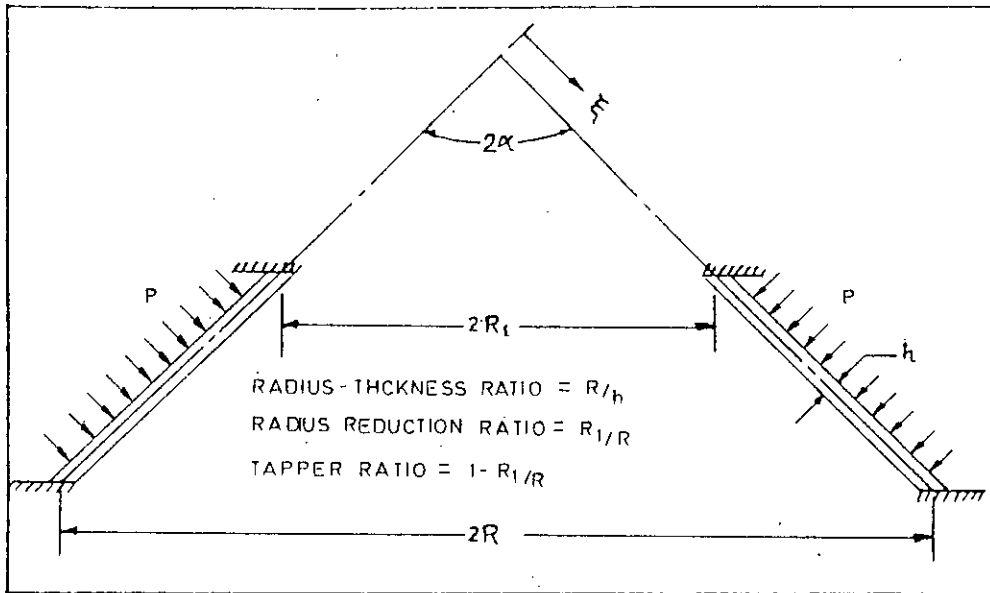


Fig. 3c Parameters of truncated conical shell element [Ref.6]

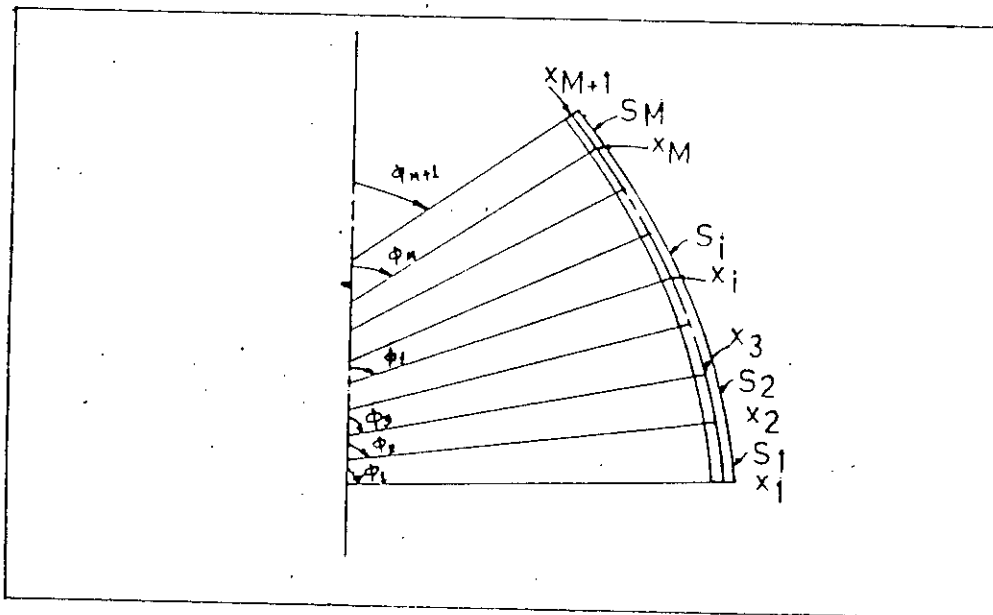


Fig. 3d Division for multisegment integration

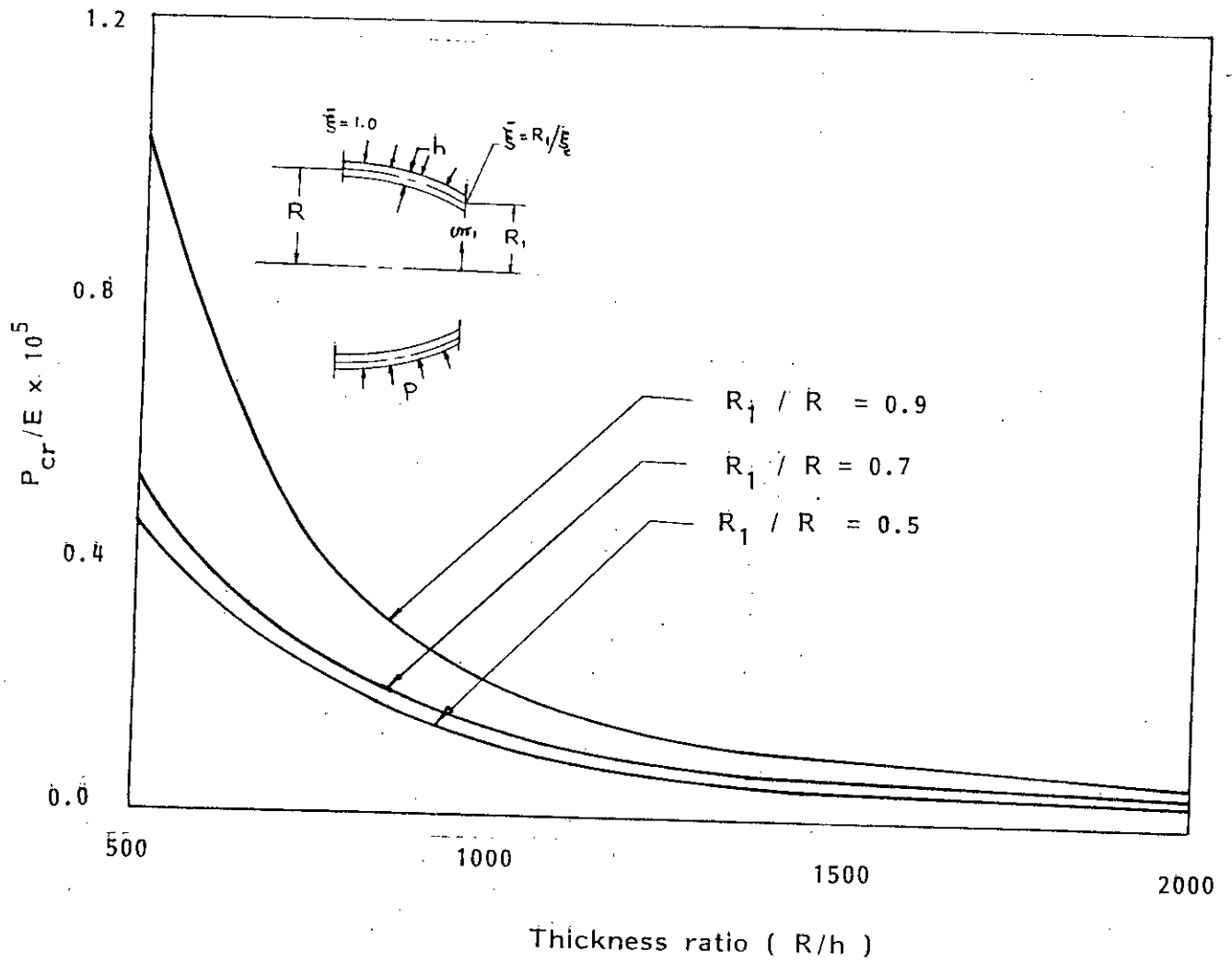


Fig. 4 Critical load versus thickness ratio
for a parabolic reducer

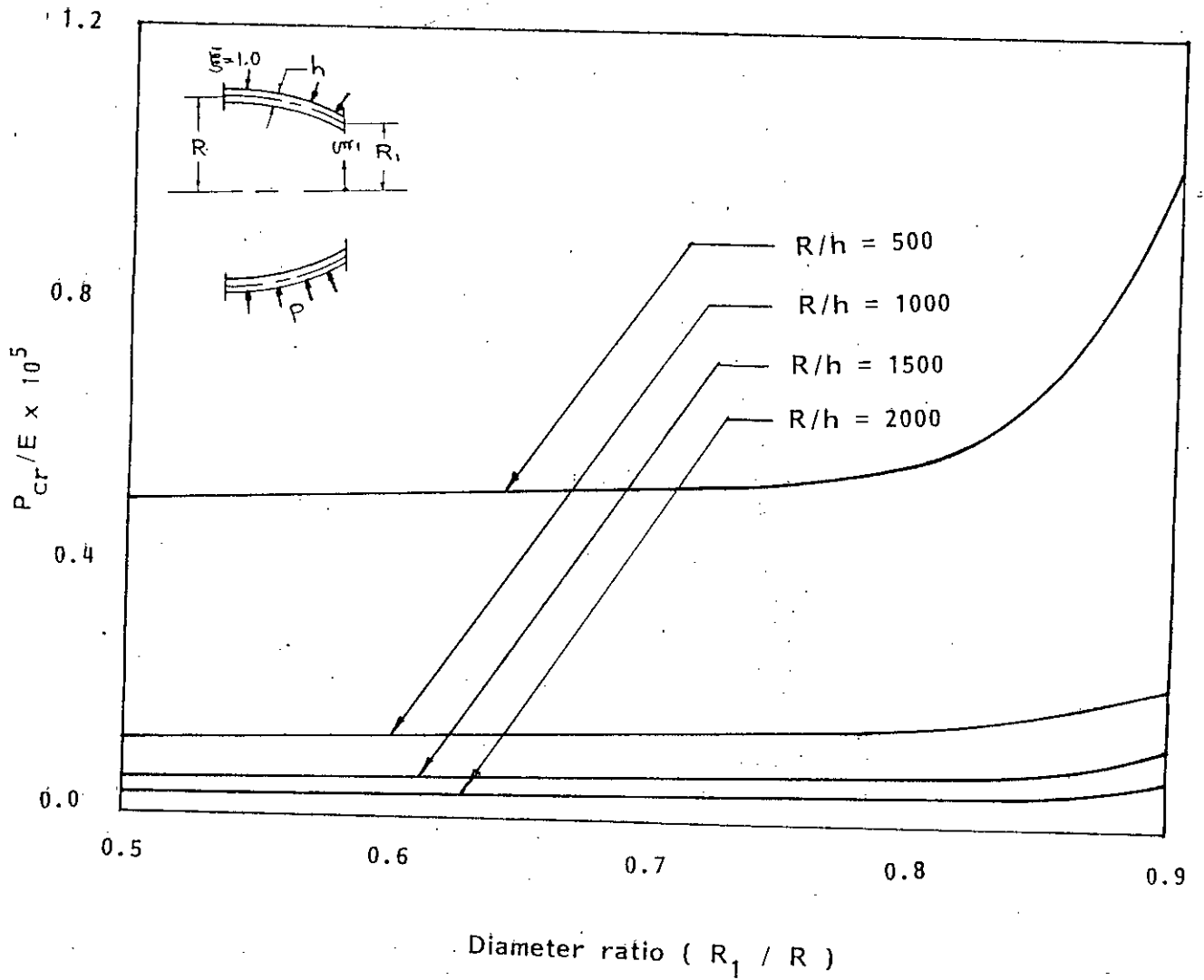


Fig. 5 Critical load versus diameter ratio
for a parabolic reducer

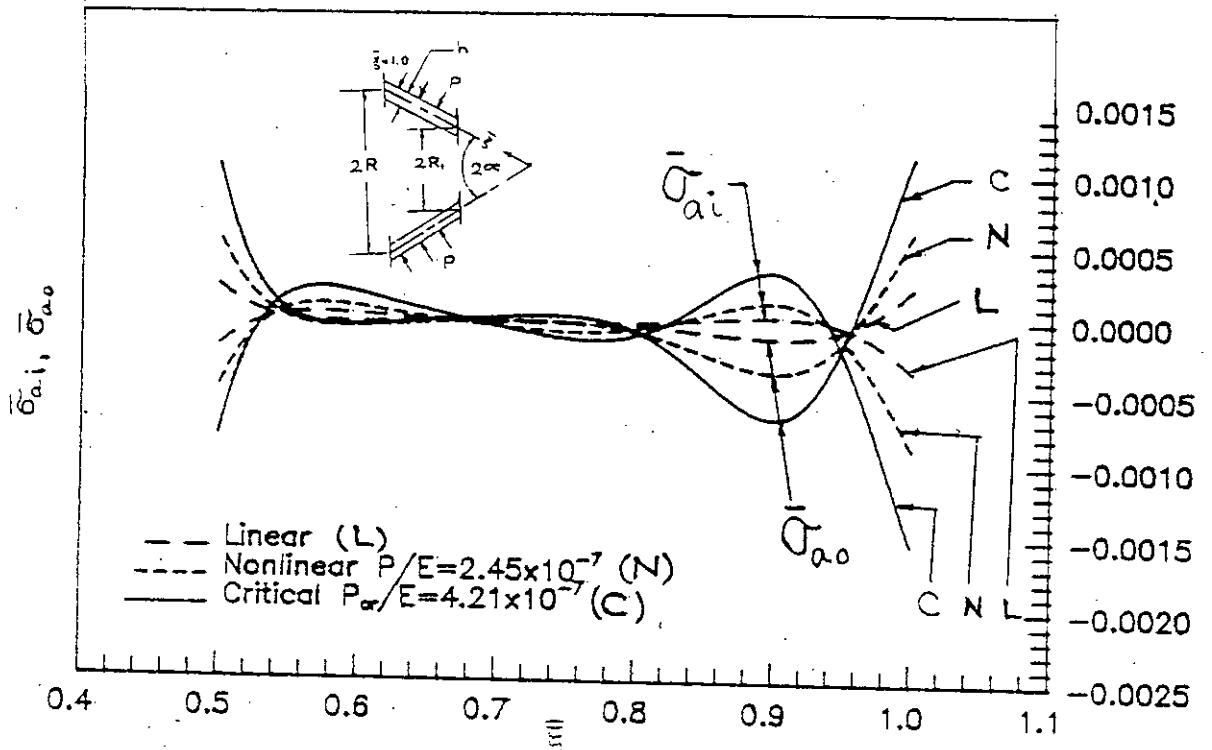


Fig.6a Meridional stresses for a 150° apex-angle frustum with thickness ratio $(R/h) = 500$ and Diameter ratio $(R_1/R) = 0.5$ [Ref.6]

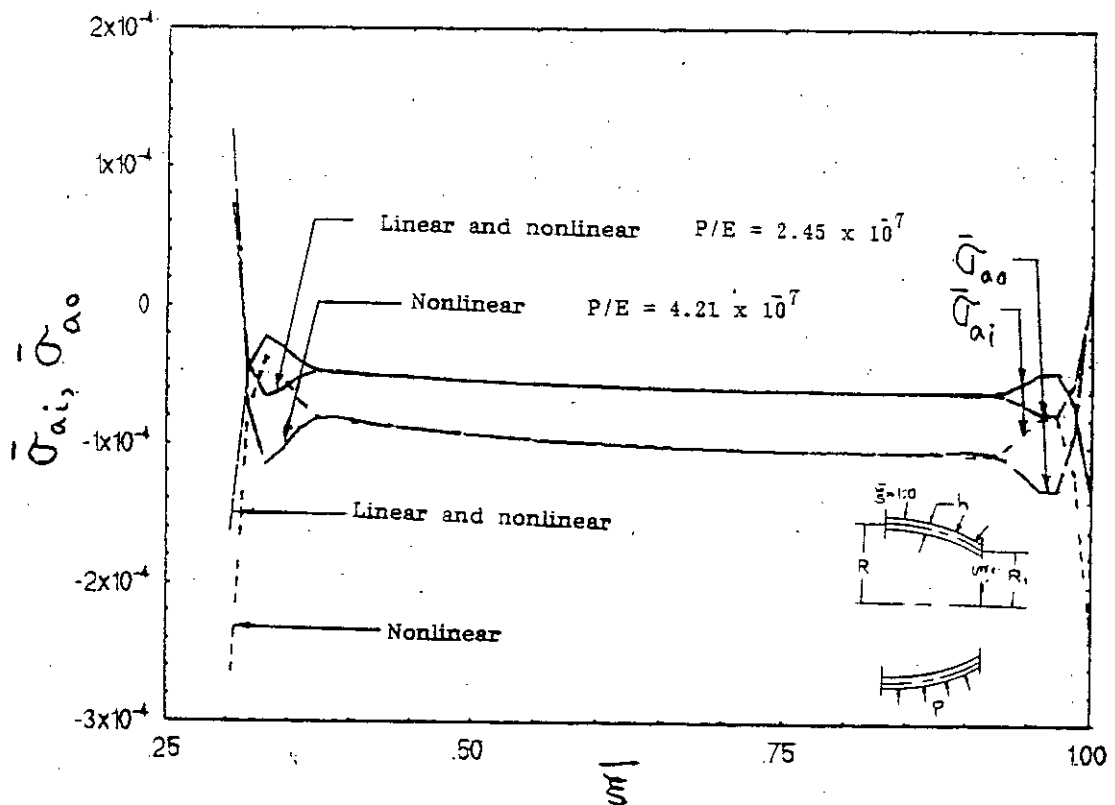


Fig.6b Meridional stresses for a Parabolic reducer with thickness ratio $(R/h) = 500$ and diameter ratio $(R_1/R) = 0.5$ [Present Analysis]

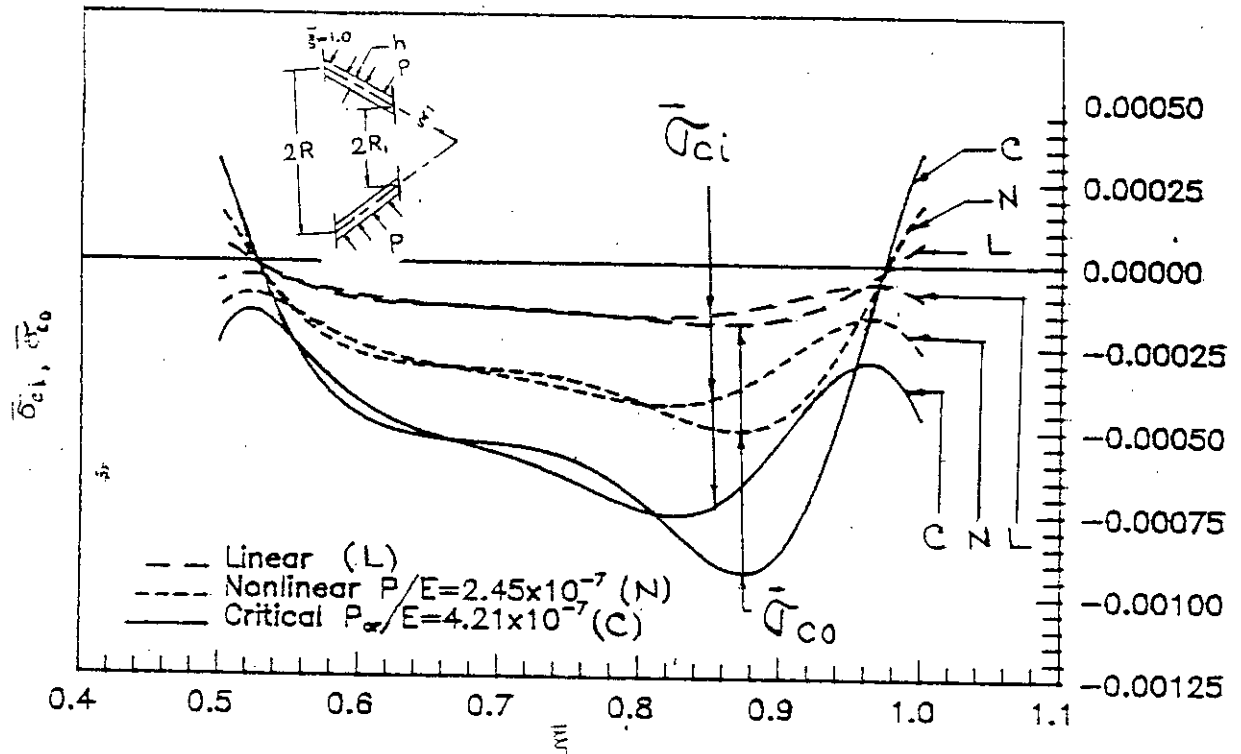


Fig.6c Circumferential stresses for a 150° apex-angle frustum with thickness ratio $(R/h)=500$ and diameter ratio $(R_1/R)=0.5$ [Ref.6]

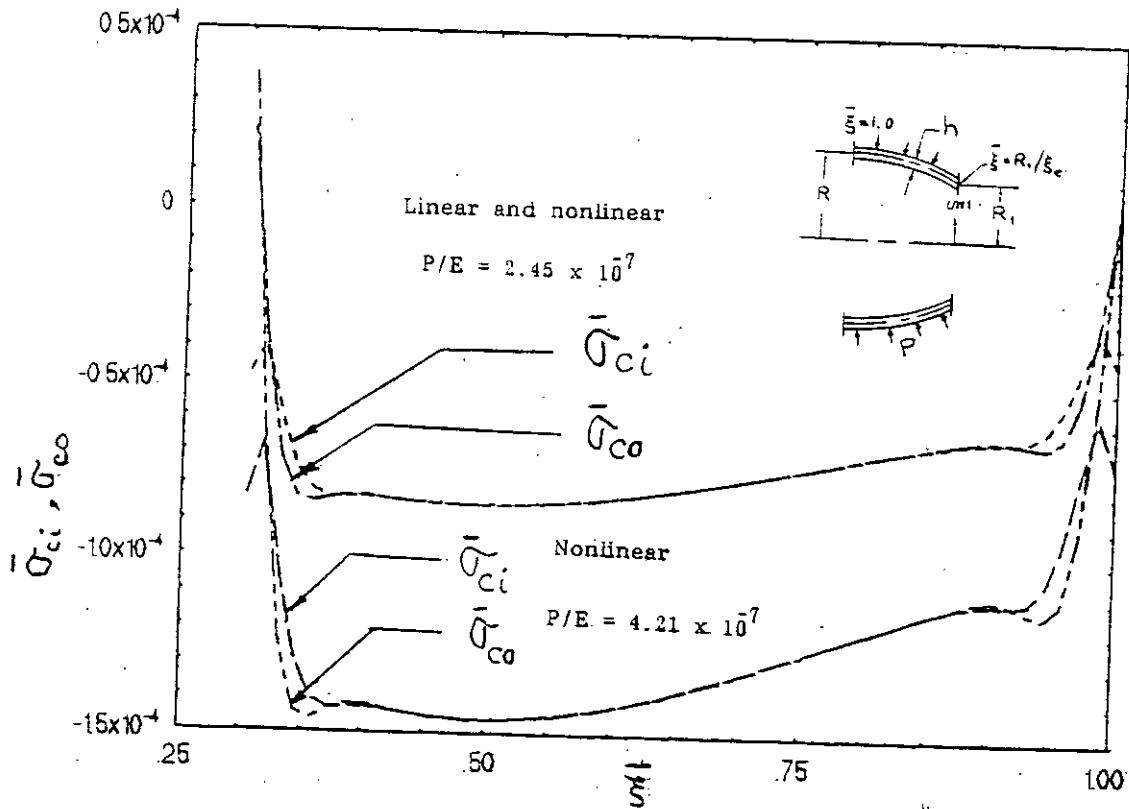


Fig. 6d Circumferential stresses for a Parabolic reducer with thickness ratio $(R/h)=500$ and diameter ratio $(R_1/R)=0.5$ [Present Analysis]

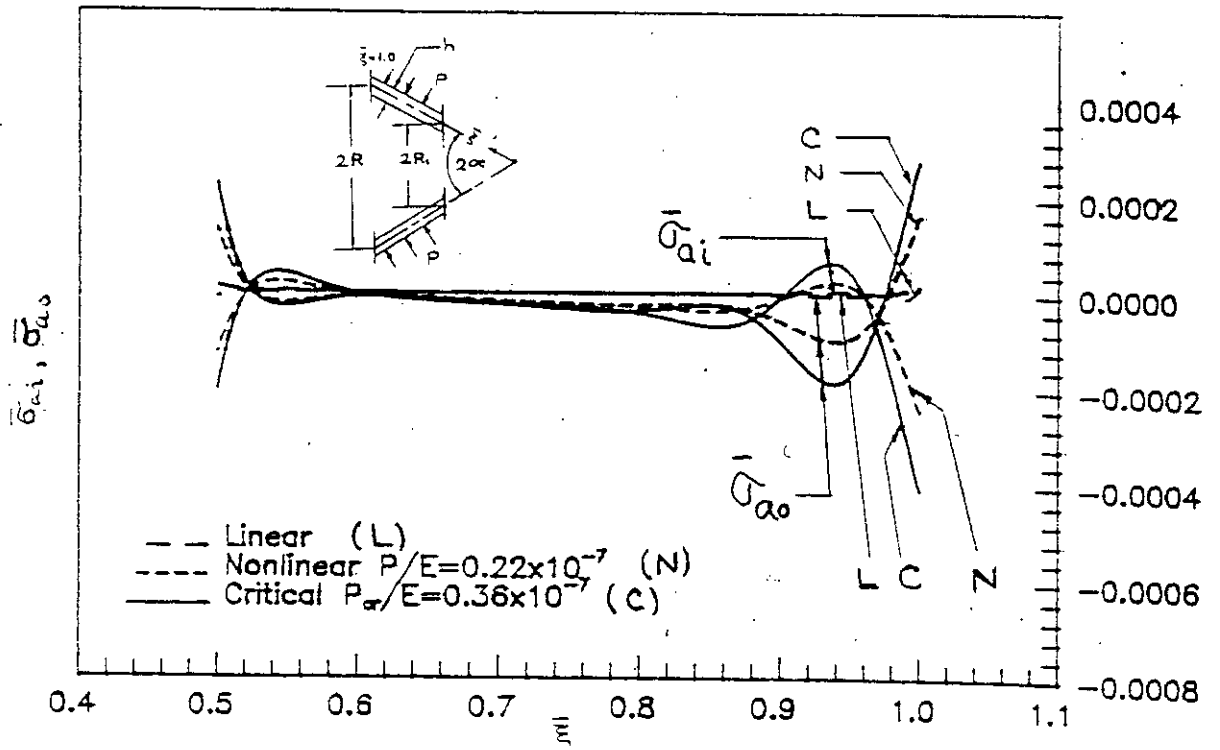


Fig.7a Meridional stresses for a 150° apex-angle frustum with thickness ratio $(R/h)=1500$ and diameter ratio $(R_1/R)=0.5$ [Ref.6]

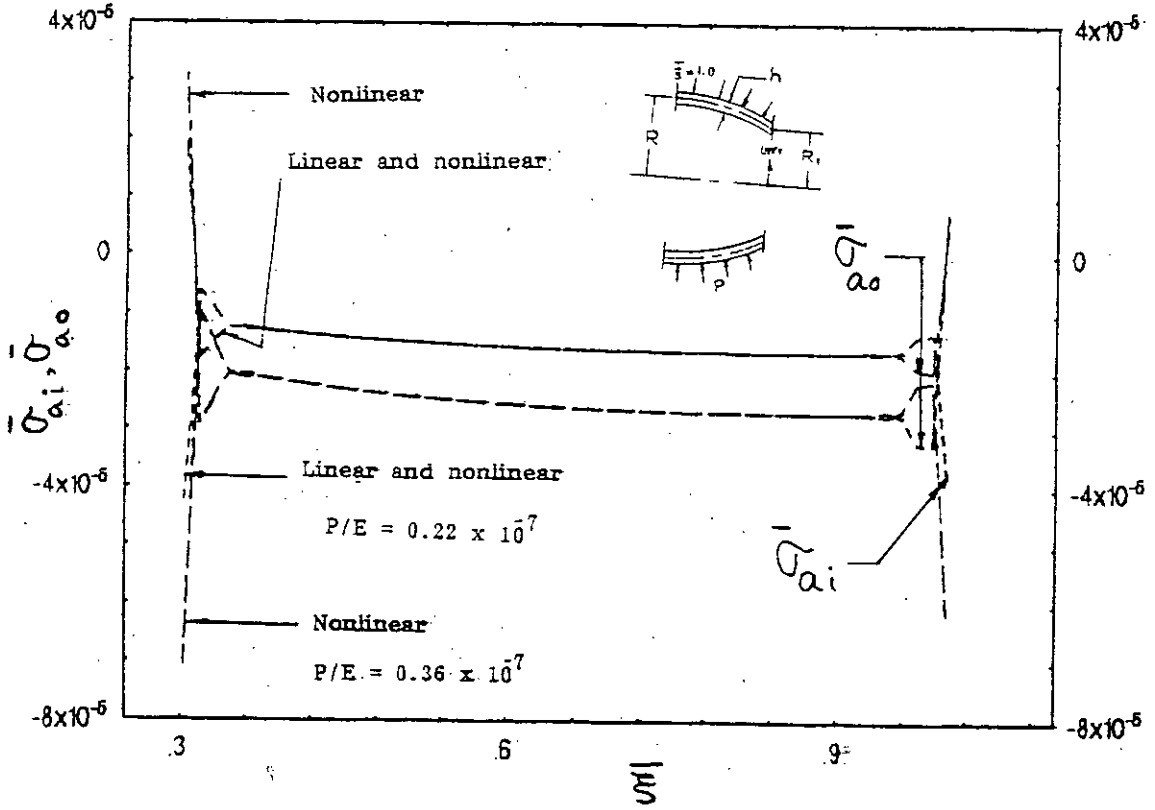


Fig. 7b Meridional stresses for a Parabolic reducer with thickness ratio $(R/h)=1500$ and diameter ratio $(R_1/R)=0.5$ [Present Analysis]

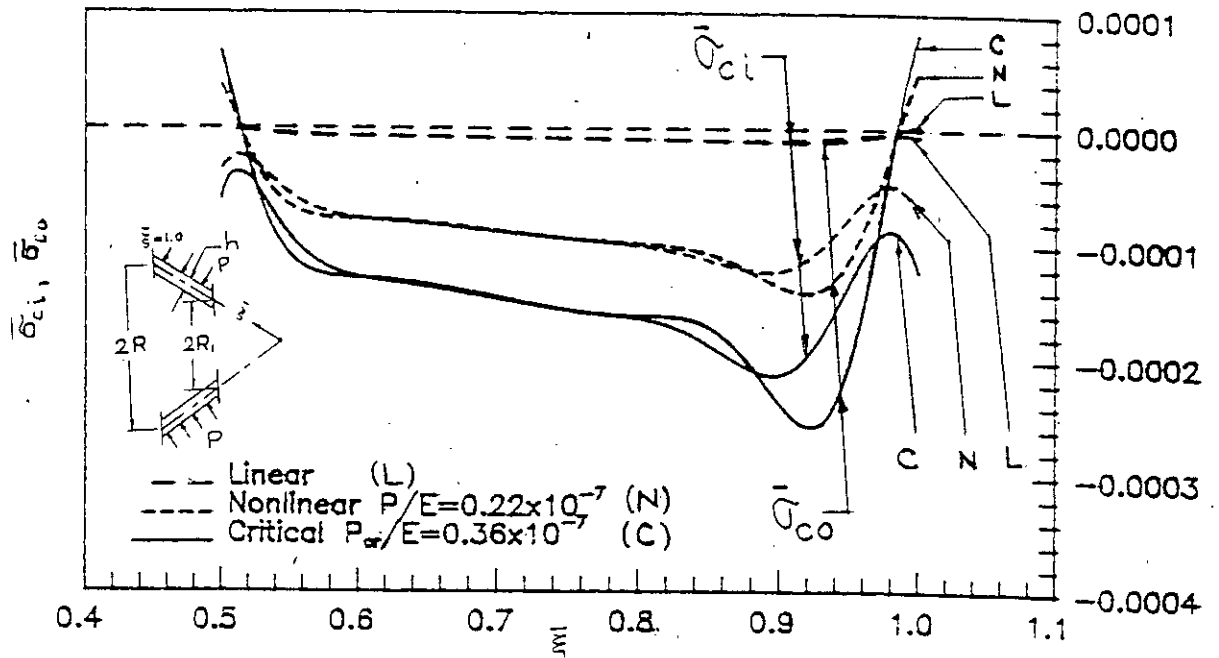


Fig.7c Circumferential stresses for a 150° apex-angle frustum with thickness ratio $(R/h)=1500$ and diameter ratio $(R_1/R)=0.5$ [Ref.6]

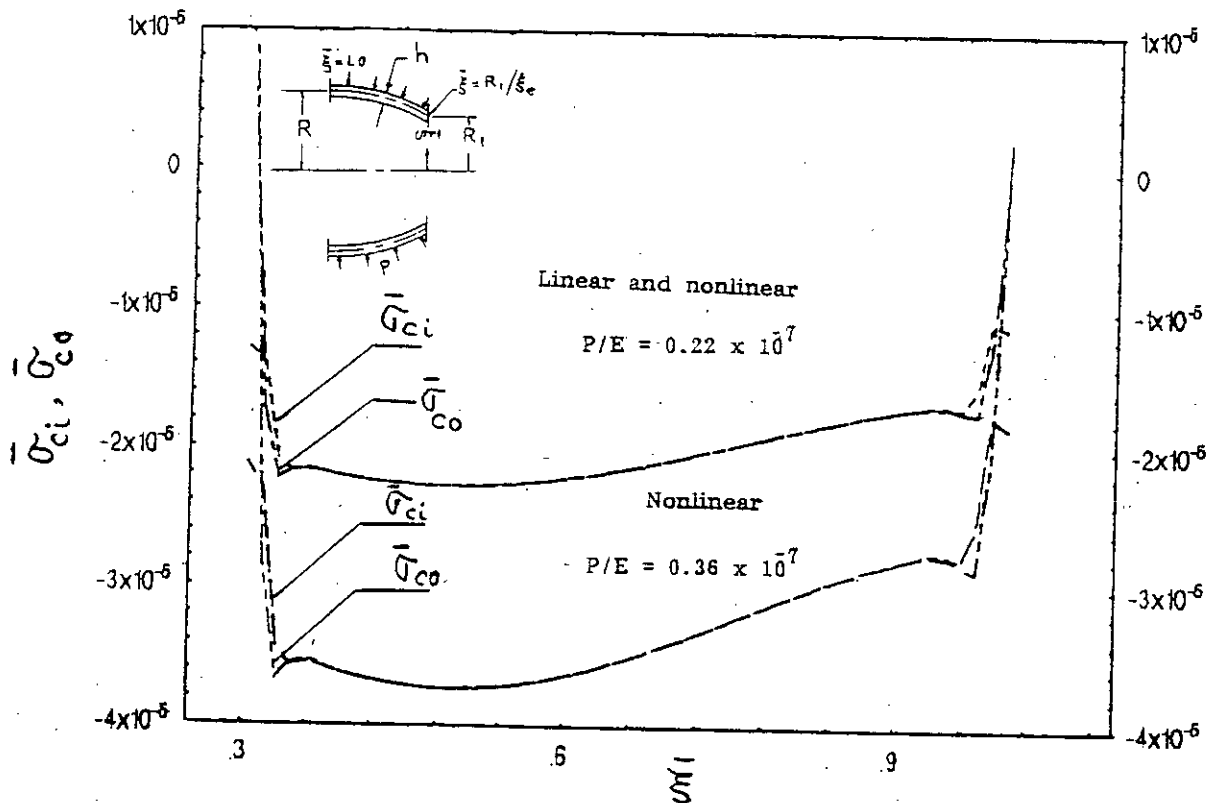


Fig.7d Circumferential stresses for a Parabolic reducer with thickness ratio $(R/h)=1500$ and diameter ratio $(R_1/R)=0.5$ [Present Analysis]

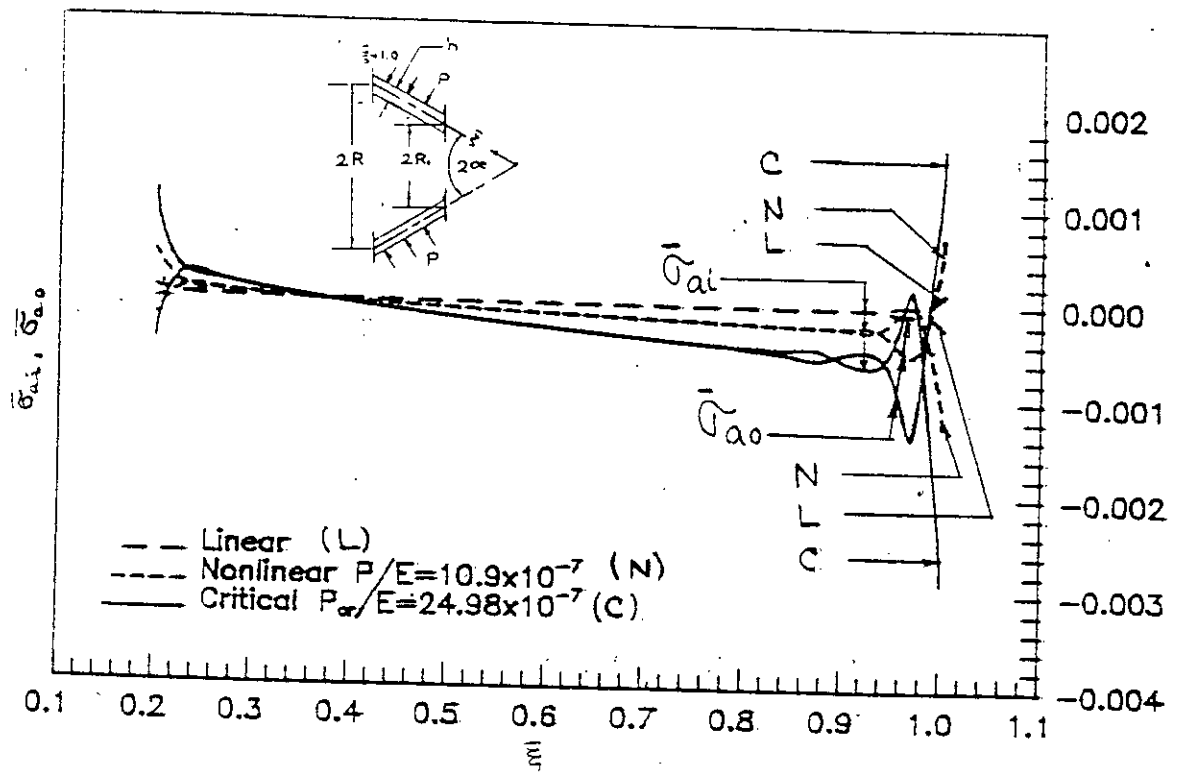


Fig.8a Meridional stresses for a 60° apex-angle frustum with thickness ratio $(R/h)=500$ and Diameter ratio $(R_1/R)=0.2$ [Ref.6]

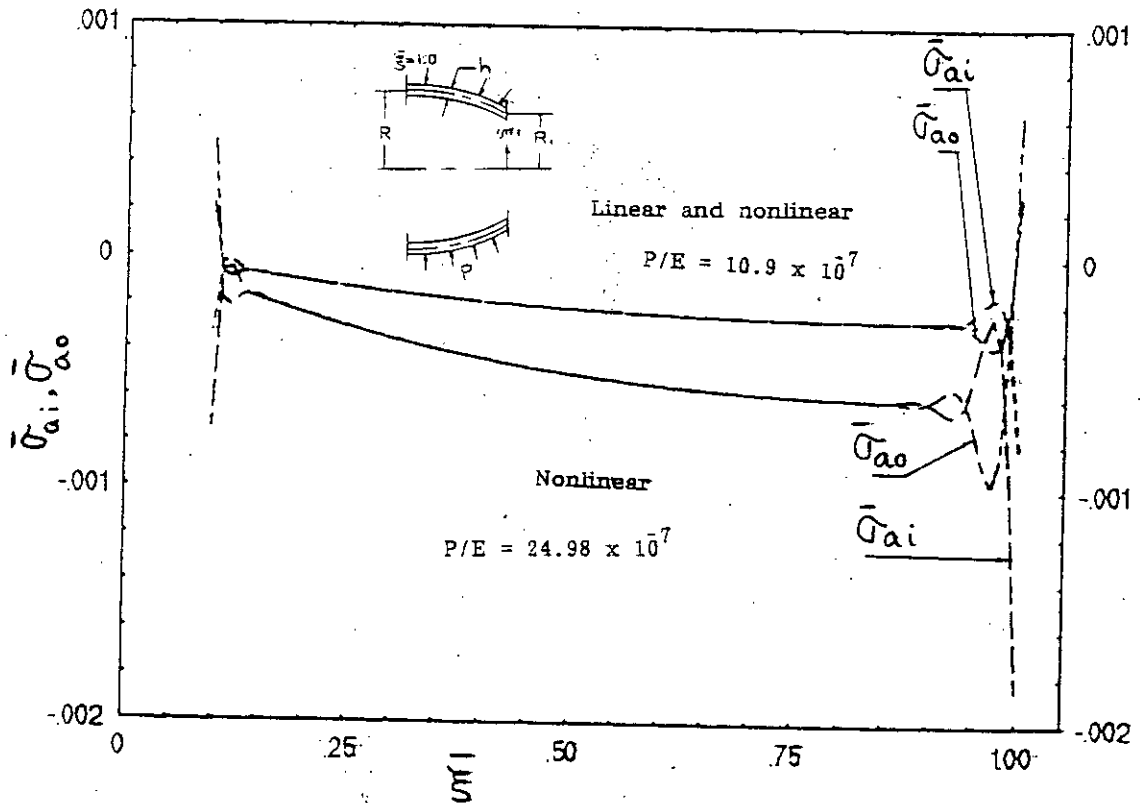


Fig.8b Meridional stresses for a Parabolic reducer with thickness ratio $(R/h)=500$ and diameter ratio $(R_1/R)=0.2$ [Present Analysis]

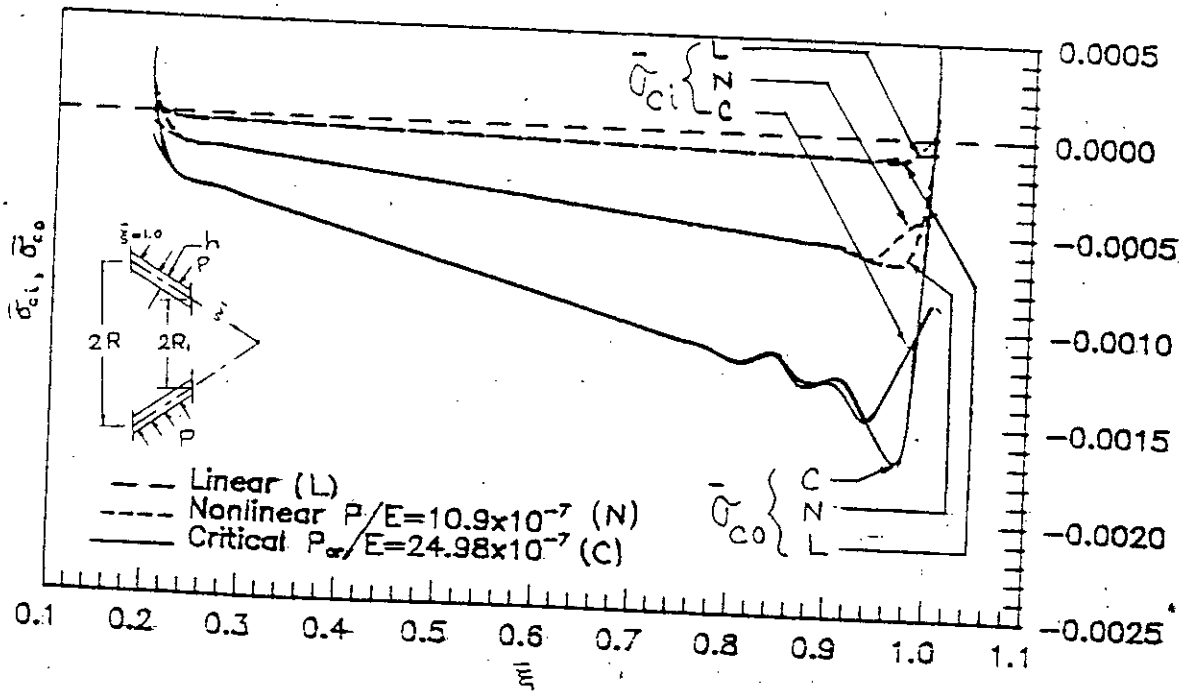


Fig. 8c Circumferential stresses for a 60° apex-angle frustum with thickness ratio $(R/h)=500$ and diameter ratio $(R_1/R)=0.2$ [Ref. 6]

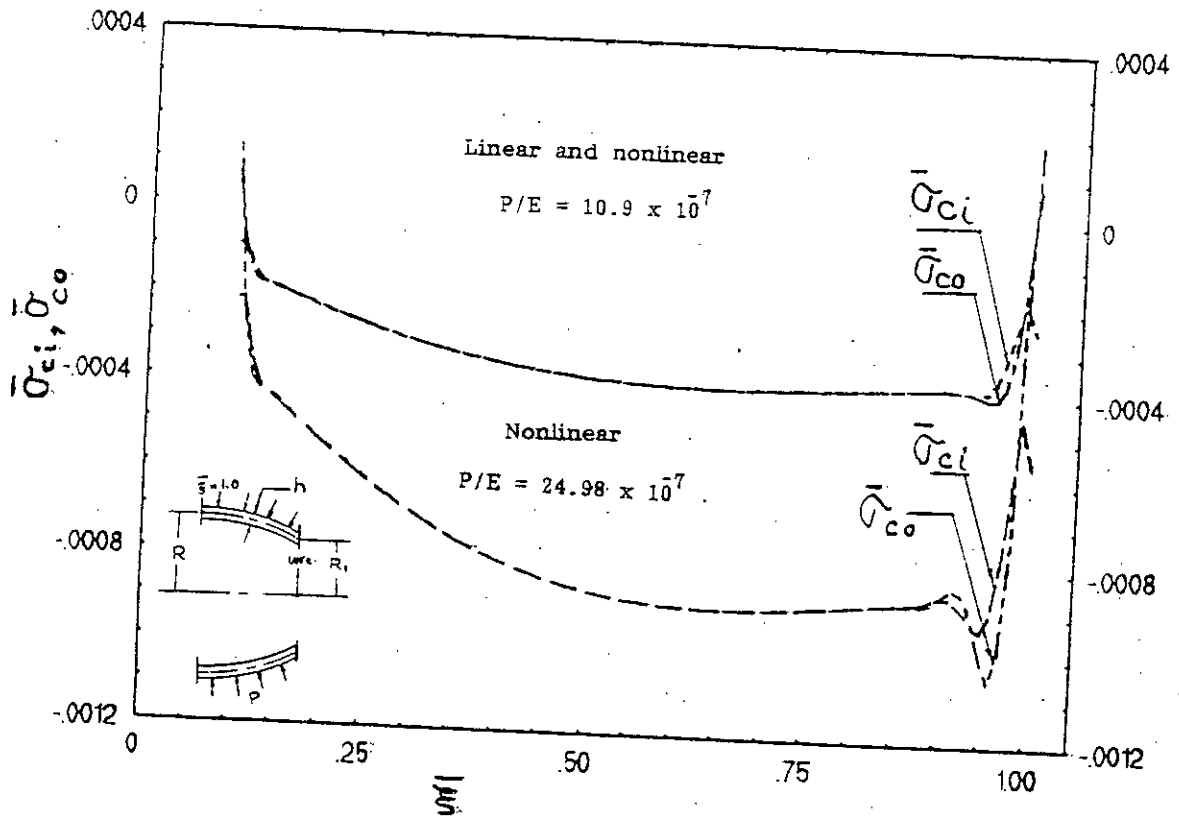


Fig. 8d Circumferential stresses for a Parabolic reducer with thickness ratio $(R/h)=500$ and diameter ratio $(R_1/R)=0.2$ [Present Analysis]

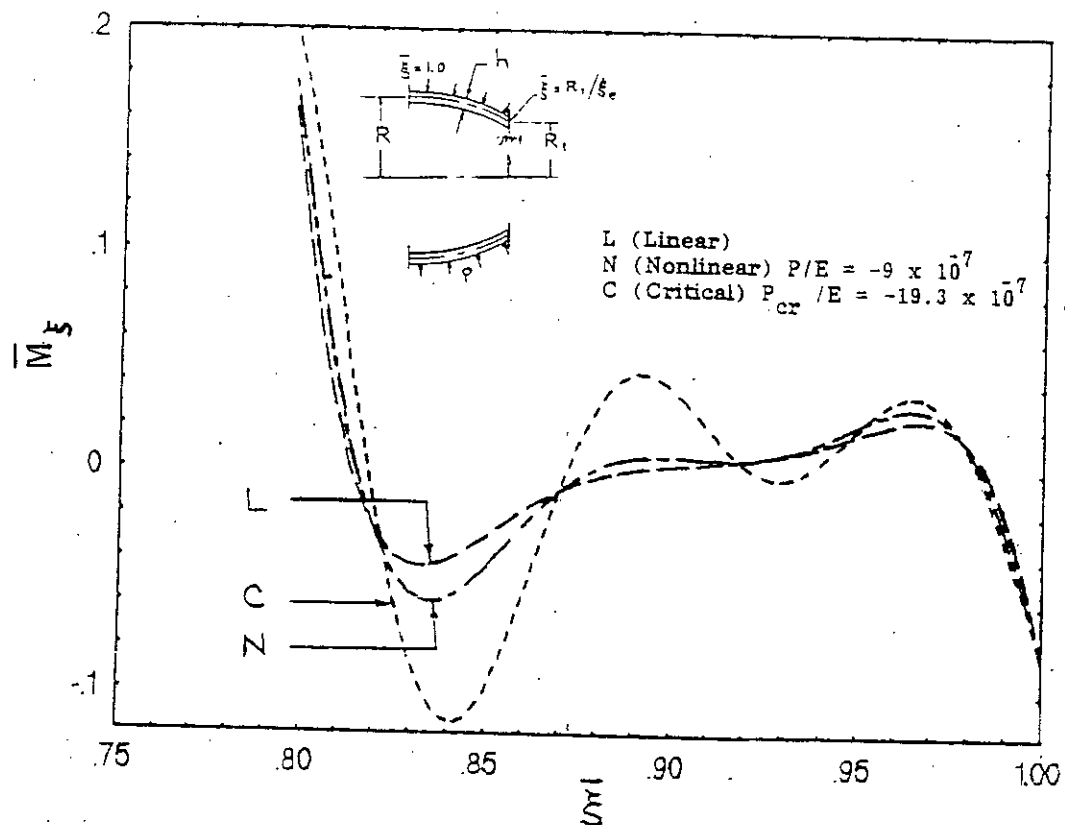


Fig.9a Meridional bending moments for a Parabolic reducer with thickness ratio $(R/h) = 1000$ and diameter ratio $(R_1/R) = 0.9$

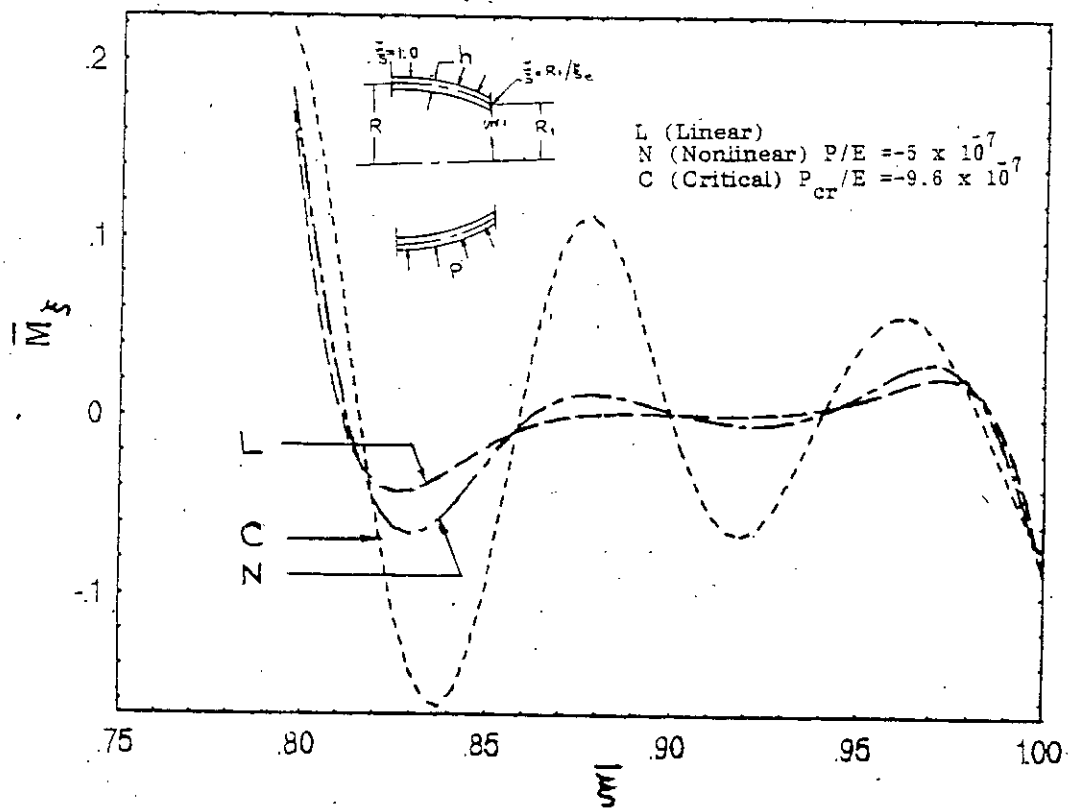


Fig.9b Meridional bending moments for a Parabolic reducer with thickness ratio $(R/h) = 1500$ and diameter ratio $(R_1/R) = 0.9$

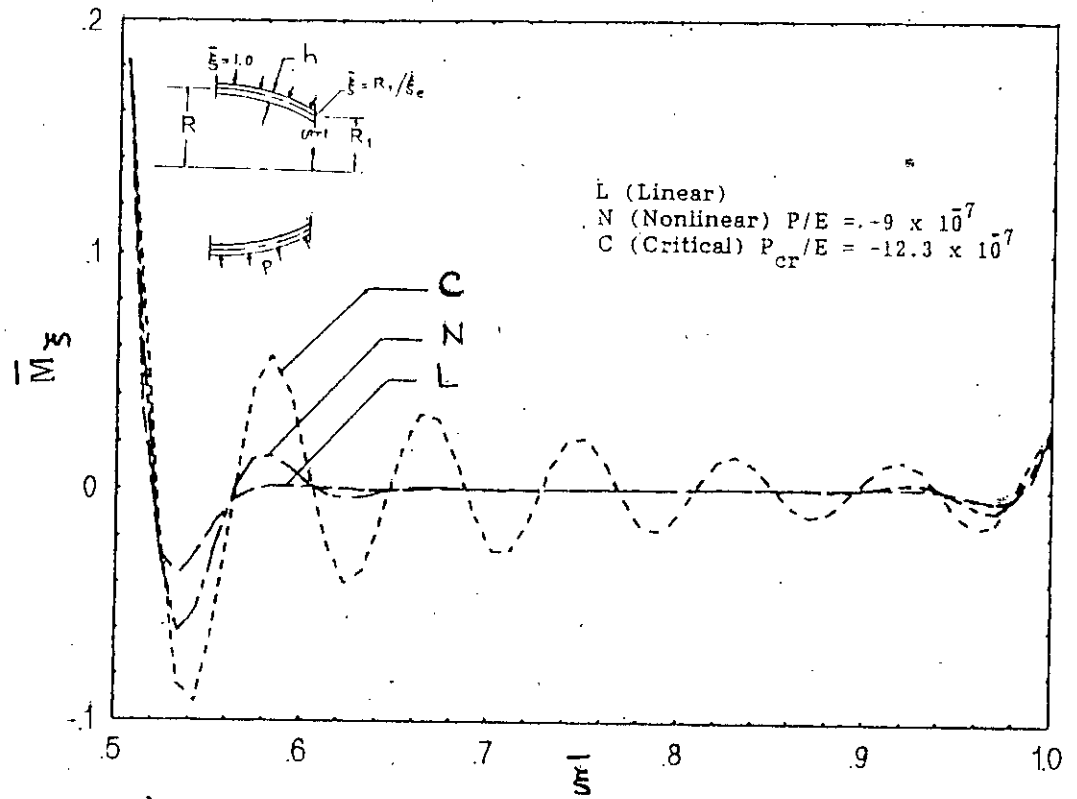


Fig.9c Meridional bending moments for a Parabolic reducer with thickness ratio $(R/h) = 1000$ and diameter ratio $(R_1/R) = 0.7$

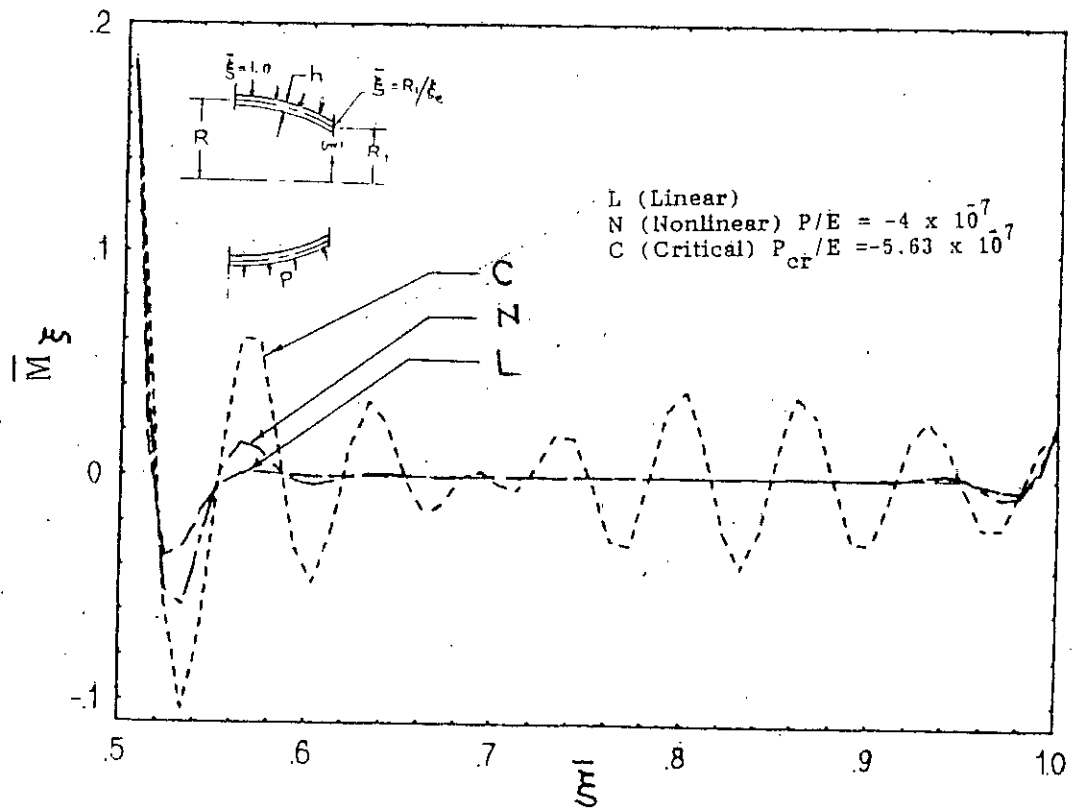


Fig.9d Meridional bending moments for a Parabolic reducer with thickness ratio $(R/h) = 1500$ and diameter ratio $(R_1/R) = 0.7$

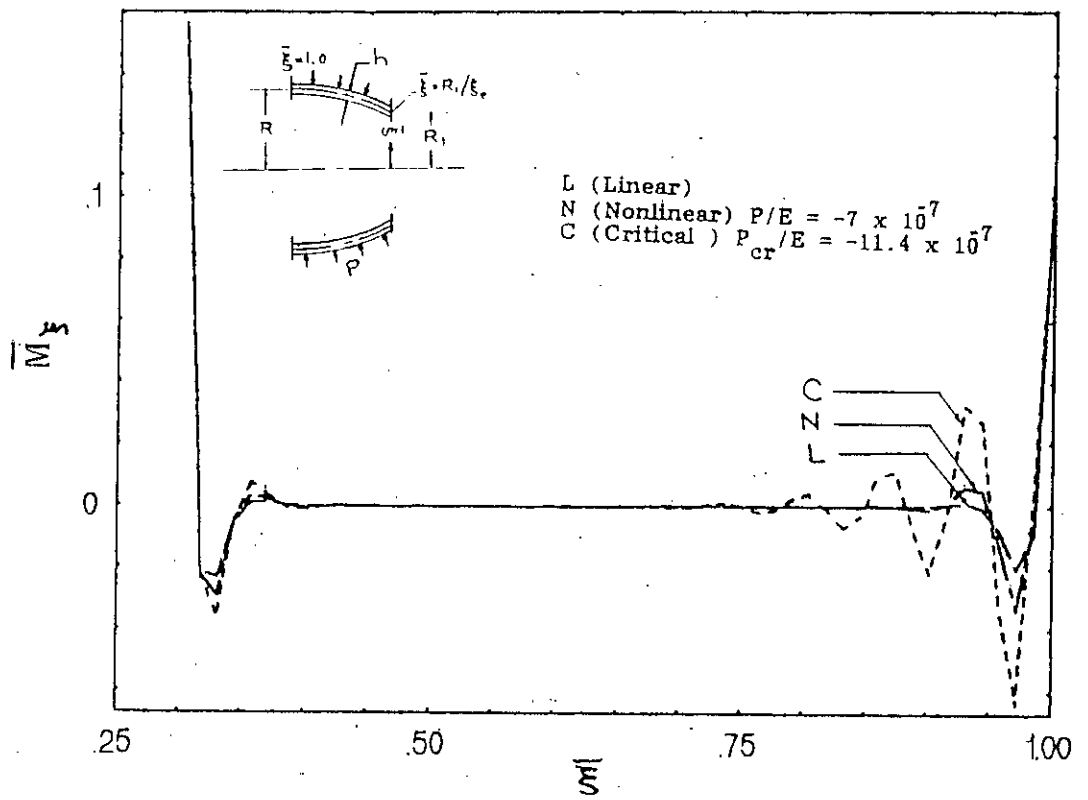


Fig.9e Meridional bending moments for a Parabolic reducer with thickness ratio $(R/h) = 1000$ and diameter ratio $(R_1/R) = 0.5$

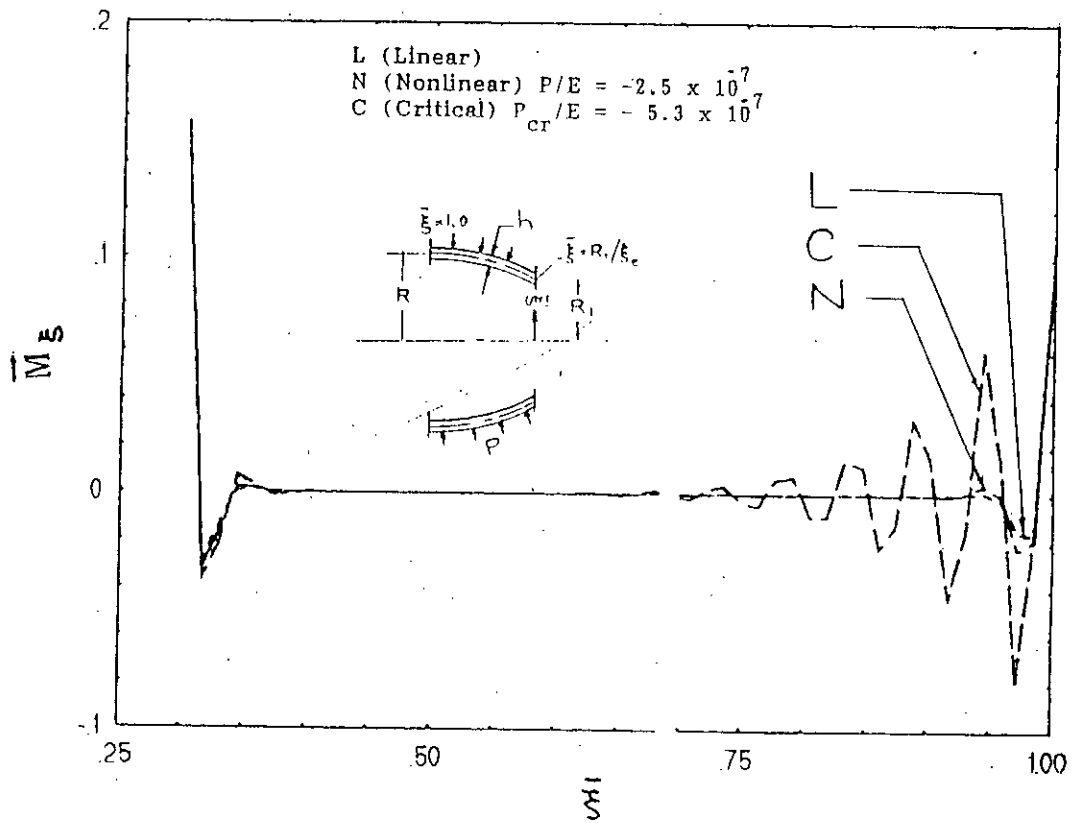


Fig.9f Meridional bending moments for a Parabolic reducer with thickness ratio $(R/h)=1500$ and diameter ratio $(R_1/R)=0.5$

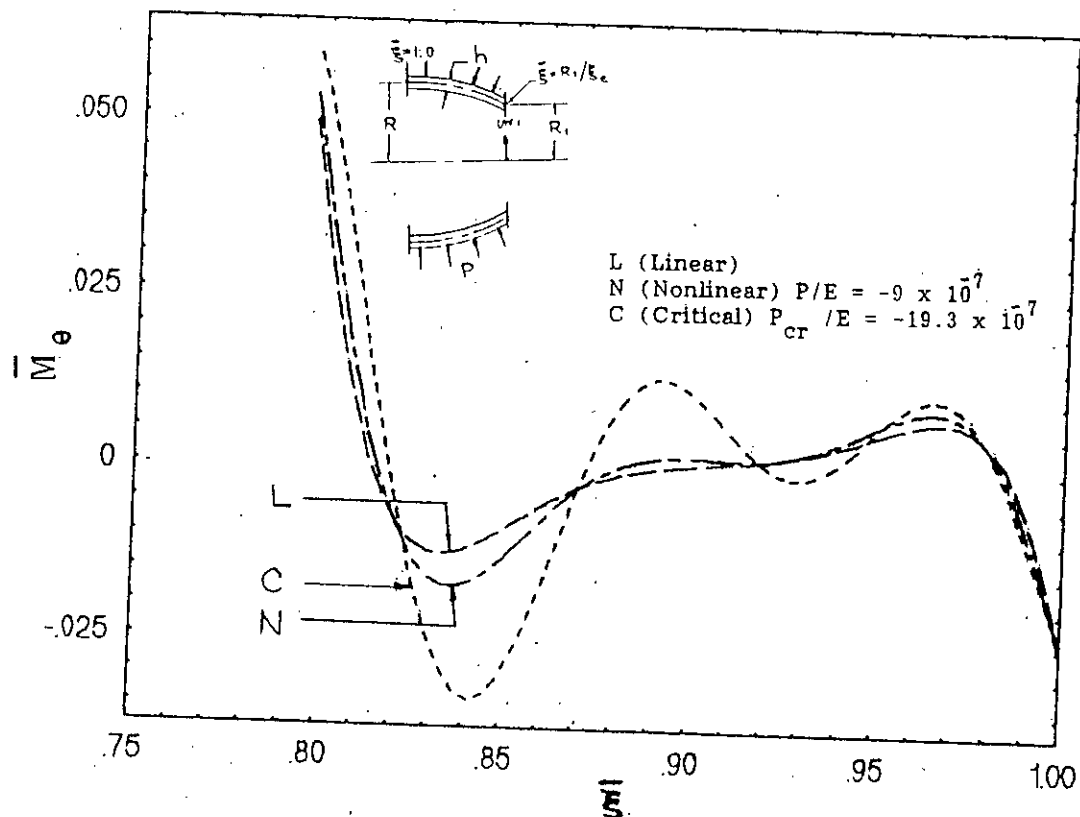


Fig. 10a Circumferential bending moments for a Parabolic reducer with thickness ratio $(R/h) = 1000$ and diameter ratio $(R_1/R) = 0.9$

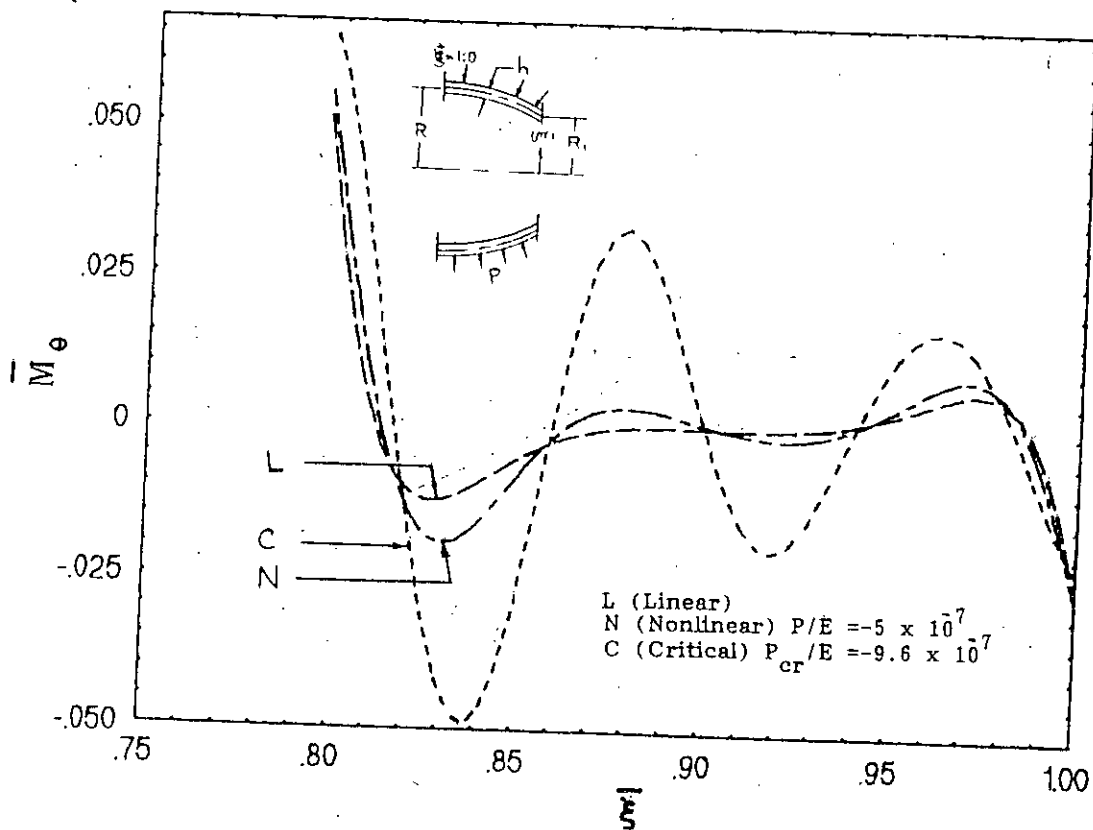


Fig. 10b Circumferential bending moments for a Parabolic reducer with thickness ratio $(R/h) = 1500$ and diameter ratio $(R_1/R) = 0.9$

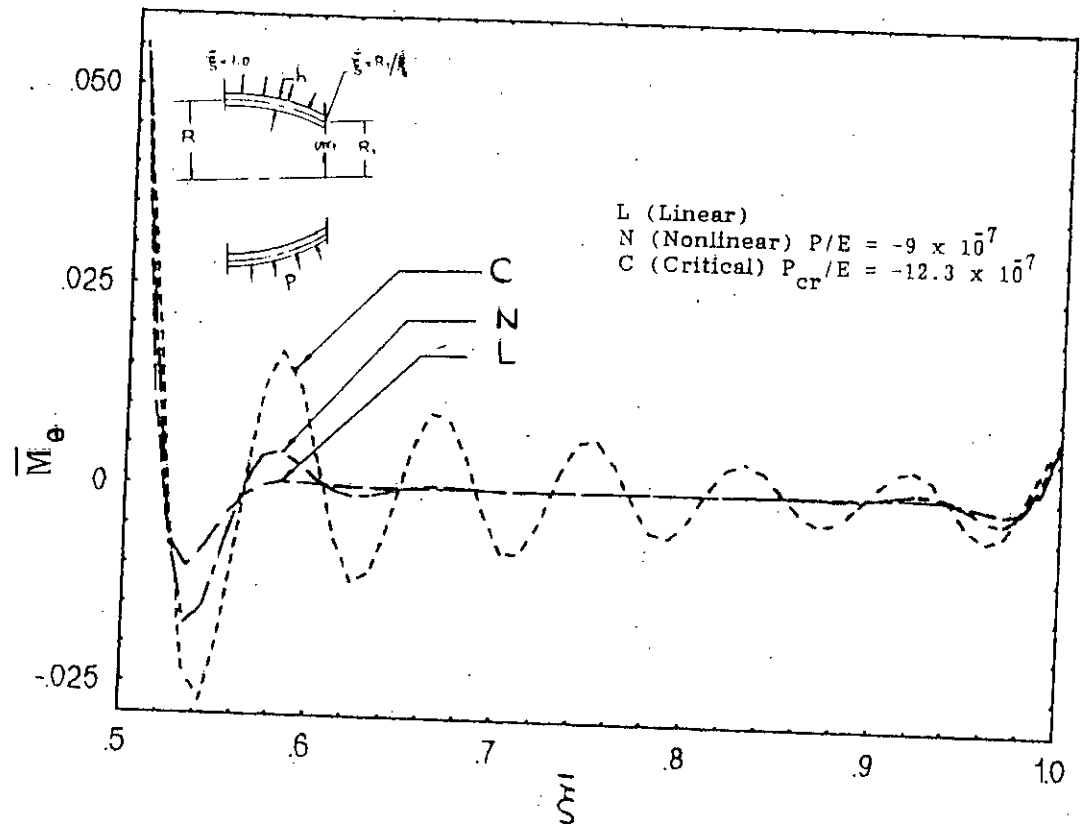


Fig. 10c Circumferential bending moments for a Parabolic reducer with thickness ratio $(R/h) = 1000$ and diameter ratio $(R_1/R) = 0.7$

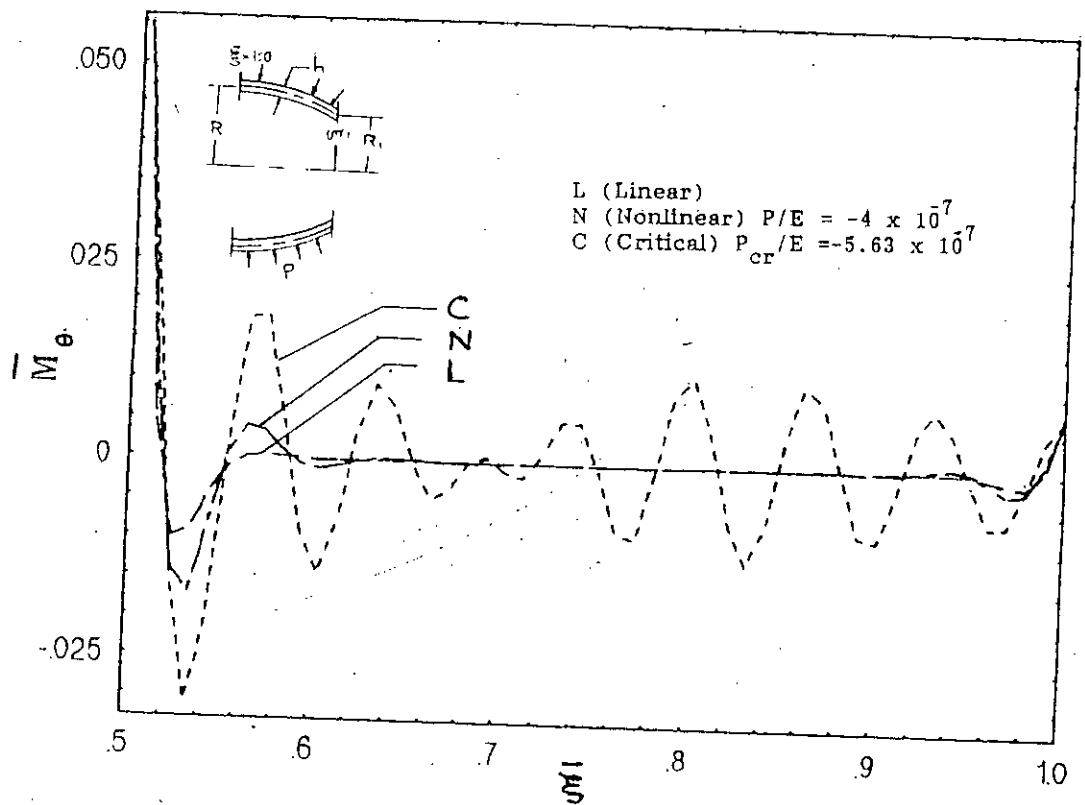


Fig. 10d Circumferential bending moments for a Parabolic reducer with thickness ratio $(R/h) = 1500$ and diameter ratio $(R_1/R) = 0.7$

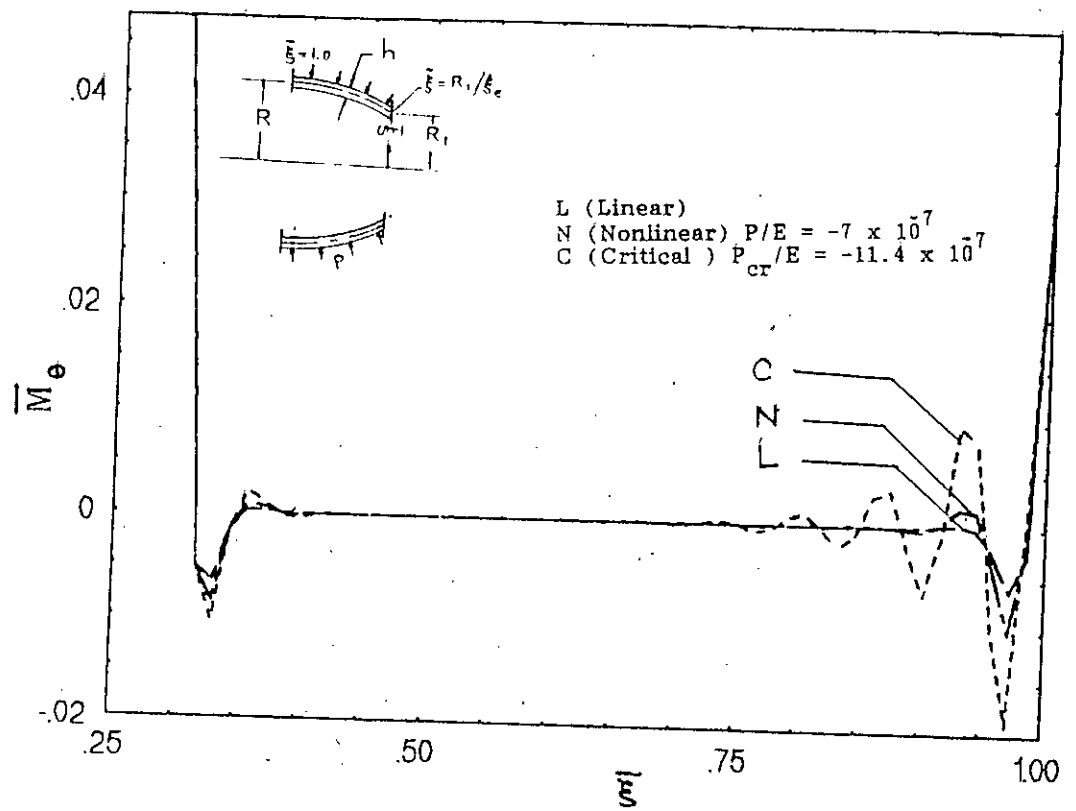


Fig. 10e Circumferential bending moments for a Parabolic reducer with thickness ratio $(R/h) = 1000$ and diameter ratio $(R_1/R) = 0.5$

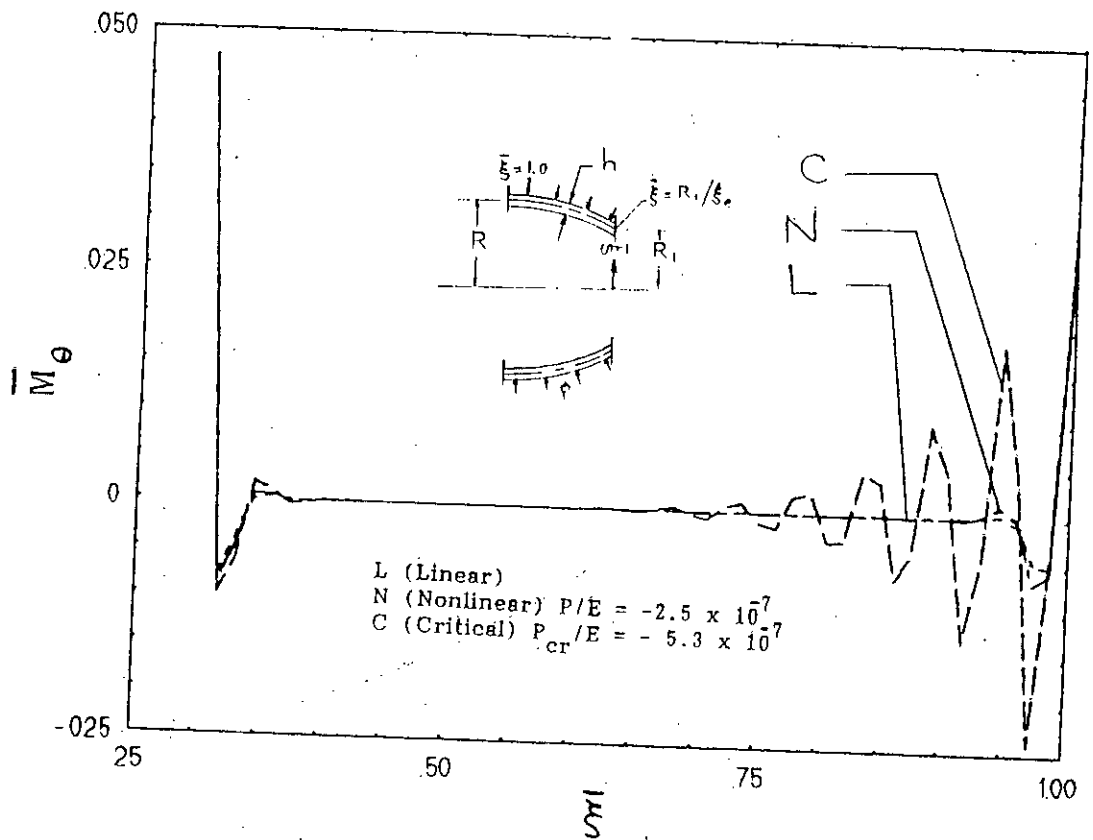


Fig. 10f Circumferential bending moments for a Parabolic reducer with thickness ratio $(R/h) = 1500$ and diameter ratio $(R_1/R) = 0.5$

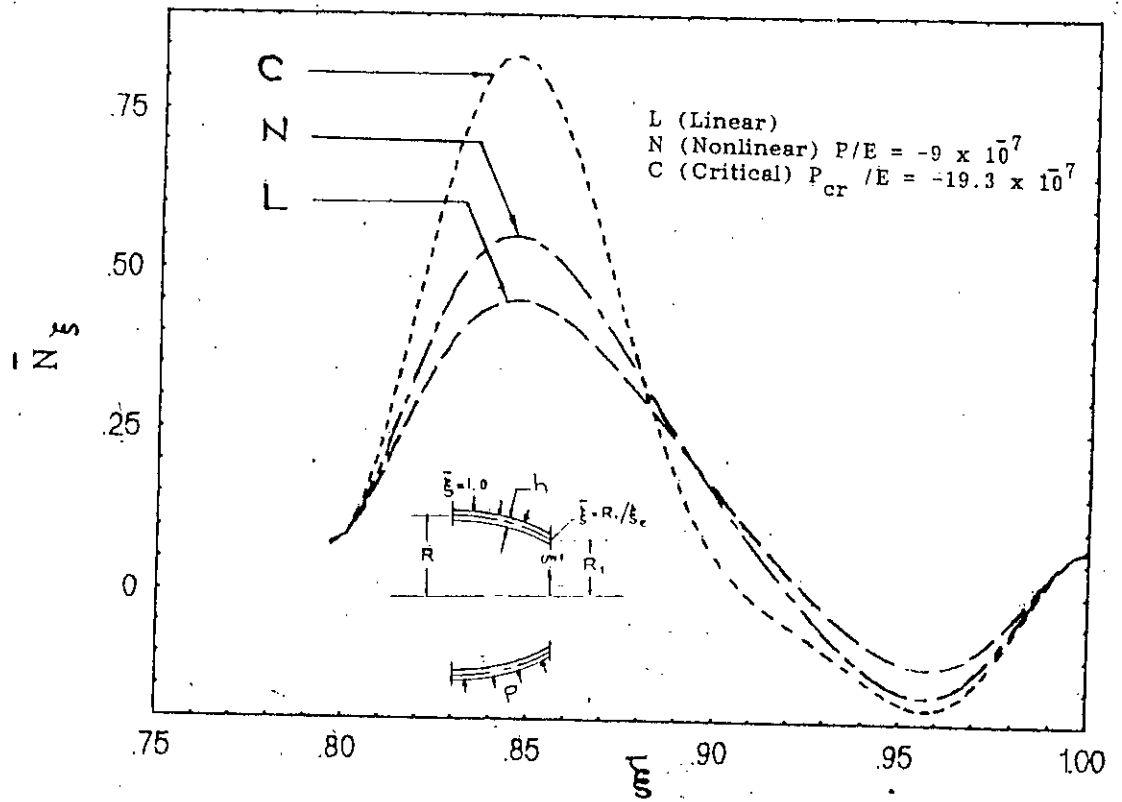


Fig. 11a Meridional stress resultants for a Parabolic reducer with thickness ratio $(R/h) = 1000$ and diameter ratio $(R_1/R) = 0.9$

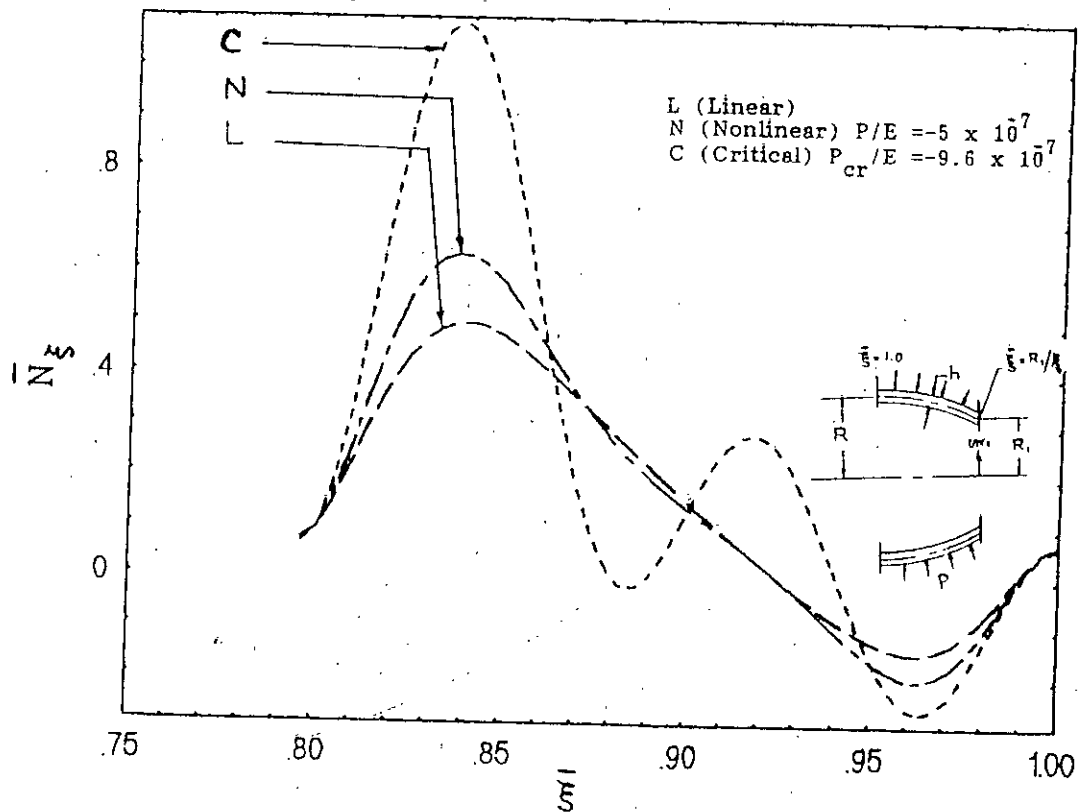


Fig. 11b Meridional stress resultants for a Parabolic reducer with thickness ratio $(R/h) = 1500$ and diameter ratio $(R_1/R) = 0.9$

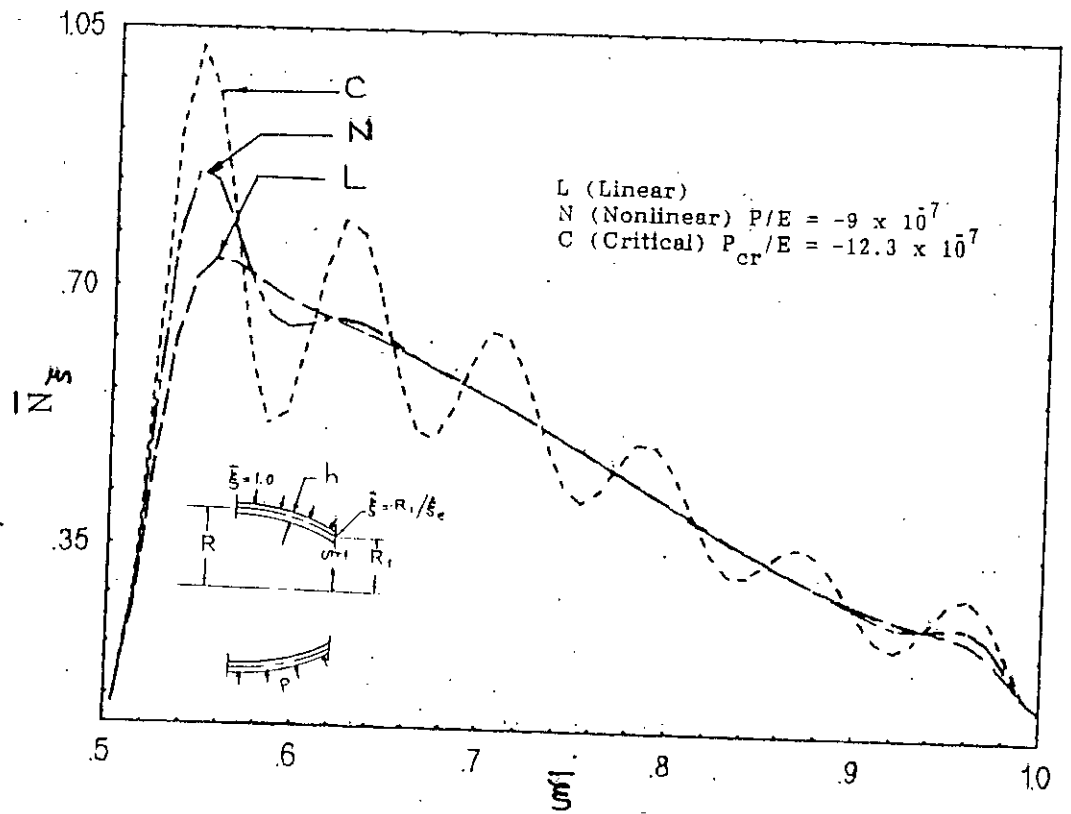


Fig. 11c Meridional stress resultants for a Parabolic reducer with thickness ratio $(R/h) = 1000$ and diameter ratio $(R_1/R) = 0.7$

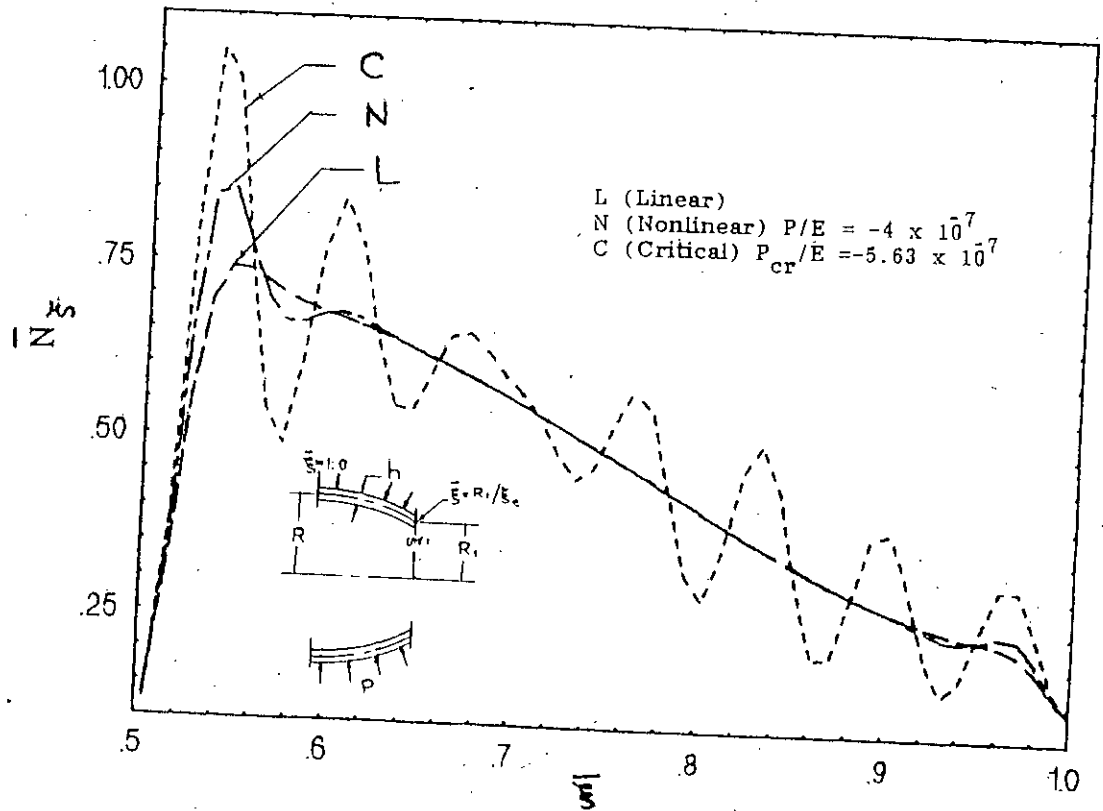


Fig. 11d Meridional stresses for a Parabolic reducer with thickness ratio $(R/h) = 1500$ and diameter ratio $(R_1/R) = 0.7$

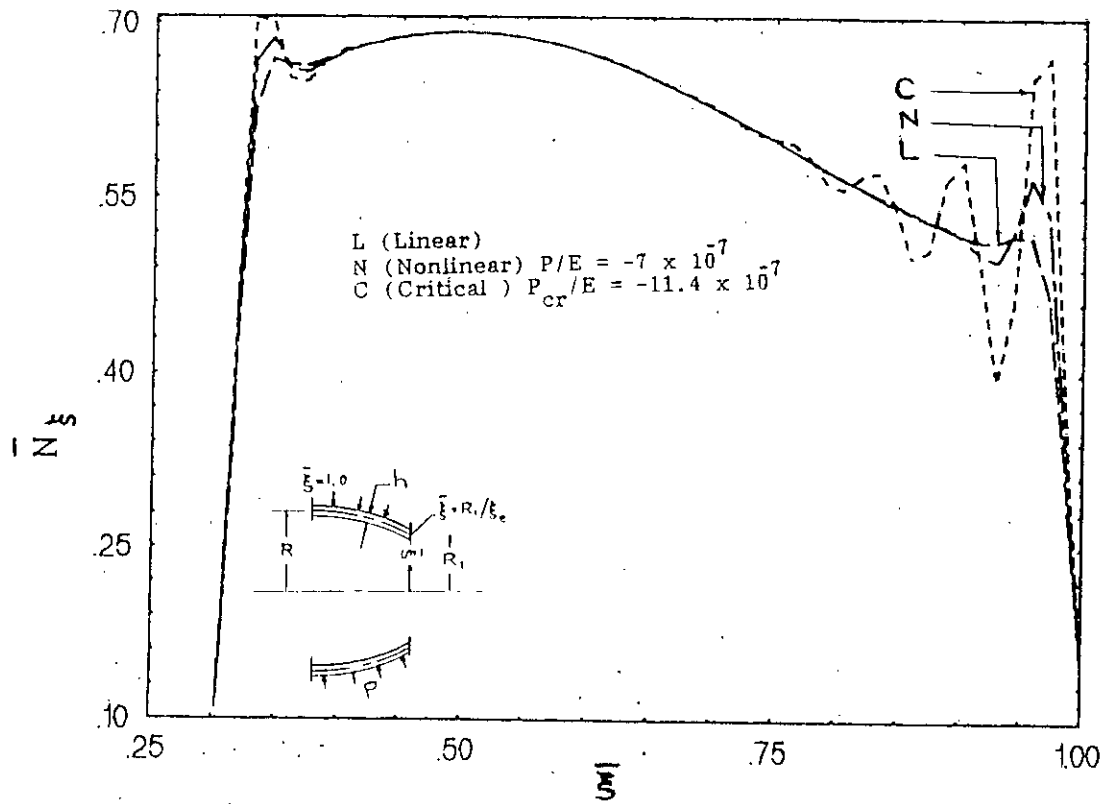


Fig. 11e Meridional stress resultants for a Parabolic reducer with thickness ratio $(R/h) = 1000$ and diameter ratio $(R_1/R) = 0.5$

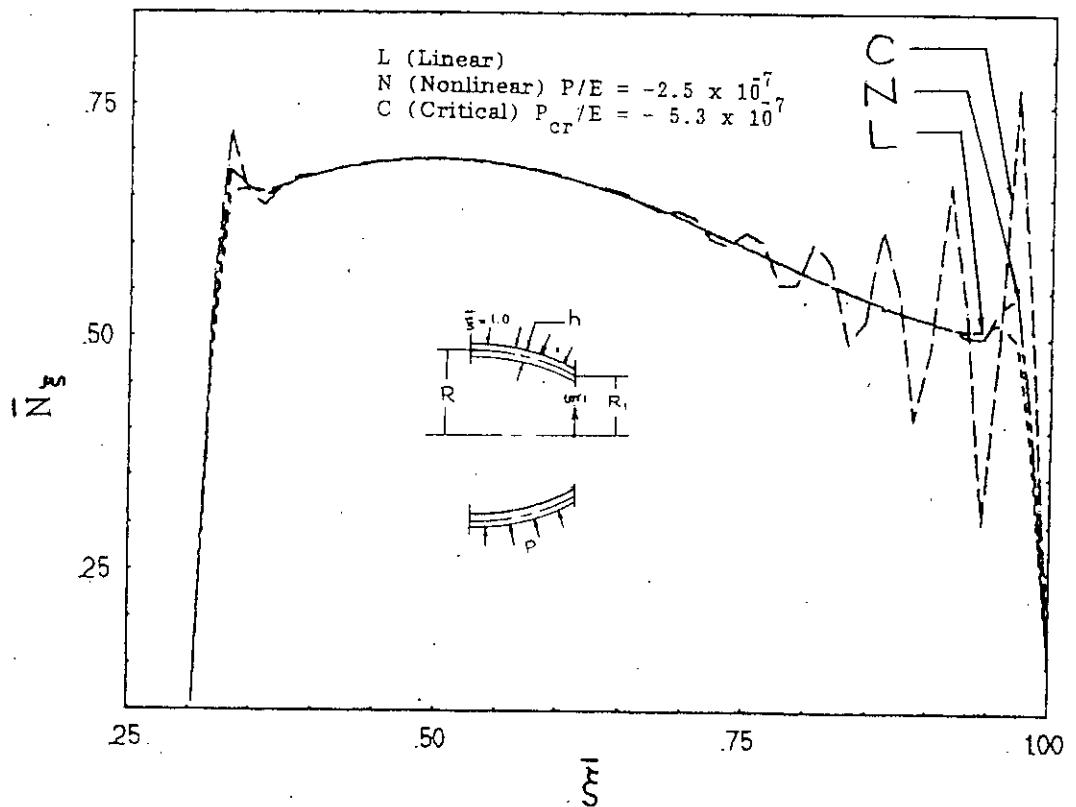


Fig. 11f Meridional stress resultants for a Parabolic reducer with thickness ratio $(R/h) = 1500$ and diameter ratio $(R_1/R) = 0.5$

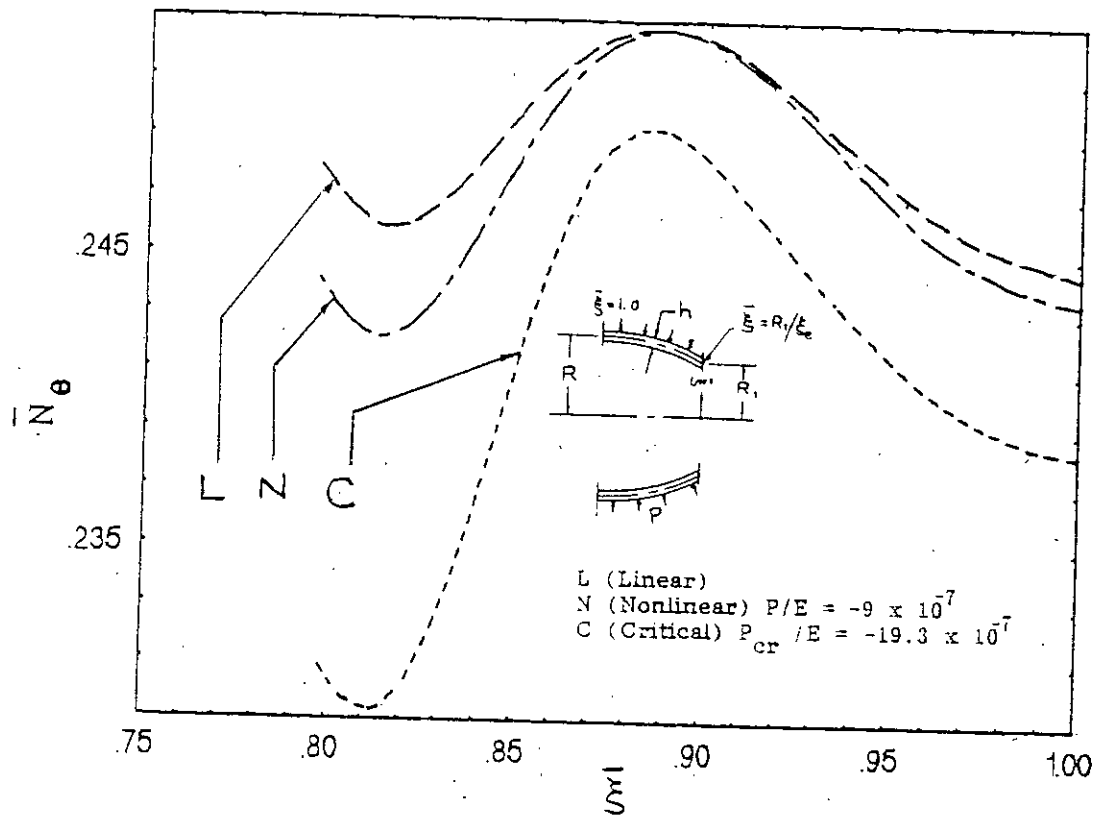


Fig. 12a Circumferential stress resultants for a Parabolic reducer with thickness ratio $(R/h) = 1000$ and diameter ratio $(R_1/R) = 0.9$

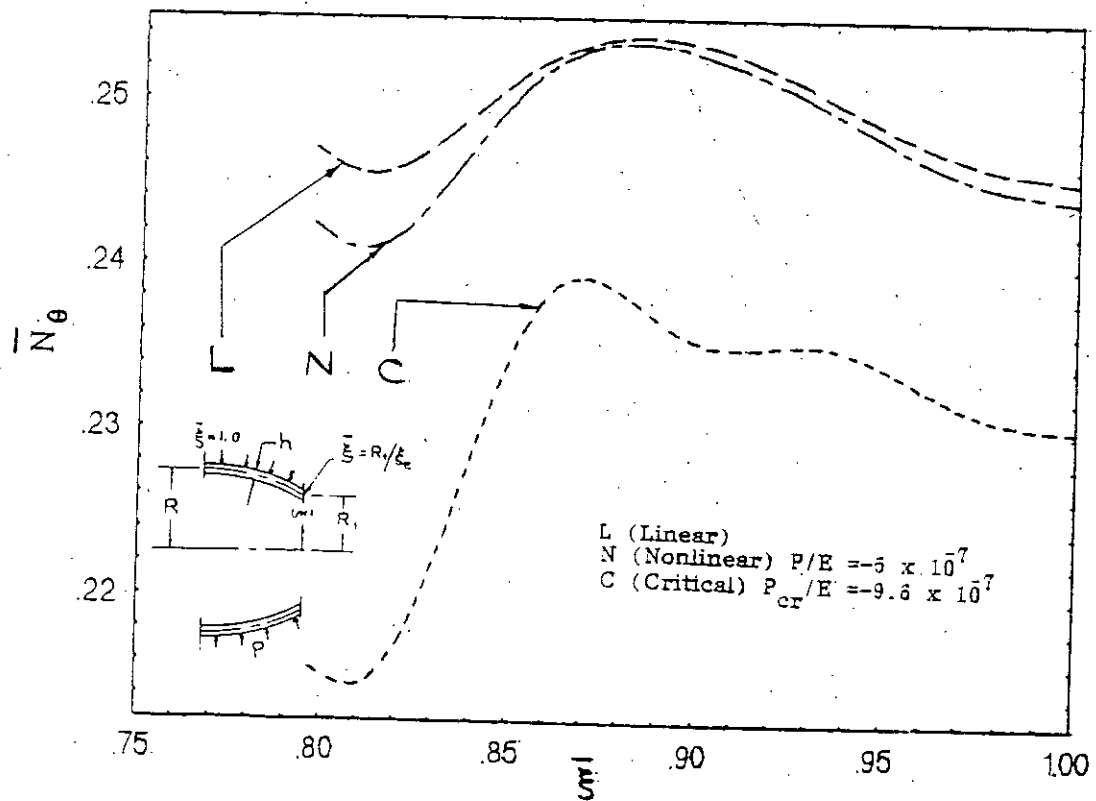


Fig. 12b Circumferential stress resultants for a Parabolic reducer with thickness ratio $(R/h) = 1500$ and diameter ratio $(R_1/R) = 0.9$

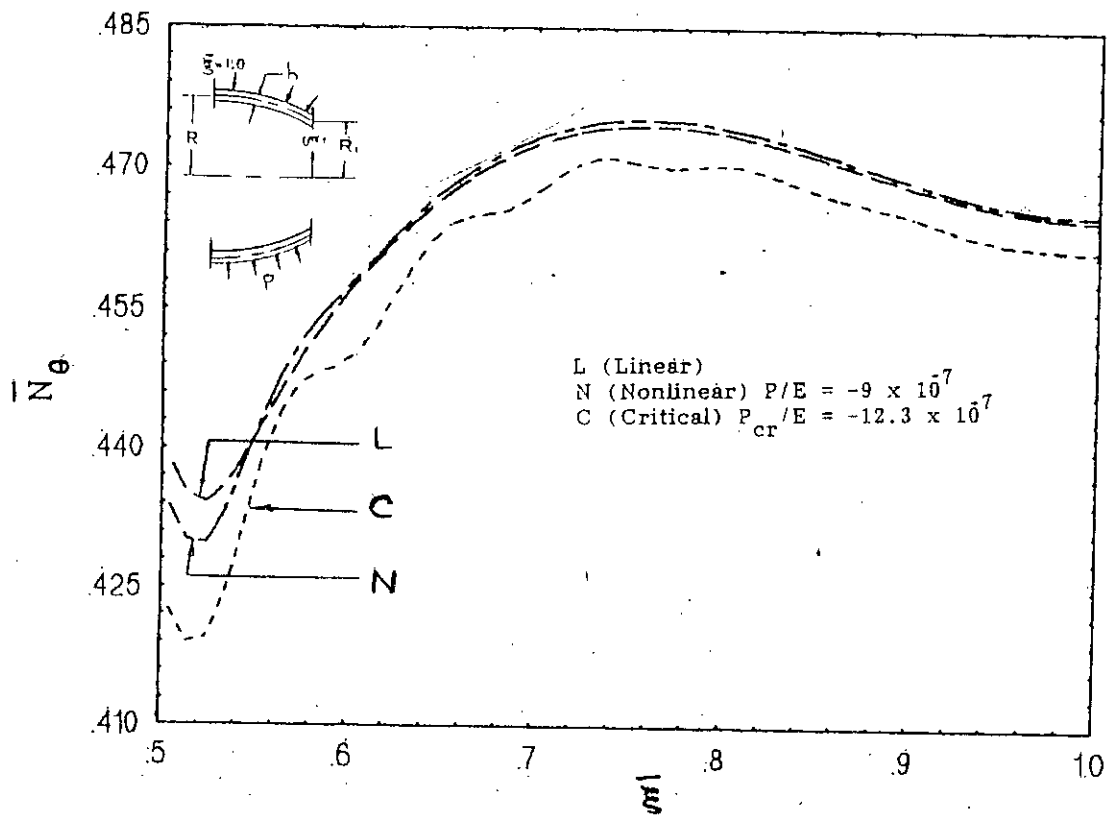


Fig.12c Circumferential stress resultants for a Parabolic reducer with thickness ratio $(R/h) = 1000$ and diameter ratio $(R_1/R) = 0.7$

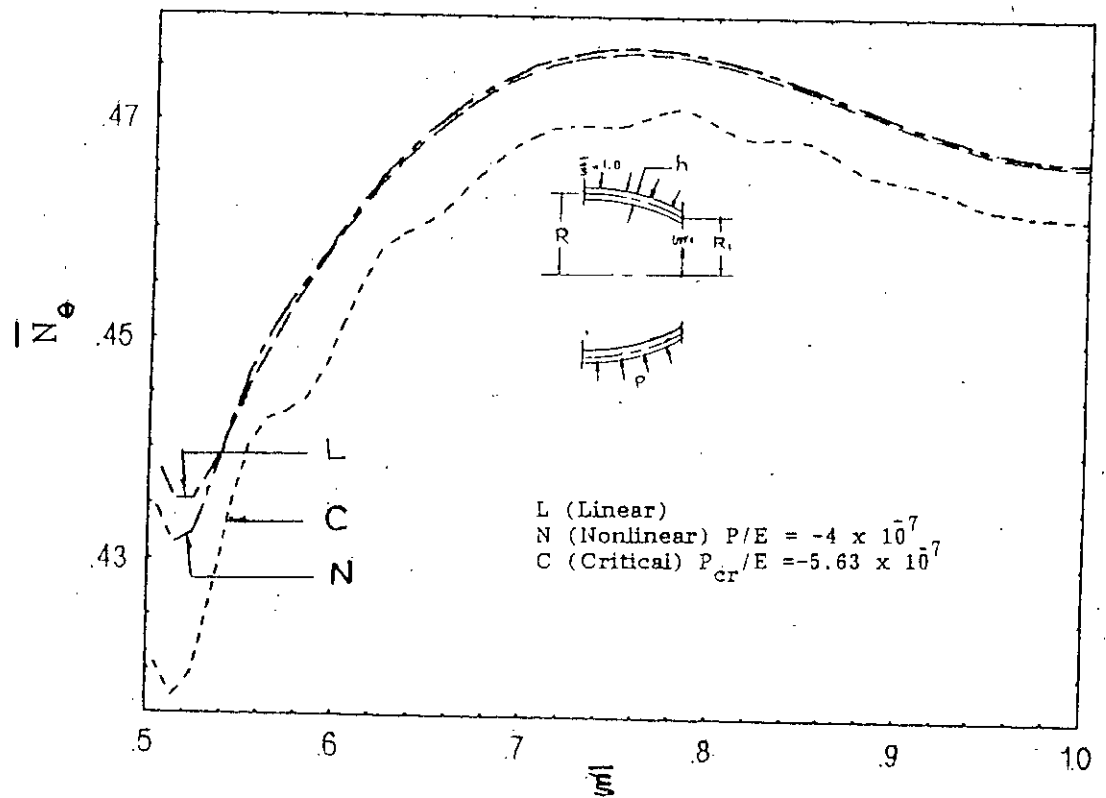


Fig.12d Circumferential stress resultants for a Parabolic reducer with thickness ratio $(R/h) = 1500$ and diameter ratio $(R_1/R) = 0.7$

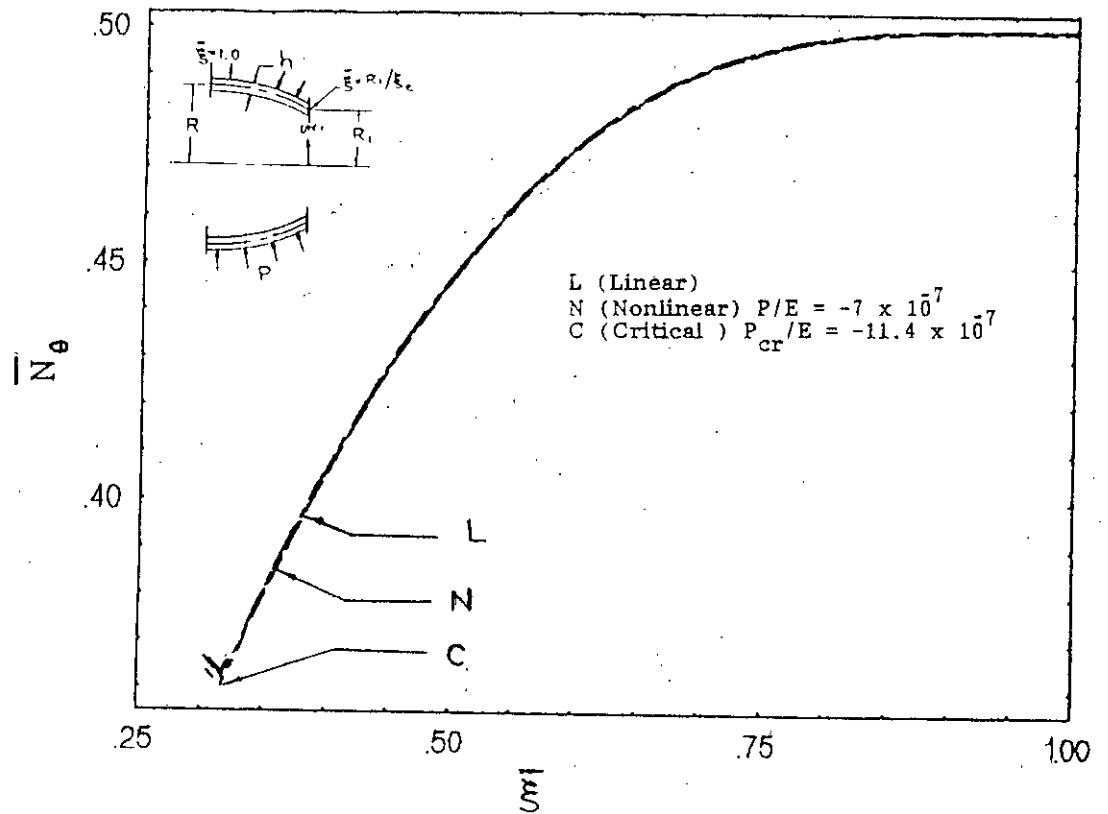


Fig.12e Circumferential stress resultants for a Parabolic reducer with thickness ratio $(R/h) = 1000$ and diameter ratio $(R_1/R) = 0.5$

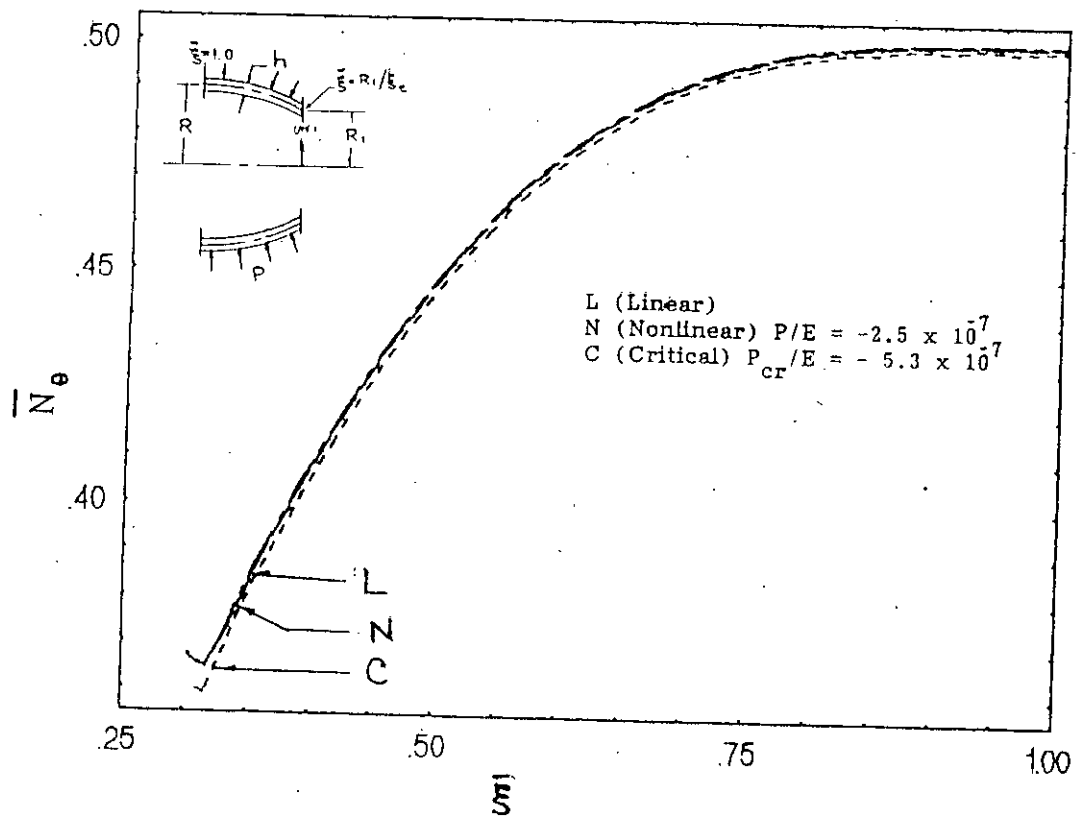


Fig.12f Circumferential stress resultants for a Parabolic reducer with thickness ratio $(R/h) = 1500$ and diameter ratio $(R_1/R) = 0.5$

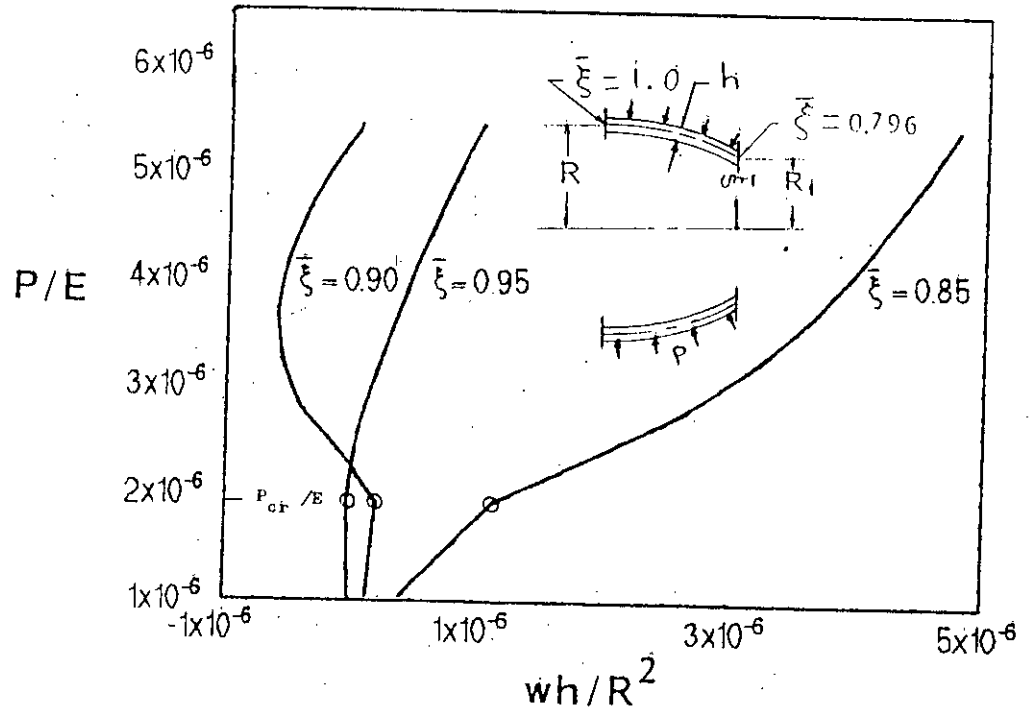


Fig. 13a Axial displacements for SHELL -1090 ($R/h=1000$, $R_1/R=0.9$)

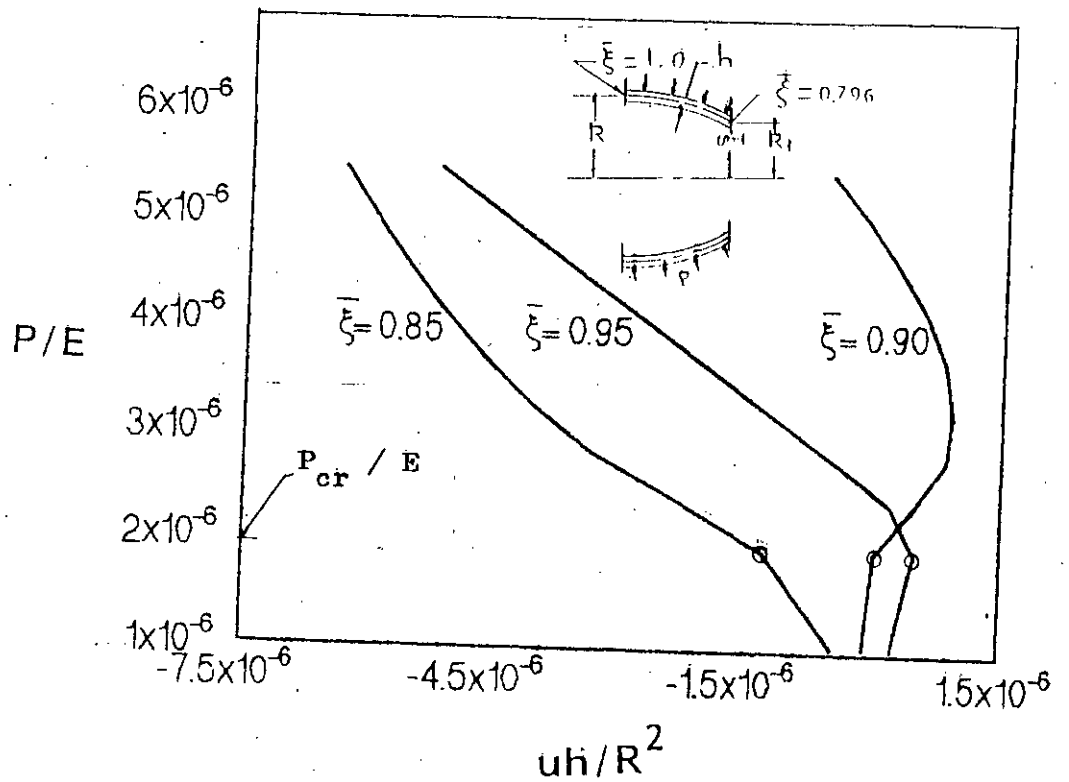


Fig. 13b Radial displacements for SHELL-1090 ($R/h=1000$, $R_1/R=0.9$)

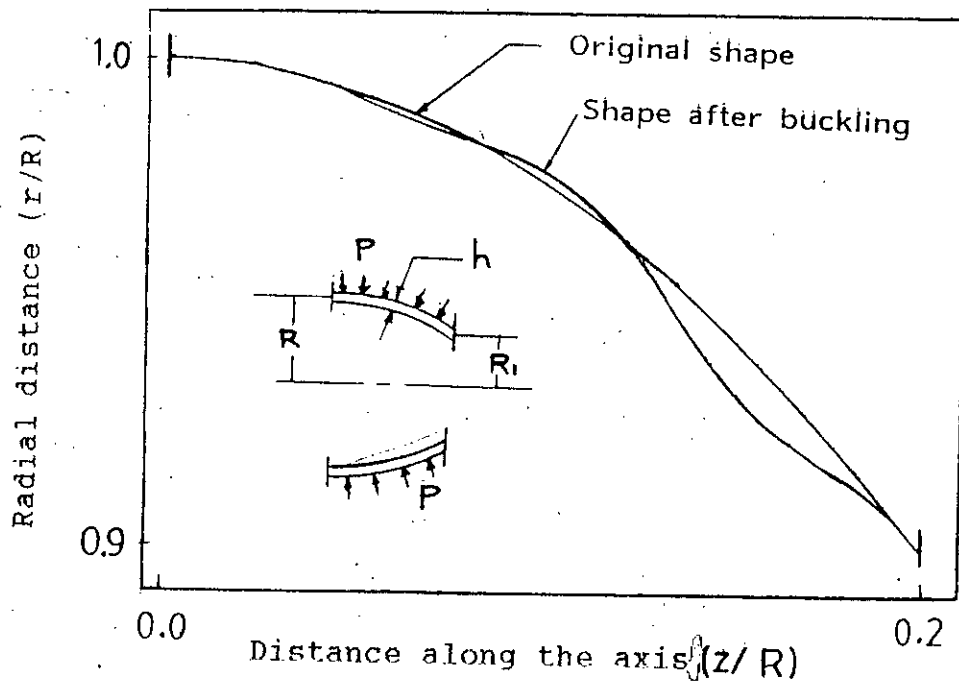


Fig.13c Buckled configuration of SHELL-1090 ($R/h=1000$, $R_1/R=0.9$)

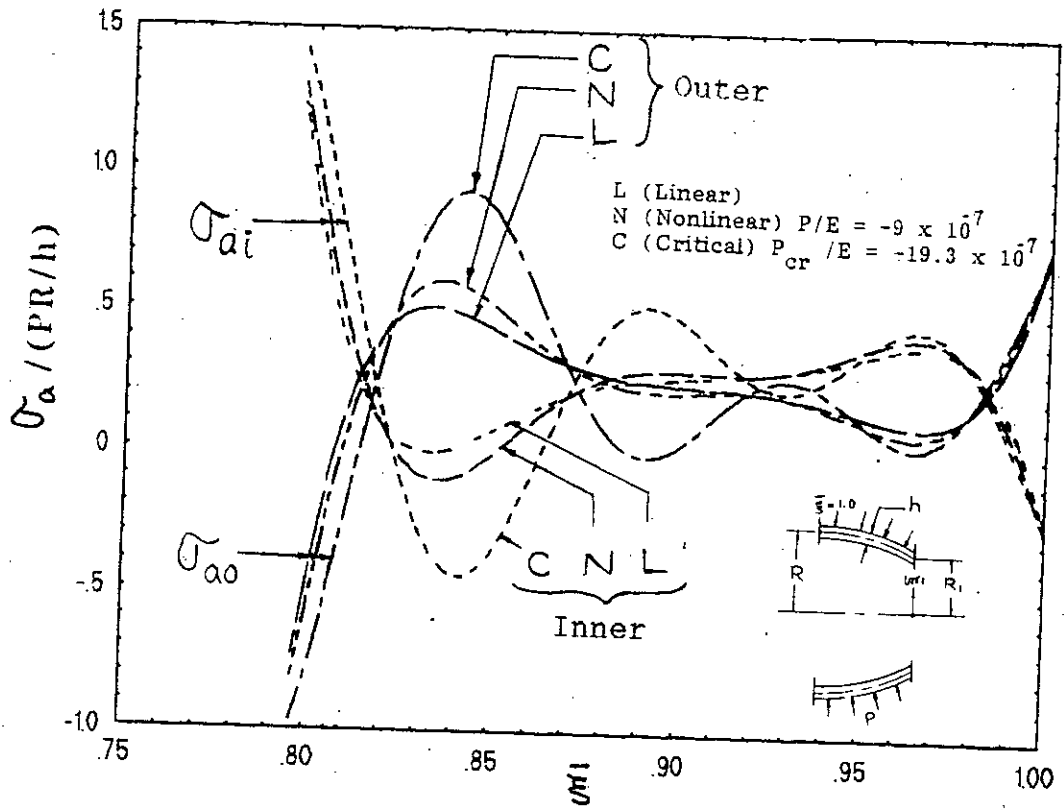


Fig. 13d Meridional stresses (inner and outer fibres) for a Parabolic reducer with $R/h=1000$ and $R_1/R=0.9$

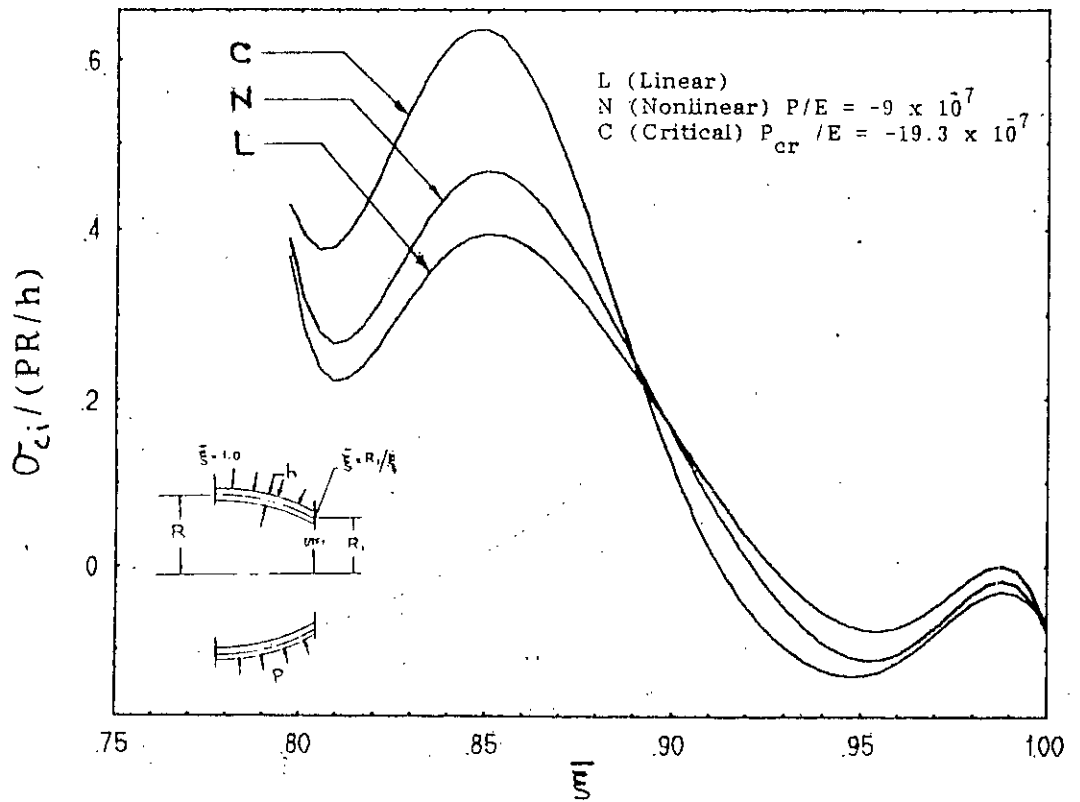


Fig. 13e Circumferential stresses (inner) for a Parabolic reducer with thickness ratio $(R/h)=1000$ and diameter ratio $(R_1/R)=0.9$

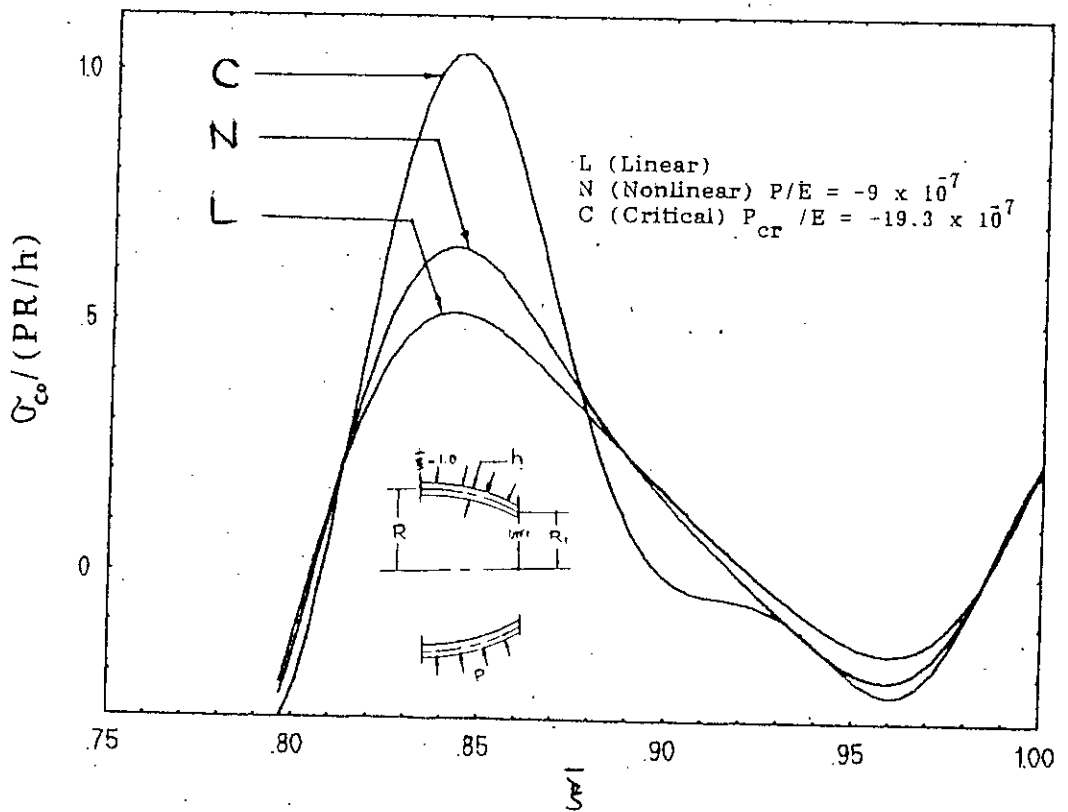


Fig. 13f Circumferential stresses (outer) for a Parabolic reducer with thickness ratio $(R/h)=1000$ and diameter ratio $(R_1/R)=0.9$

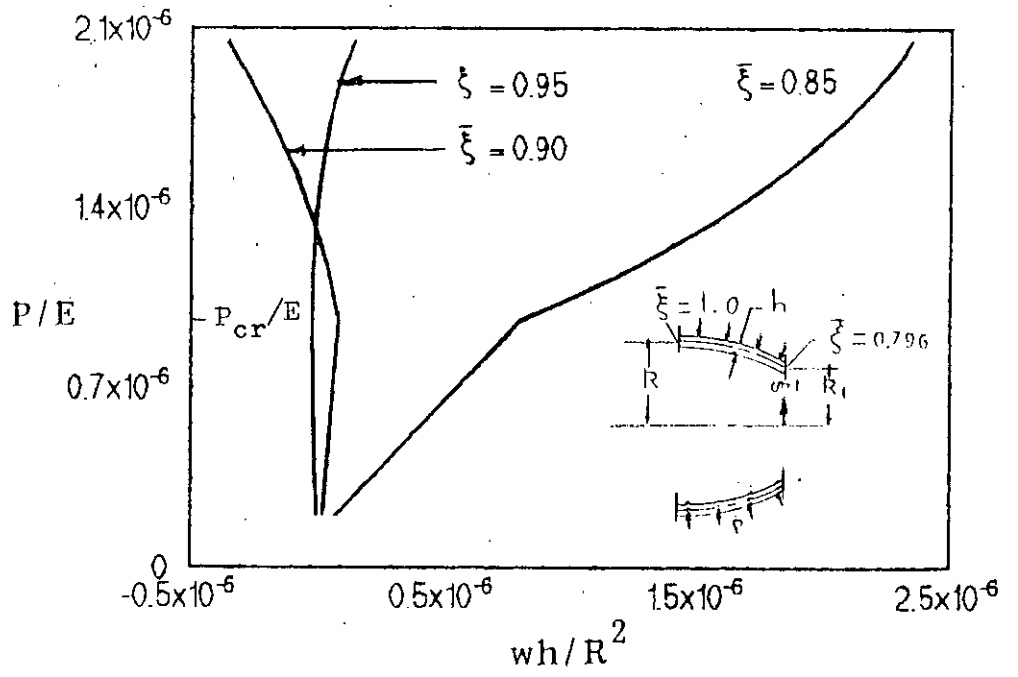


Fig. 14a Axial displacements for SHELL-1590 ($R/h=1500$, $R_1/R=0.9$)

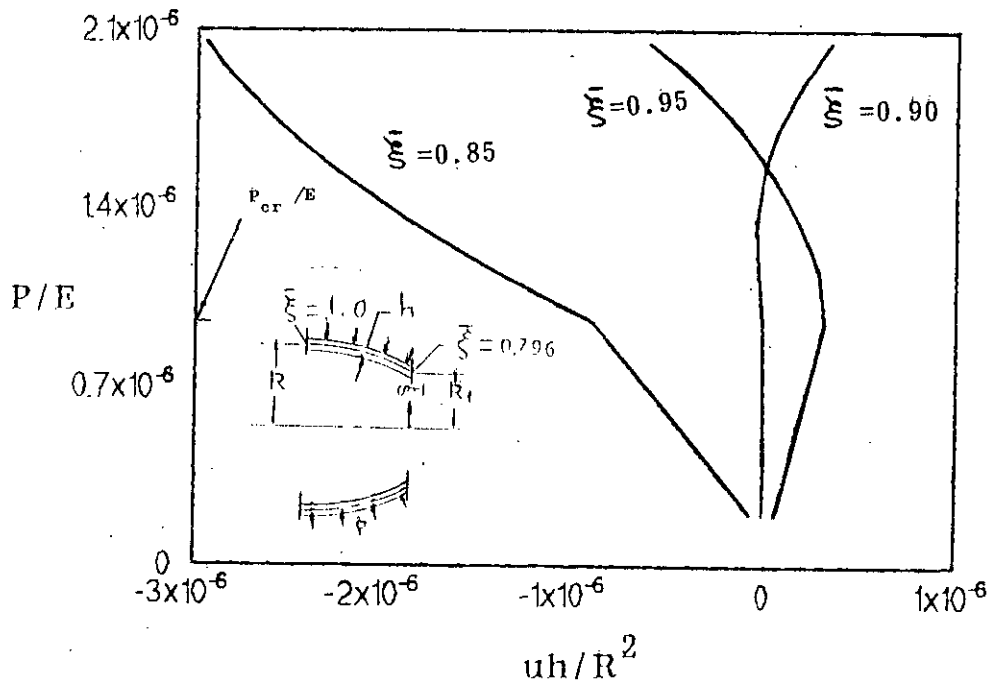


Fig. 14b Radial displacements for SHELL-1590 ($R/h=1500$, $R_1/R=0.9$)

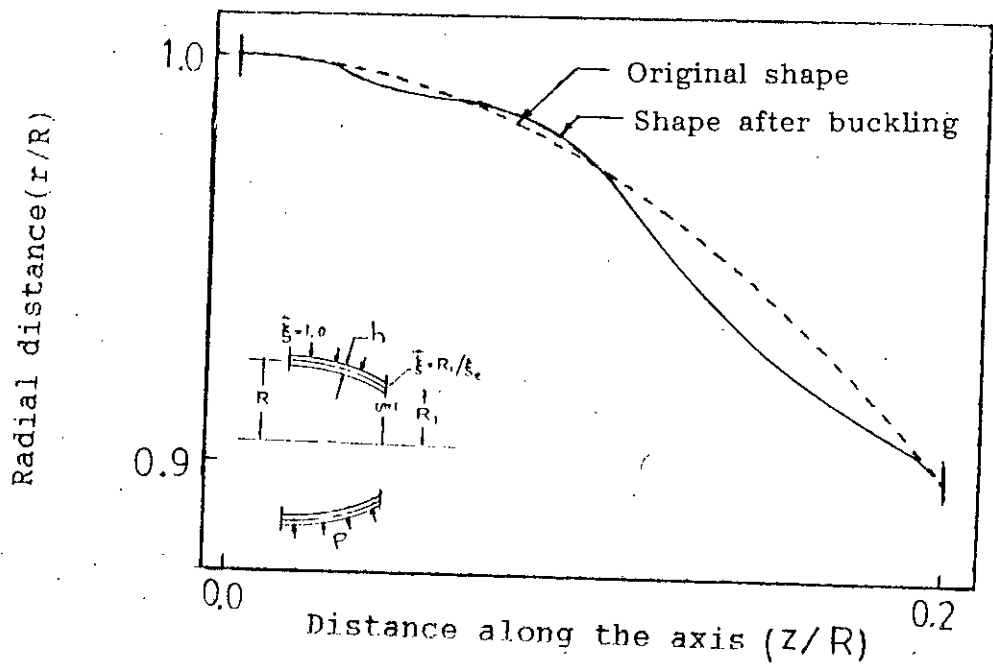


Fig.14c Buckled configuration of SHELL-1590 ($R/h=1500$, $R_1/R=0.9$)

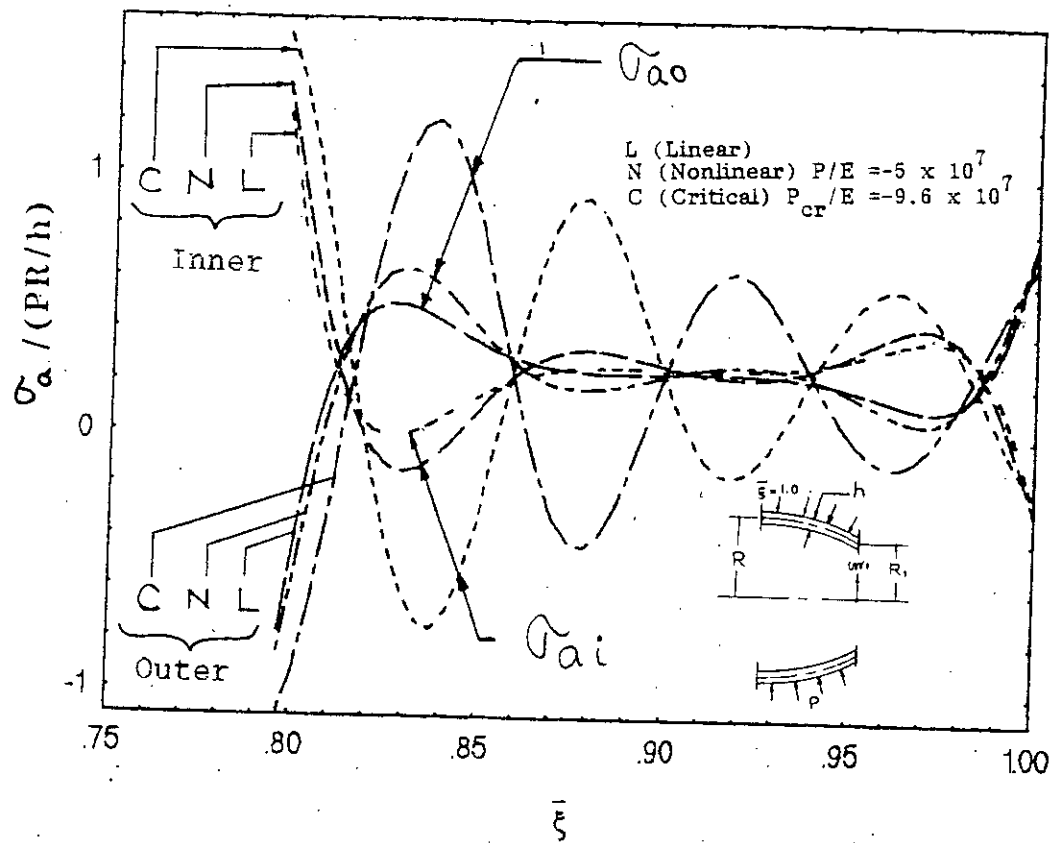


Fig. 14d Meridional stresses (inner and outer fibres) for a parabolic reducer with $R/h=1500$ and $R_1/R=0.9$

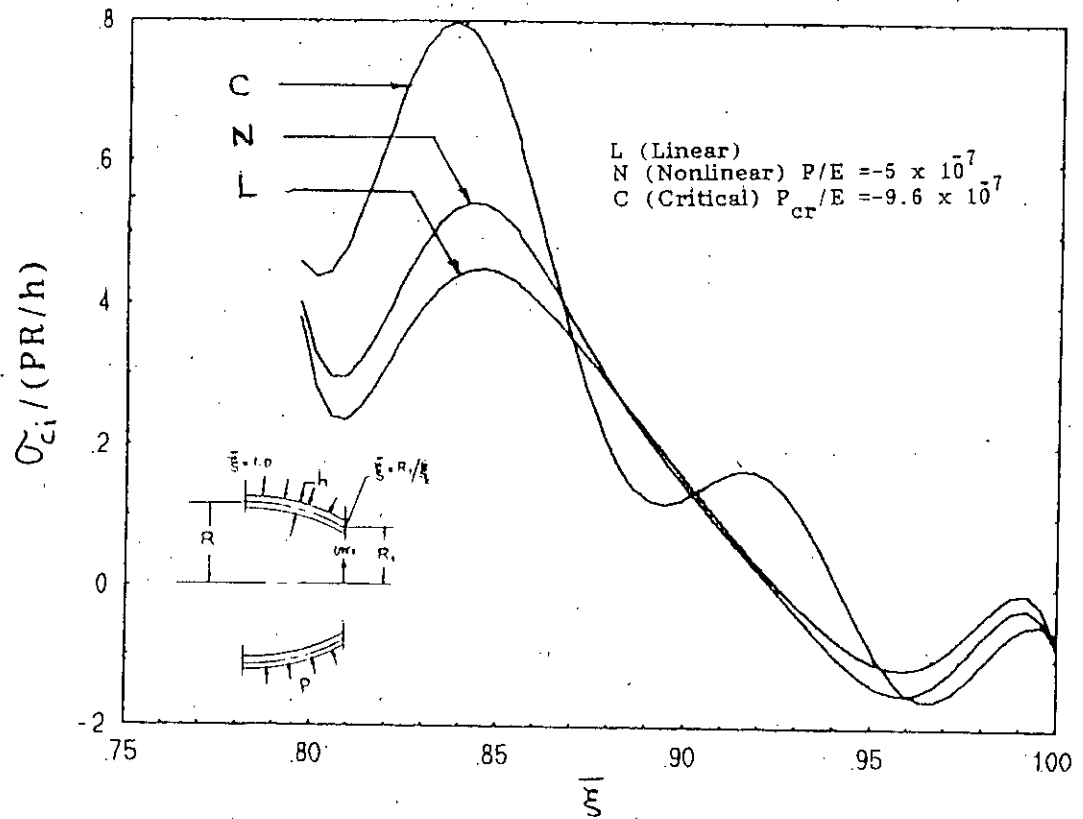


Fig.14e Circumferential stresses (inner) for a Parabolic reducer with thickness ratio $(R/h)=1500$ and diameter ratio $(R_1/R)=0.9$

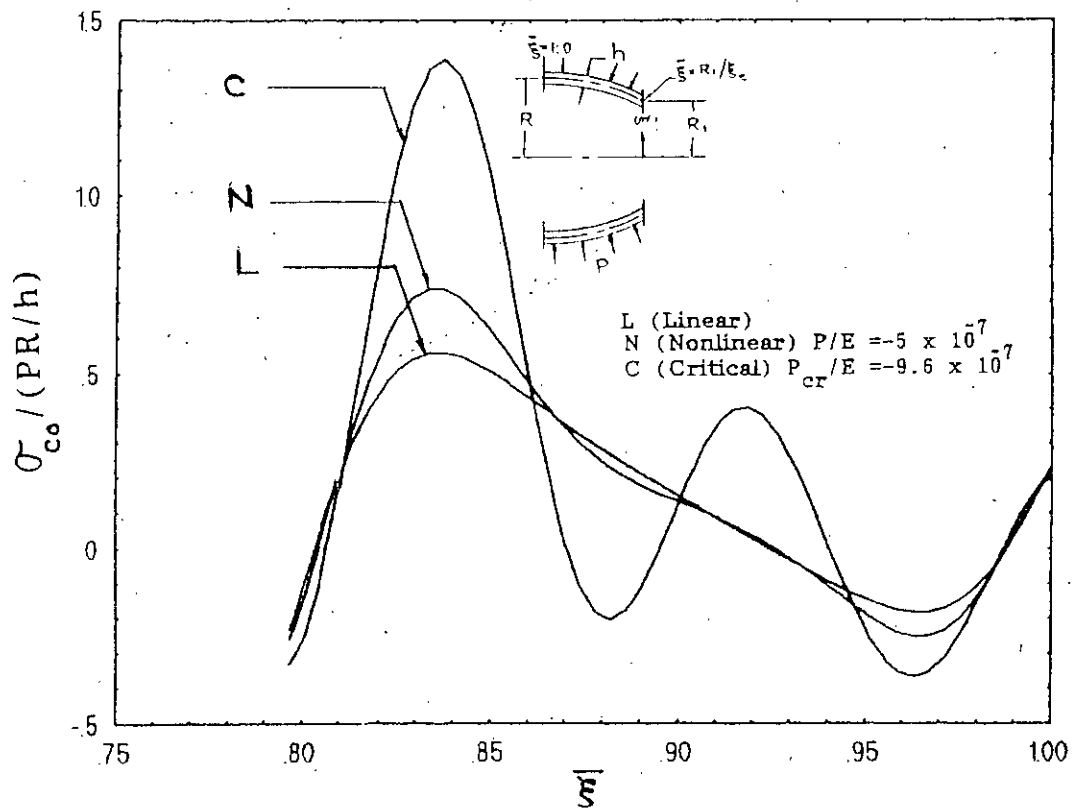


Fig.14f Circumferential stresses (outer) for a Parabolic reducer with thickness ratio $(R/h)=1500$ and diameter ratio $(R_1/R)=0.9$

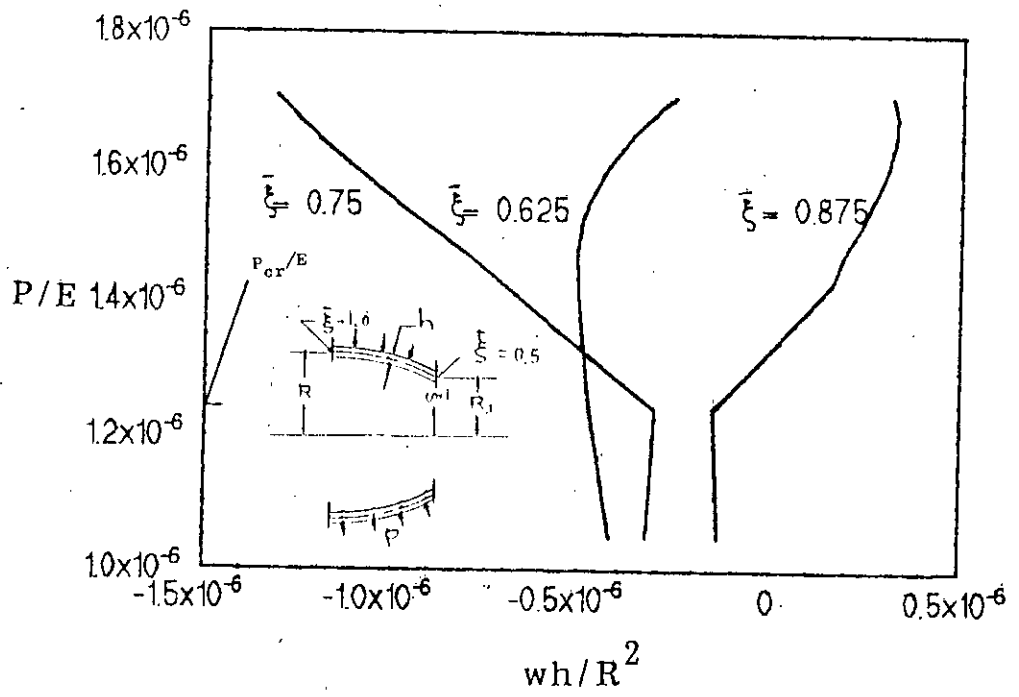


Fig. 15a Axial displacements for SHELL-1070 ($R/h=1000$, $R_1/R=0.7$)

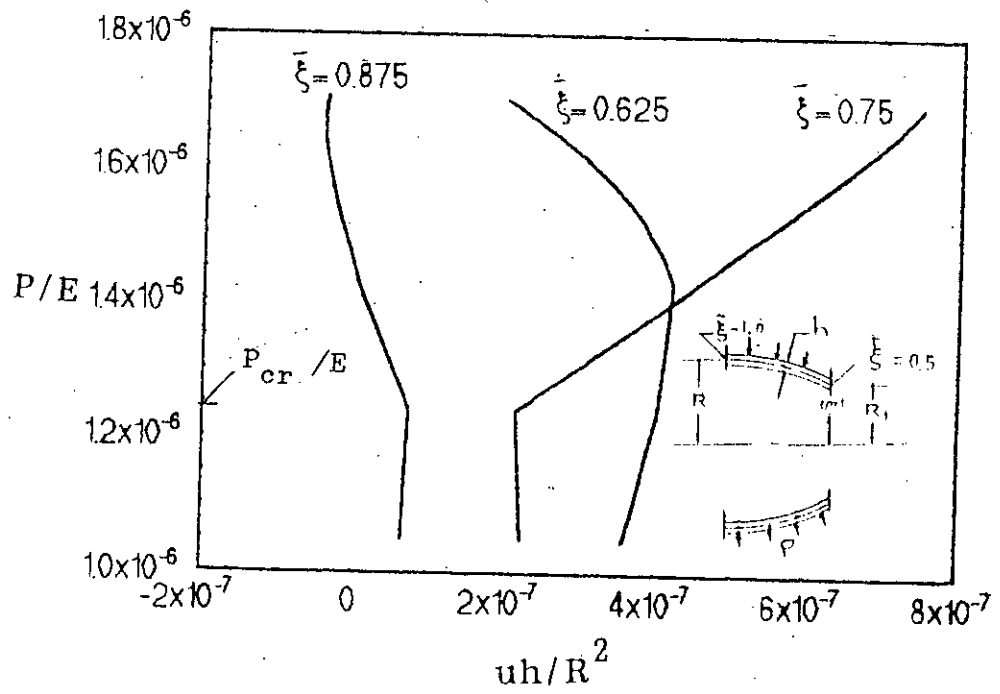


Fig. 15b Radial displacements for SHELL-1070 ($R/h=1000$, $R_1/R=0.7$)

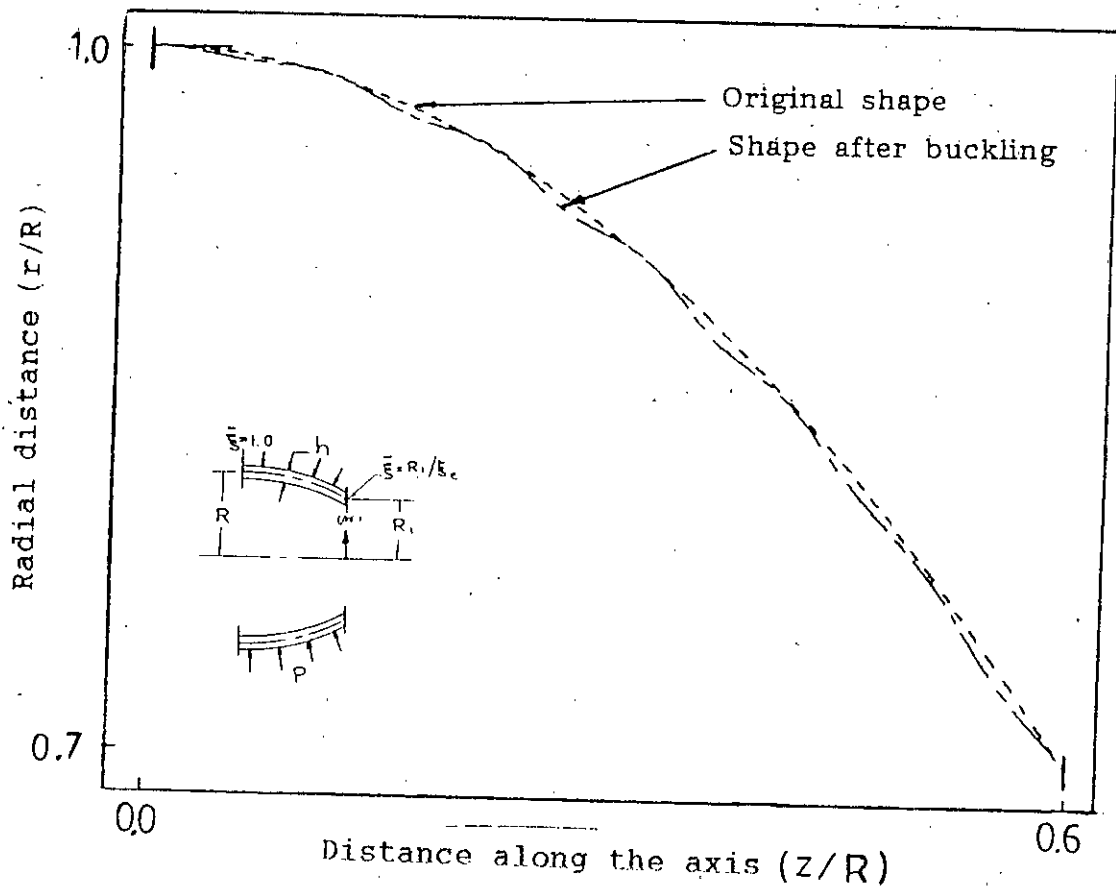


Fig.15c Buckled configuration of SHELL-1070 ($R/h=1000$, $R_1/R=0.7$)

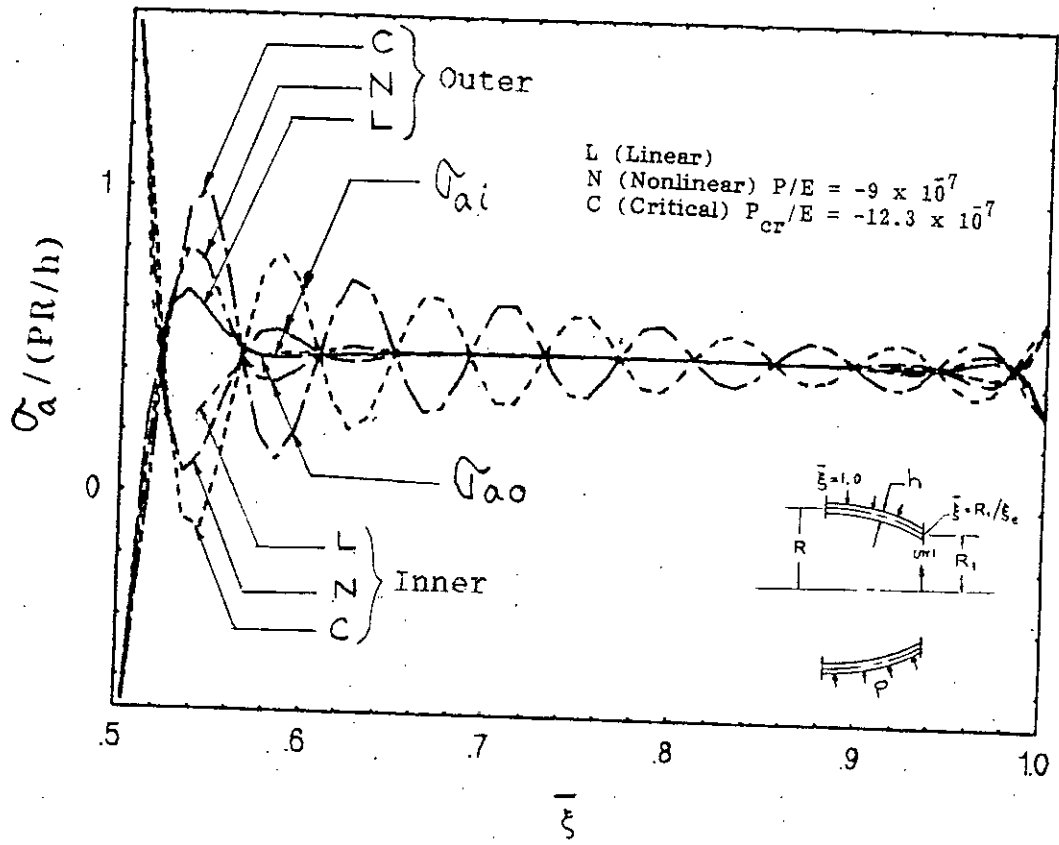


Fig. 15d Meridional stresses (inner and outer fibres) for a Parabolic reducer with $R/h=1000$ and $R_1/R=0.7$

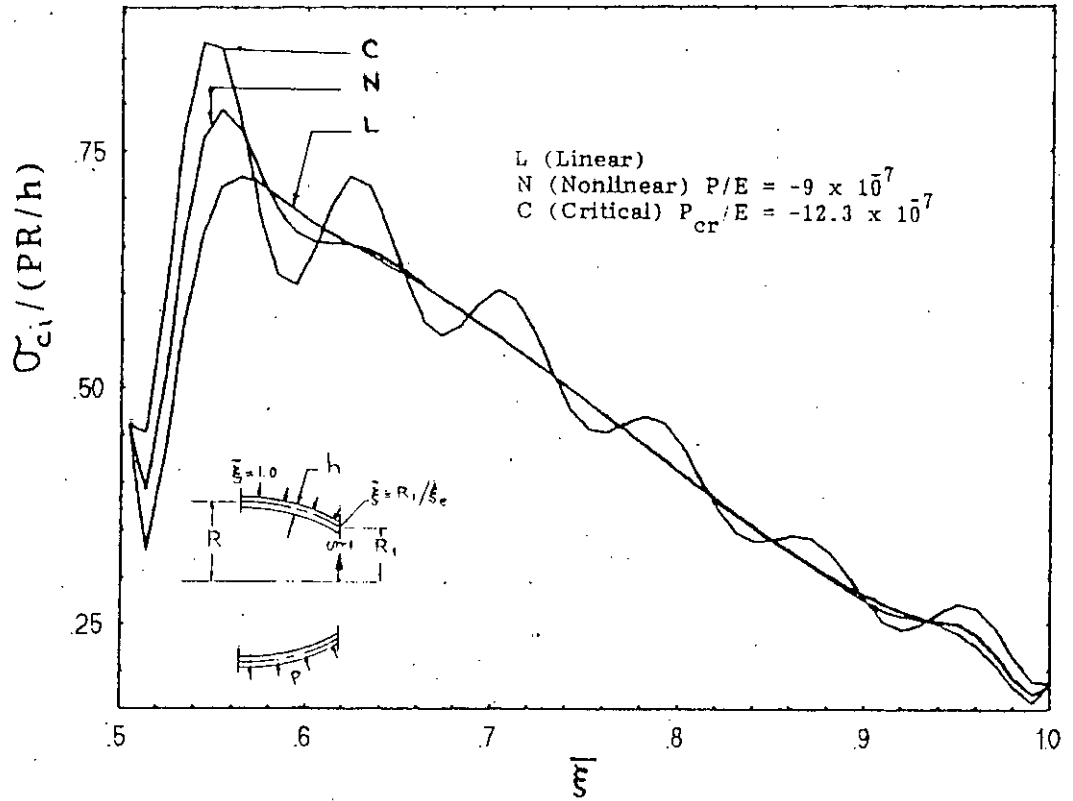


Fig.15e Circumferential stresses (inner) for a Parabolic reducer with thickness ratio $(R/h)=1000$ and diameter ratio $(R_1/R)=0.7$

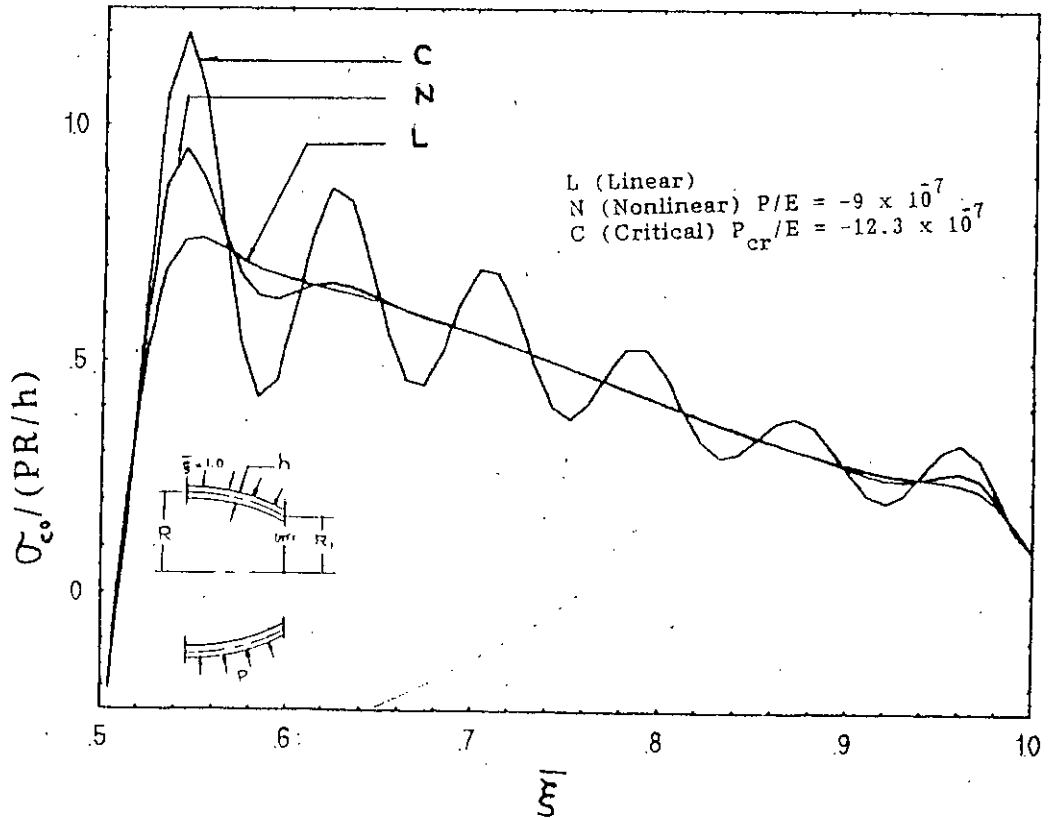


Fig.15f Circumferential stresses (outer) for a Parabolic reducer with thickness ratio $(R/h)=1000$ and diameter ratio $(R_1/R)=0.7$

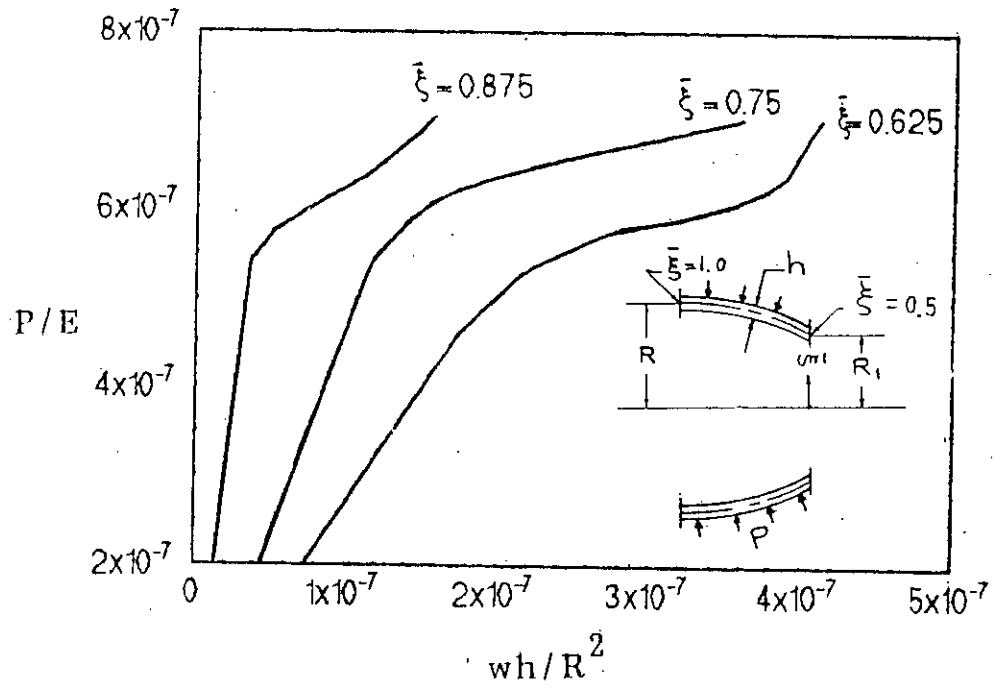


Fig.16a Axial displacements for SHELL-1570 ($R/h=1500$, $R_1/R=0.7$)

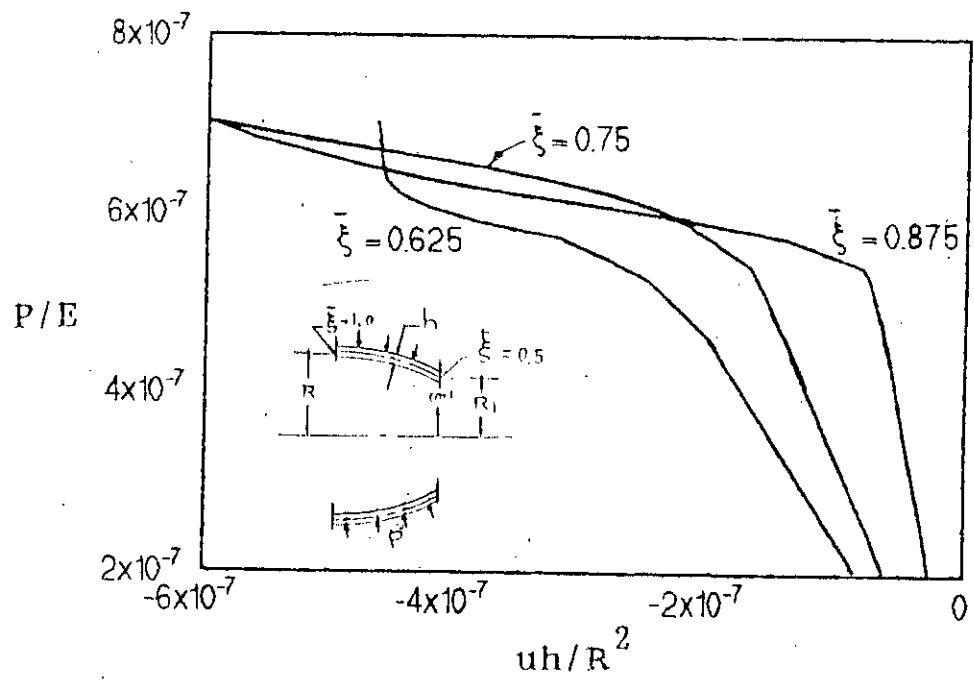


Fig.16b Radial displacements for SHELL-1570 ($R/h=1500$, $R_1/R=0.7$)

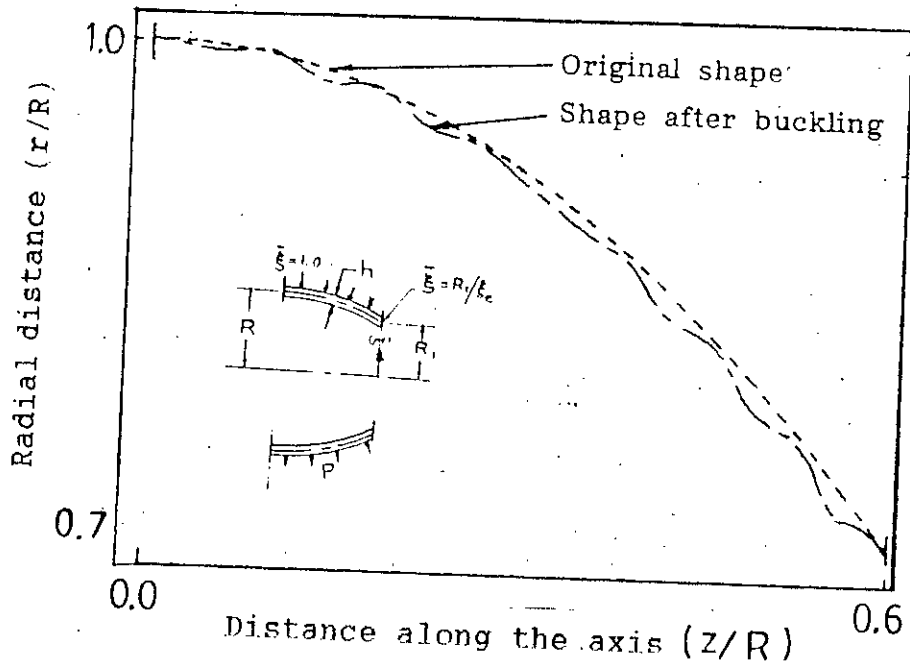


Fig. 16c Buckled configuration of SHELL-1570 ($R/h=1500$, $R_1/R=0.7$)

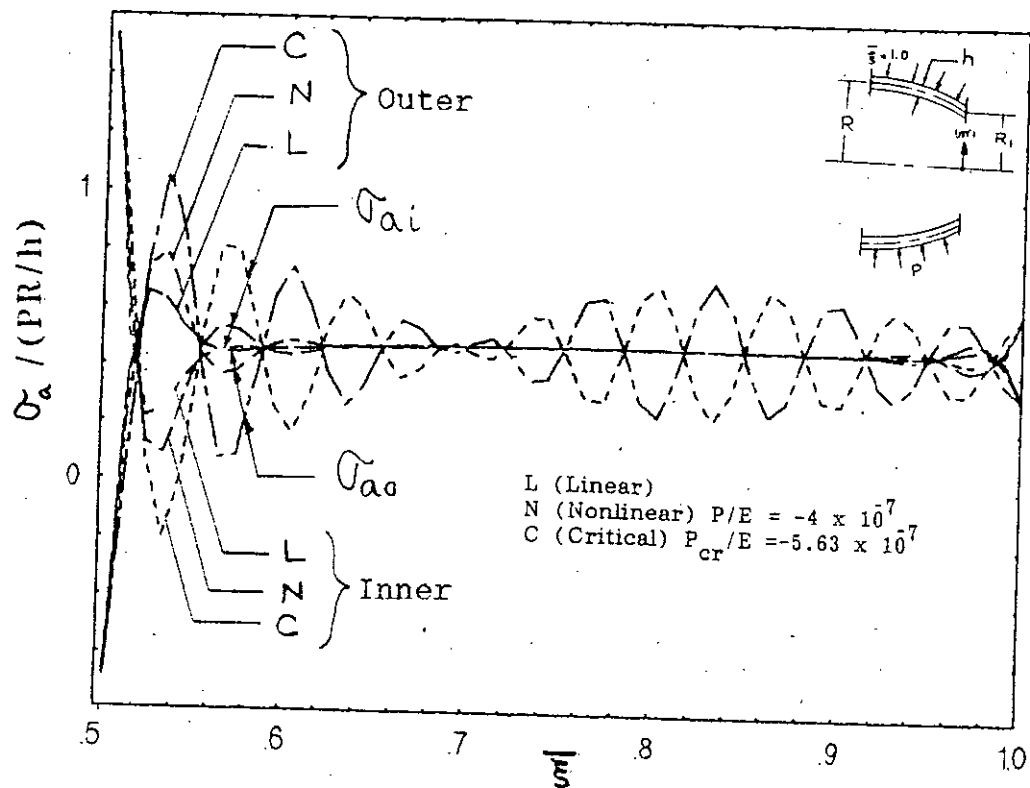


Fig. 16d Meridional stresses (inner and outer fibres) for a Parabolic reducer with $R/h=1500$ and $R_i/R=0.7$

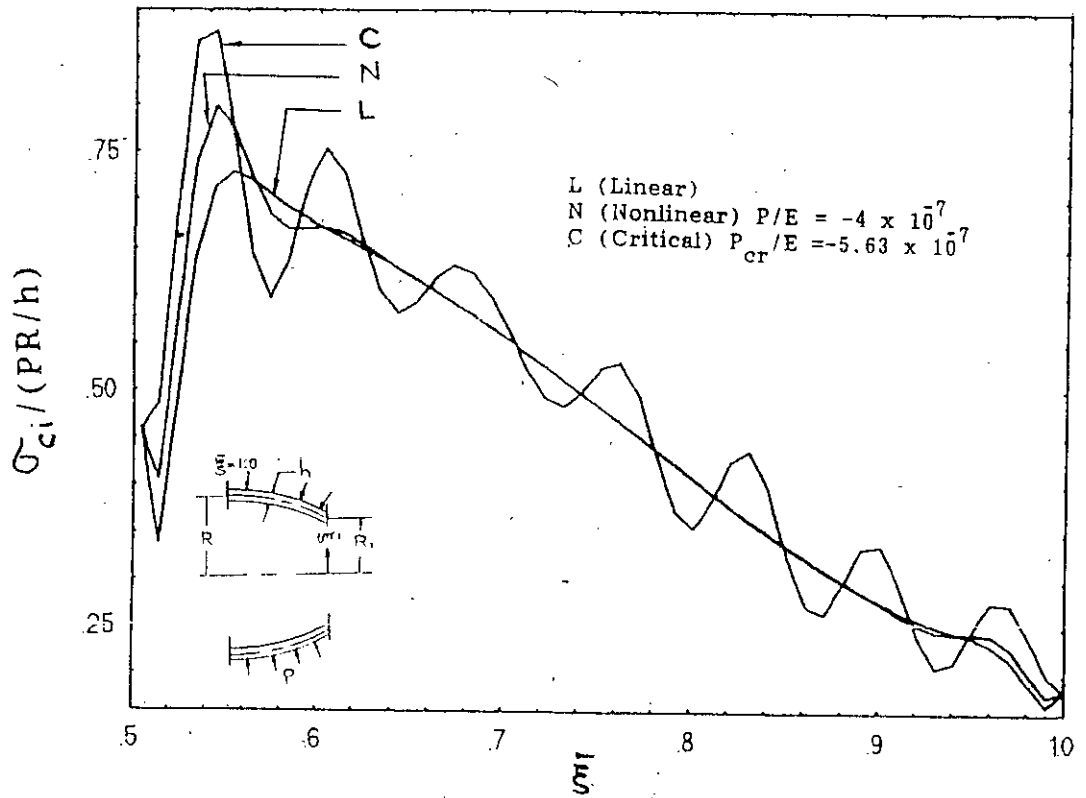


Fig. 16e Circumferential stresses (inner) for a Parabolic reducer with thickness ratio $(R/h)=1500$ and diameter ratio $(R_1/R)=0.7$

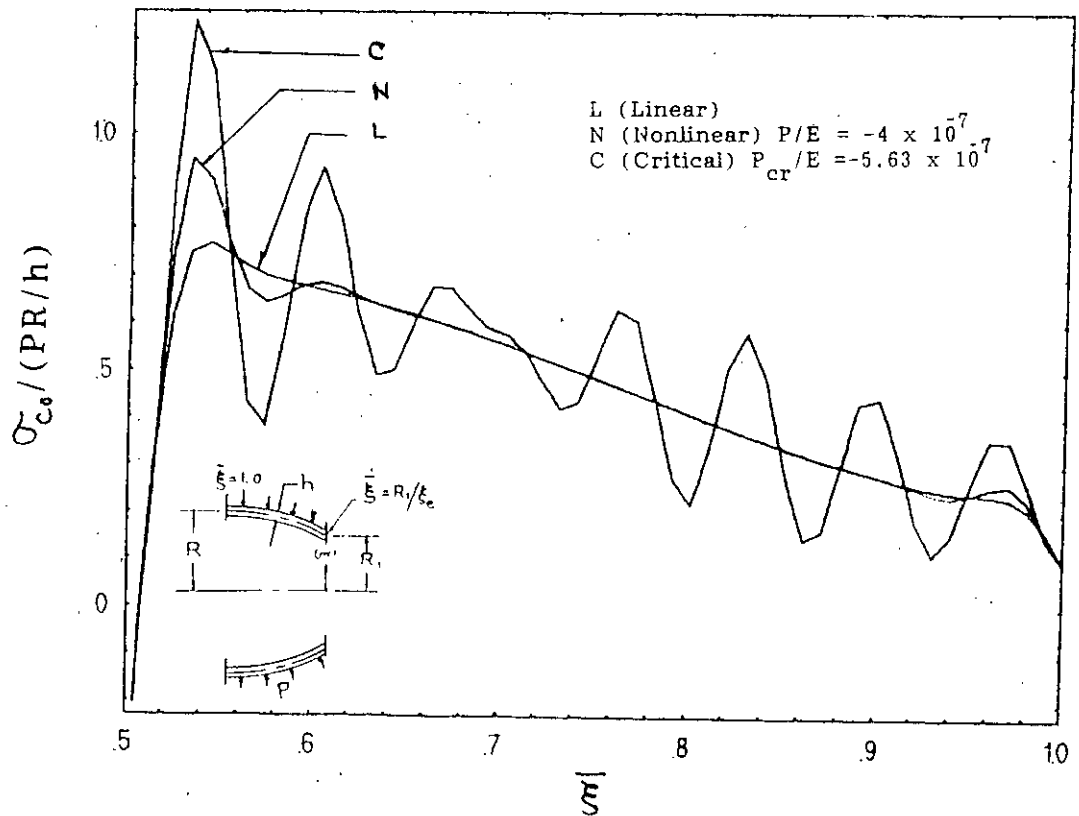


Fig. 16f Circumferential stresses (outer) for a Parabolic reducer with thickness ratio $(R/h)=1500$ and diameter ratio $(R_1/R)=0.7$

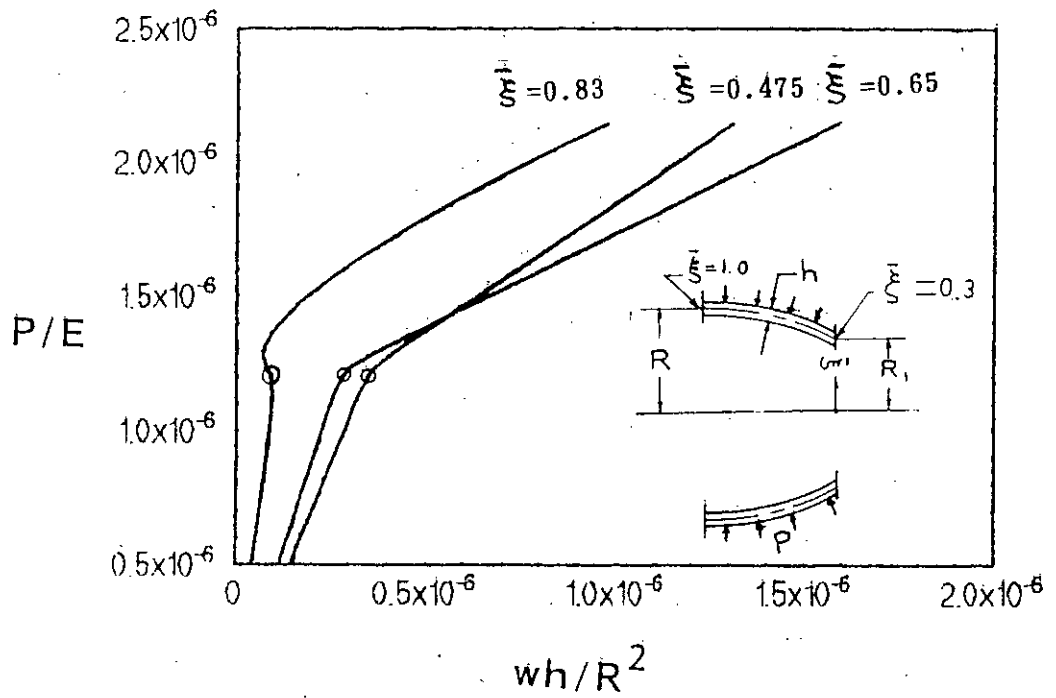


Fig. 17a Axial displacements for SHELL-1050 ($R/h=1000$, $R_1/R=0.5$)

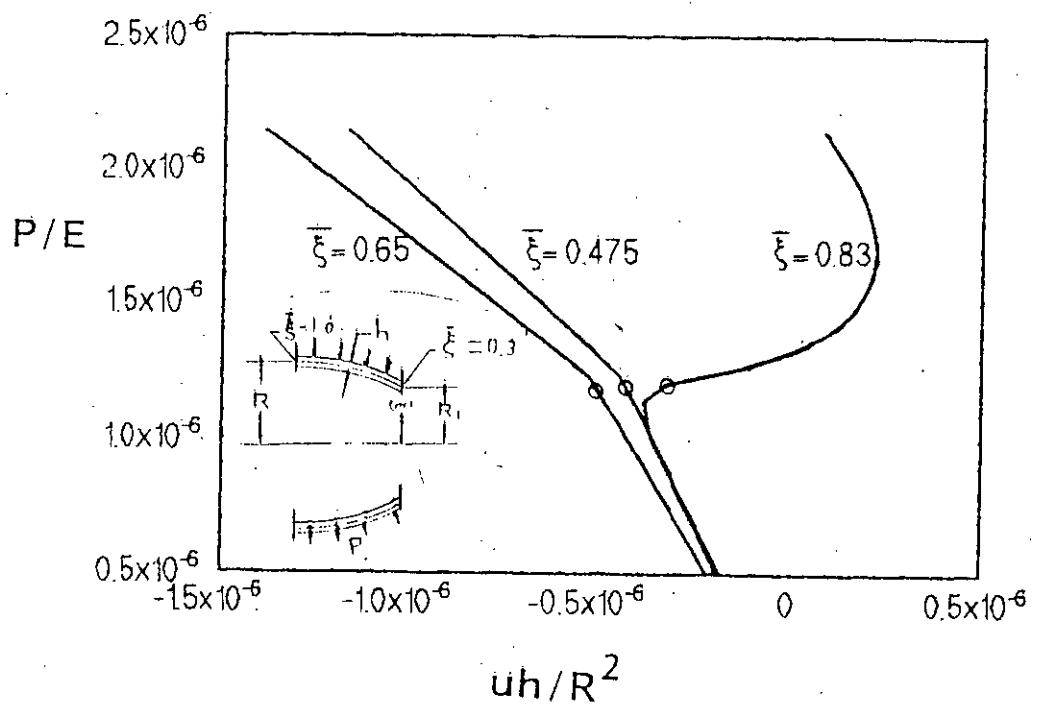


Fig. 17b Radial displacements for SHELL-1050 ($R/h=1000$, $R_1/R=0.5$)

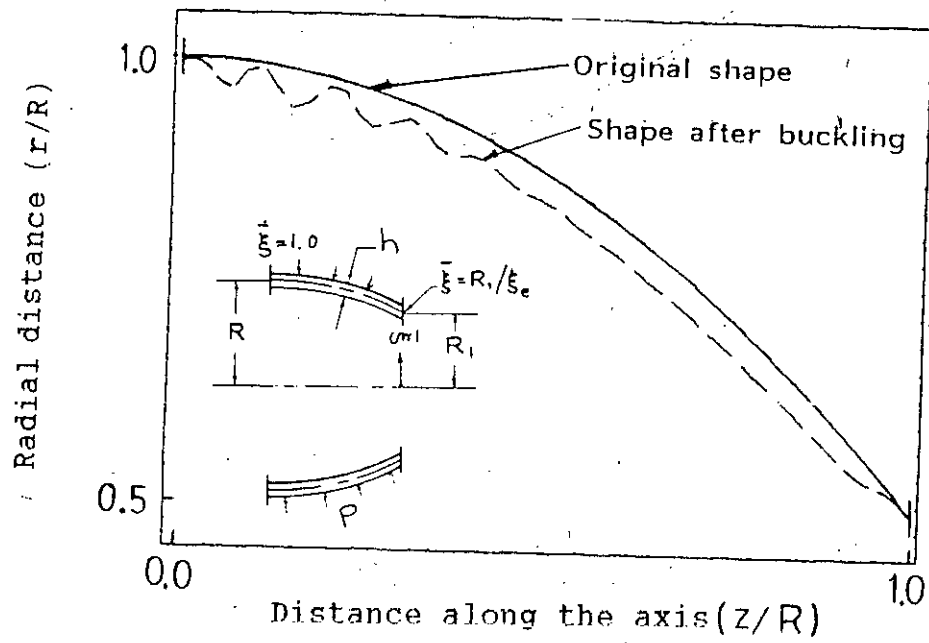


Fig.17c Buckled configuration of SHELL-1050 ($R/h=1000$, $R_1/R=0.5$)

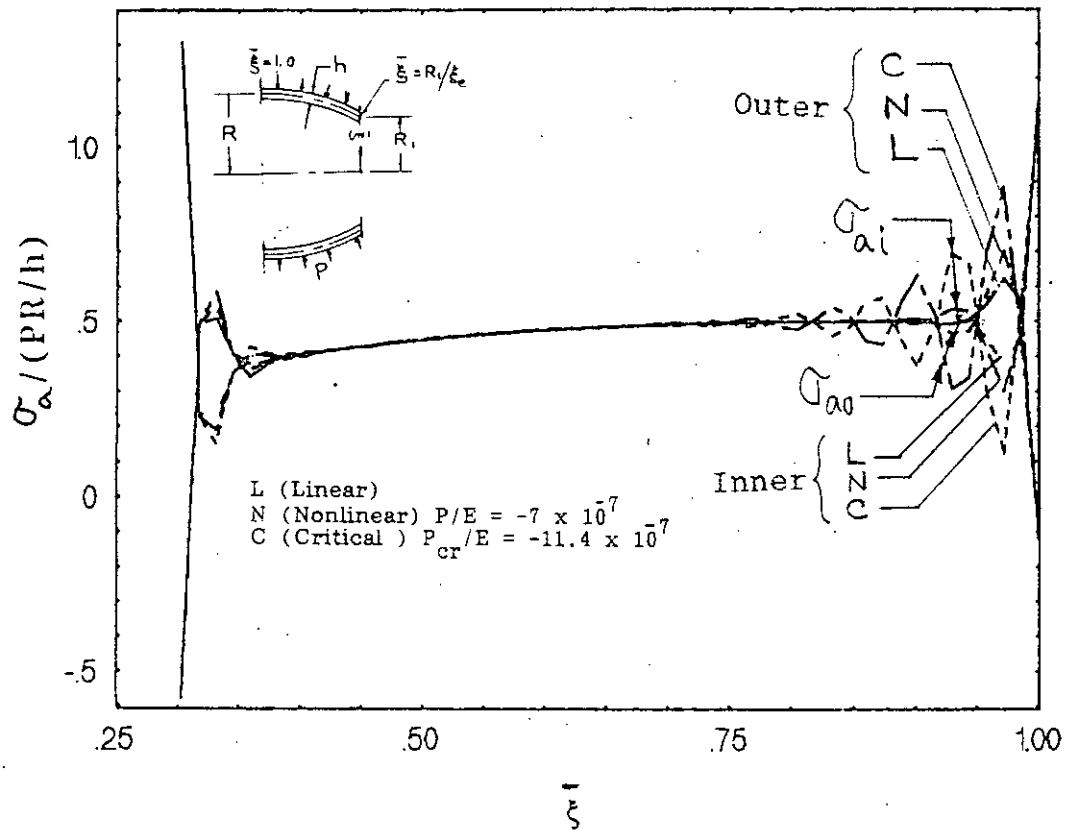


Fig. 17d Meridional stresses (inner and outer fibres) for a Parabolic reducer with $R/h=1000$ and $R_1/R=0.5$

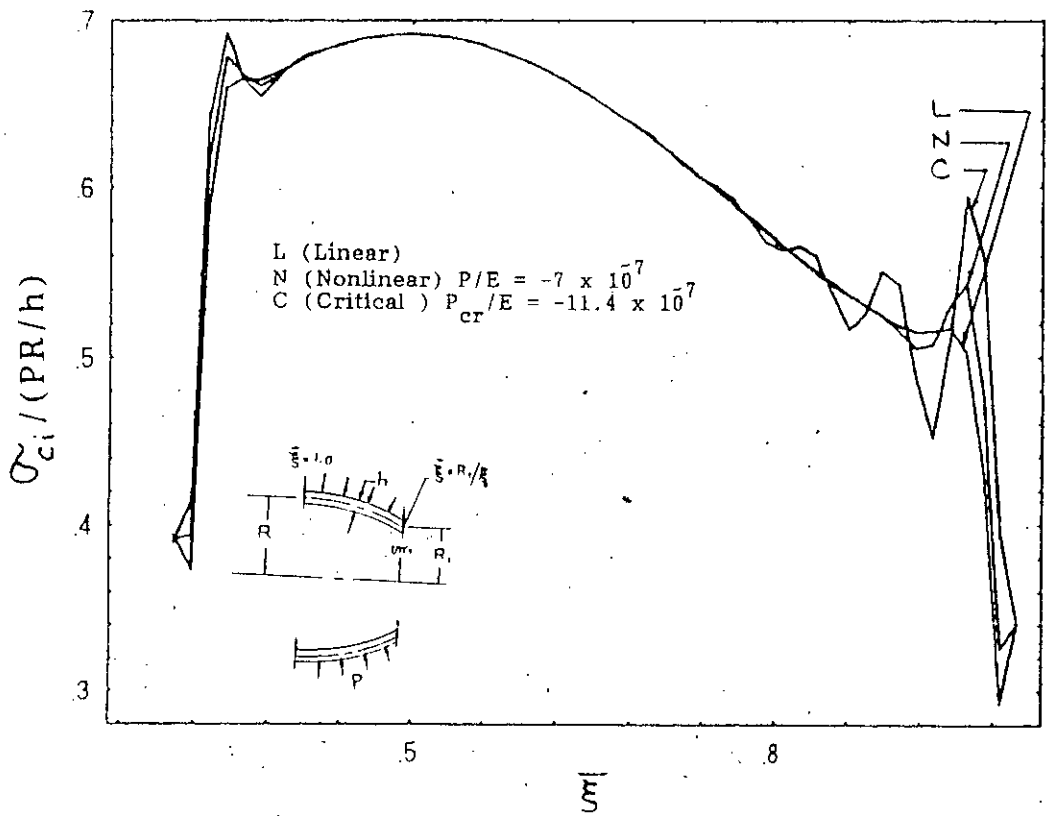


Fig.17e Circumferential stresses (inner) for a Parabolic reducer with thickness ratio $(R/h)=1000$ and diameter ratio $(R_1/R)=0.5$

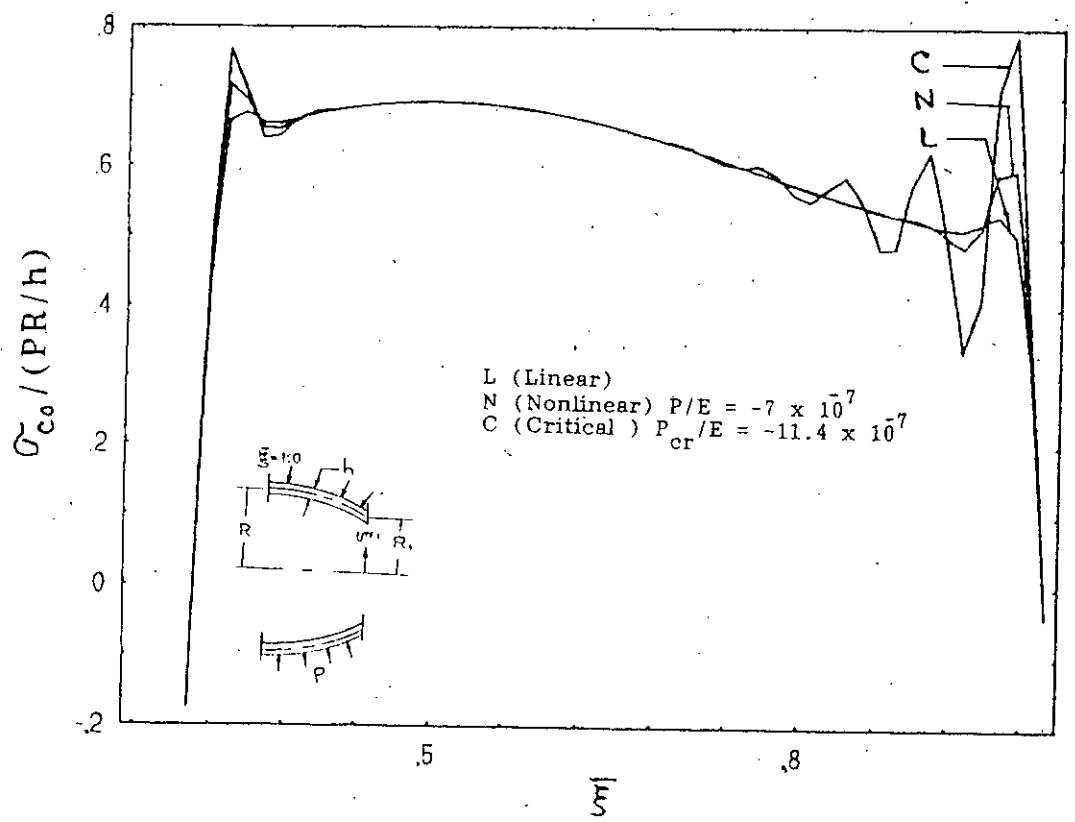


Fig.17f Circumferential stresses (outer) for a Parabolic reducer with thickness ratio $(R/h)=1000$ and diameter ratio $(R_1/R)=0.5$

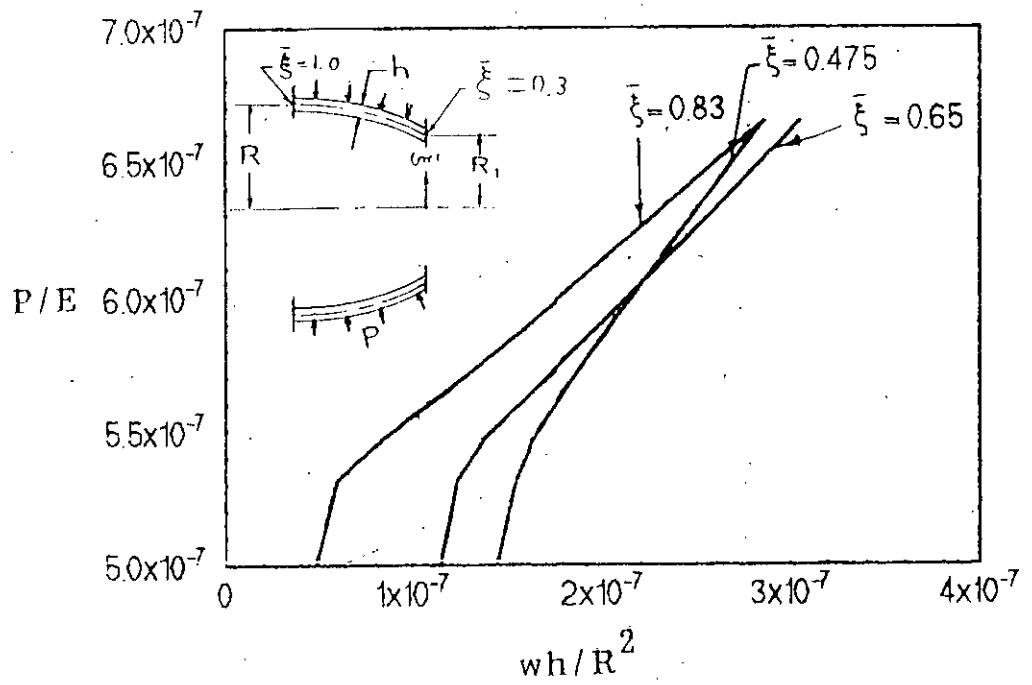


Fig. 18a Axial displacements for SHELL-1550 ($R/h=1500$, $R_1/R=0.5$)

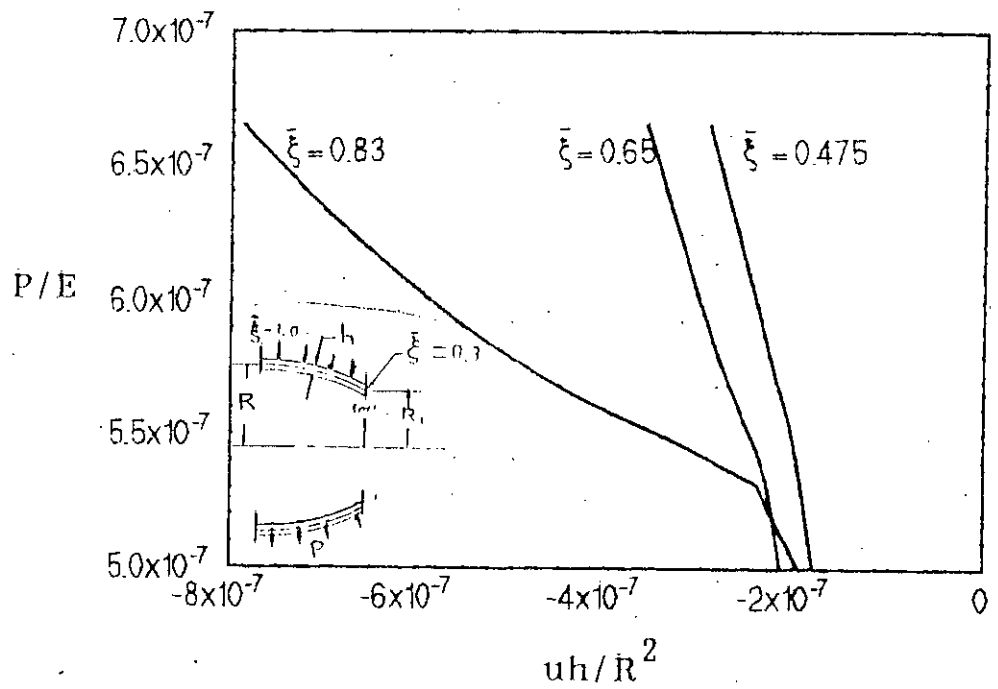


Fig. 18b Radial displacements for SHELL-1550 ($R/h=1500$, $R_1/R=0.5$)

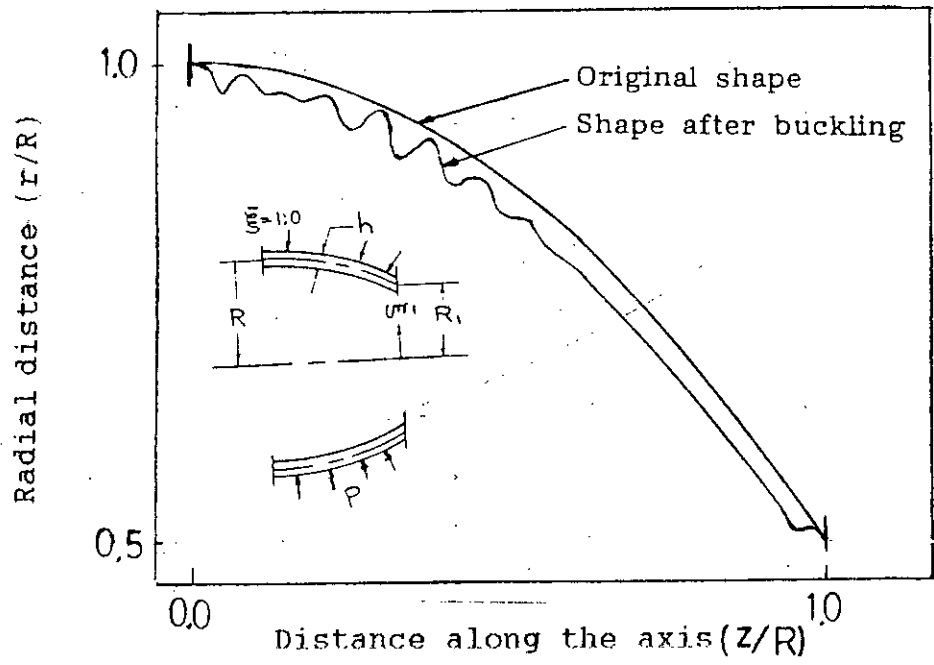


Fig.18c Buckled configuration of SHELL-1550 ($R/h=1500$, $R_1/R=0.5$)

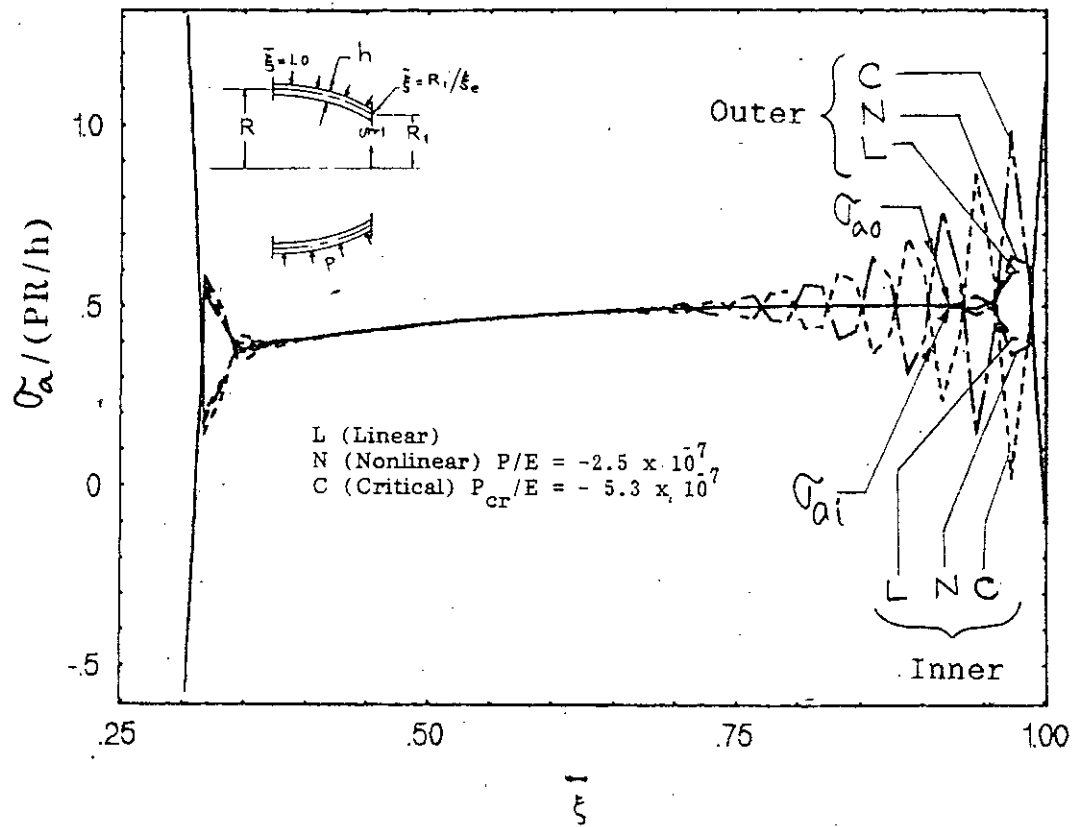


Fig. 18d Meridional stresses (inner and outer fibres) for a parabolic reducer with $R/h=1500$ and $R_1/R=0.5$

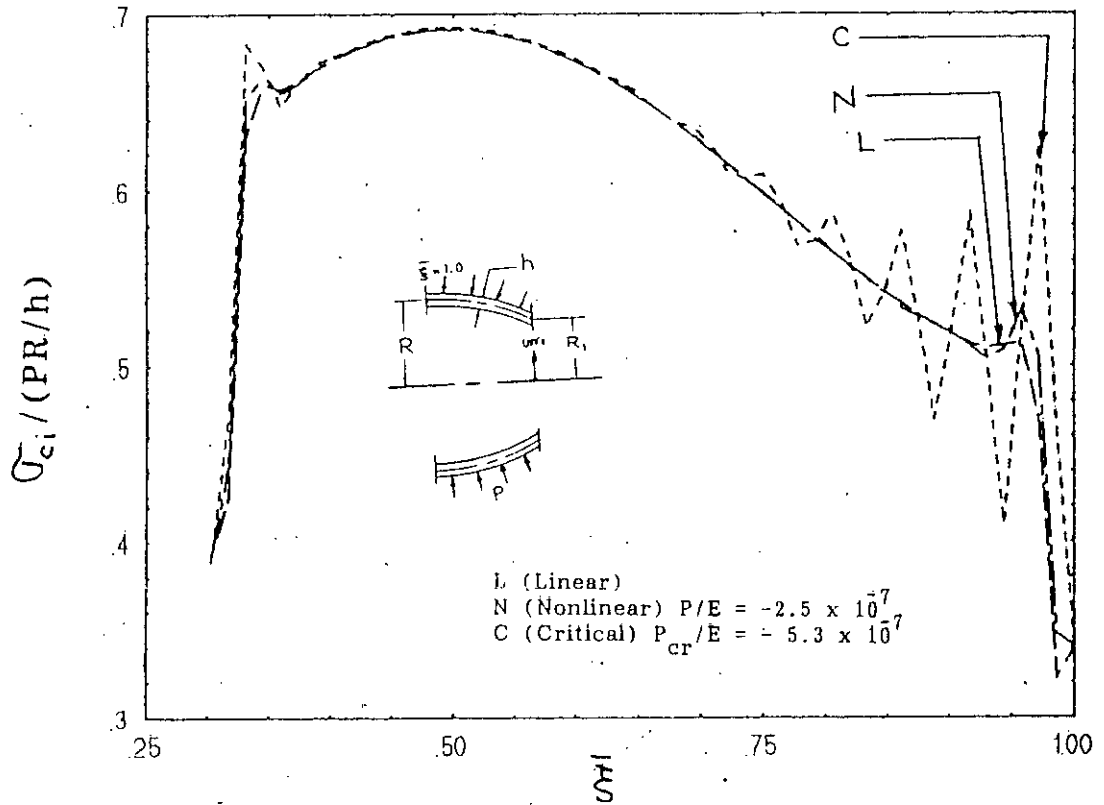


Fig. 18e Circumferential stresses (inner) for a Parabolic reducer with thickness ratio $(R/h)=1500$ and diameter ratio $(R_1/R)=0.5$

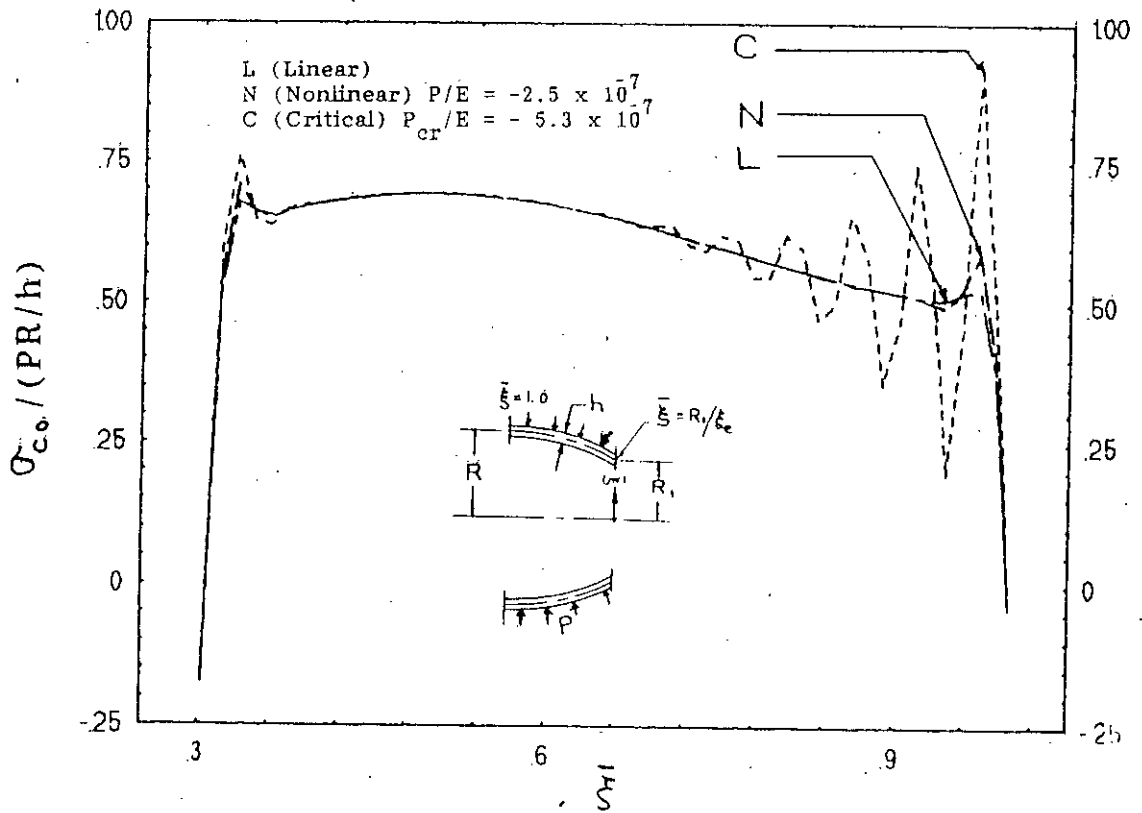


Fig. 18f Circumferential stresses (outer) for a Parabolic reducer with thickness ratio $(R/h)=1500$ and diameter ratio $(R_1/R)=0.5$

APPENDIX - A

PROGRAMMING FEATURES

A.1 GENERAL FEATURES

The computer program used in the present investigation is adopted from that of Uddin [95] with necessary modifications to suit the requirements of solving stability problems of truncated parabolic shell elements under uniform external pressure. The program is based on Reissner's nonlinear theory of axisymmetric deformation of shells of revolution [69] while the multisegment method of integration developed by Kalnins and Lestingi [37] takes care of solving the governing equations and the integration process is carried out by a predictor-corrector method. The predictor and corrector are given, respectively, by formulas (19.16) and (19.17) of Ref. 49. To secure the six starting values necessary for the application of this pair of predictor and corrector, the six-point formulas (19.10-19.14) of Ref. 49 are being used. It should be noted here that all these formulas contain an error of the order of H^7 where H is the distance between two consecutive computational points, and, thus, they are highly sophisticated.

The shell meridian is divided into eleven computational points. The program first prints out the values of the fundamental variables (\bar{u} , $\bar{\beta}$, \bar{w} , \bar{V} , \bar{H} , \bar{M}_ξ) based on linear theory which is followed by the print-out of nonlinear results for the same loading parameter. From here on, the program will produce nonlinear results for increasing loading steps.

The program also prints out detail results in terms of radial displacement \bar{u} , axial displacement \bar{w} , circumferential moment \bar{M}_θ , meridional moment \bar{M}_ξ , circumferential stress resultant \bar{N}_θ , meridional stress resultant \bar{N}_ξ , circumferential stress at the inner surface $\sigma_{ci}/(PR/h)$, circumferential stress at the outer surface $\sigma_{co}/(PR/h)$, meridional stress at inner surface $\sigma_{ai}/(PR/h)$, and meridional stress at the outer surface $\sigma_{ao}/(PR/h)$ in that order, columnwise.

A.2 TREATMENT OF BOUNDARY CONDITIONS

Equations (4.13a) written in terms of normalized fundamental variables and in accordance with the statement of Eqs. (3.7c) appear as

$$\begin{bmatrix} 1 & 0 & 0 & 0 & 0 & 0 \\ 0 & 1 & 0 & 0 & 0 & 0 \\ 0 & 0 & 1 & 0 & 0 & 0 \\ 0 & 0 & 0 & 1 & 0 & 0 \\ 0 & 0 & 0 & 0 & 1 & 0 \\ 0 & 0 & 0 & 0 & 0 & 1 \end{bmatrix} \begin{bmatrix} \bar{u} \\ \bar{\beta} \\ \bar{w} \\ \bar{V} \\ \bar{H} \\ \bar{M}_\xi \end{bmatrix} = \begin{bmatrix} \bar{u} \\ \bar{\beta} \\ \bar{w} \\ \bar{V} \\ \bar{H} \\ \bar{M}_\xi \end{bmatrix} \quad (\text{A-1})$$

In the matrix Eqs. (A-1) the elements of the column matrix on the left hand side remain in the same order, whereas, those on the right hand side should be arranged in such a manner that the three prescribed elements at the boundary become the first three elements of this column matrix. According to Eqs. (3.7c), if \bar{u} is specified at the boundary, the first and the 5th rows of the unit-matrix of (A-1) remain the same, while specification of \bar{H} at the boundary will require the interchange of these two rows which will interchange \bar{u} and \bar{H} in the column matrix on the right hand side. Similarly, if $\bar{\beta}$ is specified at the boundary, the

second and the last rows remain as they are, and interchanged when \bar{M}_ξ is specified. Lastly, the third and the fourth rows of the unit-matrix are kept the same or interchanged depending on whether \bar{w} or \bar{V} is specified at the boundary. The same operation is carried out for both the boundary points. The transformed unit matrices of (A-1) are then designated by T_1 at the starting boundary and by T_{M+1} at the finishing boundary.

A.3 ON THE USE OF THE PROGRAM

In order to use the program for obtaining solutions of different problems the knowledge of the definitions of input and output variables is essential. Therefore these variables with their definitions are given in the table at the end of Appendix A.

In part A of the program the necessary information required for the solution of a problem is read in. The first three 'READ' statements read the initial values of the loading parameter 'EM', the value of incremental step of the loading parameter 'EM1', the number to which the shell meridian will have to be divided 'M', Poisson ratio of the shell material 'AN', the number of loading steps 'SOBI', radius-thickness ratio 'T', and the diameter ratio 'XL'. The next 'READ' statement reads the arbitrary given values of the independent variable $X(J,1)$ and the initial values of the six fundamental variables $X(J,I)$, ($I=2,7$), for nodal points J , ($J = 1, M+1$). The value of the independent variable is later on adjusted based on the diameter ratio 'XL'. The boundary values for any three of the six fundamental variables at the starting boundary are accepted by the fifth 'READ'

statement. In case of the present analysis of clamped ends parabolic reducers, the prescribed boundary conditions are:

$$\begin{aligned} \text{XX (1,1)} &= \bar{u} = 0.0 \\ \text{XX (2,1)} &= \bar{\beta} = 0.0 \\ \text{XX (3,1)} &= \bar{w} = 0.0 \end{aligned}$$

The sixth 'READ' statement reads in the three prescribed boundary conditions at the final boundary. For the present analysis, these three boundary conditions are:

$$\begin{aligned} \text{XY (1,1)} &= \bar{w} = 0.0 \\ \text{XY (2,1)} &= \bar{u} = 0.0 \\ \text{XY (3,1)} &= \bar{\beta} = 0.0 \end{aligned}$$

The values of the boundary conditions indicators at the starting are read in by the seventh 'READ' statement. The appropriate values of the indicators 'IS1', 'IS2', and 'IS3' are given in the following table:

Specified quantity	Indicator and its value
\bar{u}	IS1 = 0
$\bar{\beta}$	IS2 = 0
\bar{w}	IS3 = 0
\bar{V}	IS3 = 1
\bar{H}	IS1 = 1
\bar{M}_F	IS2 = 1

The eighth and the last 'READ' statement accepts the boundary condition indicators at the final boundary. Their appropriate value are given in the above table where the quantities 'IS1', 'IS2', and 'IS3' should be replaced by 'IF1', 'IF2', and 'IF3', respectively. In the initialization block of part A of the program, certain quantities are initialized and certain fixed parameter of the shell are calculated.

Part B of the program deals with the problem of adjusting the given boundary conditions with regard to the solutions of the matrix equations. Part C of the program concerns with the calculation of normalized constants involving shell parameters, material constants, and loading. Under part D of the program the output of the results is handled. The remaining portion of the program deals with the integration of different systems of differential equations and the solution of matrix equations.

A.4 OUTPUT OF THE PROGRAM

The first output will be the given initial nodal values of the independent variable $\bar{\xi}$ and the six fundamental variables \bar{u} , $\bar{\beta}$, \bar{w} , \bar{V} , \bar{H} and \bar{M}_ξ , in their written order column wise, and in tabular form. The first output will also accompany the various input parameters and indices. The second output gives the value of number of pass, residue- the sum of the differences of the absolute values of the fundamental variables at the nodal points of the two recent consecutive passes, and the present value of the normalized load.

The first output is then repeated for solution based on linear theory. The next output presents the details of the solution based on the linear theory. Here the

following quantities are printed out in tabular form and in the order of $\bar{\xi}$, \bar{u} , \bar{w} , \bar{M}_θ , \bar{M}_ξ , \bar{N}_θ , \bar{N}_ξ , $\sigma_{ci}/(PR/h)$, $\sigma_{co}/(PR/h)$, $\sigma_{ai}/(PR/h)$, $\sigma_{ao}/(PR/h)$ column wise. For each segment these quantities are printed out at six equidistant points. This can be changed to twenty-one or eleven points by simply changing the increment of the loop parameter of part D of the program that handles the output of results. With the results of first linear output, the linear solution is repeated once again to get better solution. After the print-out of the second linear solution, there will be repetition of the second and first out-put (now based on nonlinear theory) for a number of times until the solution converges. When convergence is attained the details of the nonlinear solution will be printed out. The solution at the nodal points are printed out twice, first-based on the initial value integration and second-based on the solution of matrix equations, to check the accuracy of the results.

From this point onward the nonlinear solutions will be repeatedly printed out for increasing loadings.

The output files 'AX', 'RD' and 'SHAPE' are opened additionally for the convenience of plotting the load-deflection curves and the deformed shell meridian. The first column of the output file 'AX' prints out the absolute value of the loading parameter (P/E) while the rest of the columns print out the axial displacements (wh/R^2) for the nodal points along the shell meridian. Similarly, the output file 'RD' prints out the radial displacements (uh/R^2). In the output file 'SHAPE' the first and the third columns print out the points along the shell axis while the second and the fourth columns print out the corresponding points along the shell meridian before and after deformation for the increasing values of the loading parameter.

A.5 TABLE OF INPUT-OUTPUT VARIABLES OF THE PROGRAM

Variable	Definition
EM	EM = P/E, Normalized load
EM1	Increasing step of EM
FOC	$a/(R-R_1)$, FOC=1 for the present analysis
SOB1	Number of desired loading step
M	Number of segments
PH(I)	Meridional angle at the nodal point I
RC	Constant $\bar{R} = \xi_e/R$
AN	Poisson's ratio ν
XL	R_1/R , Diameter ratio
TK	R/h , thickness ratio
X(1,I)	$\bar{\xi}$ at the nodal point I
X(2,I)	\bar{u} at the nodal point I
X(3,I)	$\bar{\beta}$ at the nodal point I
X(4,I)	\bar{w} at the nodal point I
X(5,I)	\bar{V} at the nodal point I
X(6,I)	\bar{H} at the nodal point I
X(7,I)	\bar{M}_ξ at the nodal point I
XX(1,I)	value of \bar{u} or \bar{H} at the starting boundary
XX(2,I)	value of $\bar{\beta}$ or \bar{M}_ξ at the starting boundary
XX(3,I)	value of \bar{w} or \bar{V} at the starting boundary
XY(1,I)	value of \bar{u} or \bar{H} at the finishing boundary
XY(2,I)	value of $\bar{\beta}$ or \bar{M}_ξ at the finishing boundary
XY(3,I)	value of \bar{w} or \bar{V} at the finishing boundary
IS1,IS2,IS3	indicators of boundary conditions at the starting boundary
IF1,IF2,IF3	indicators of boundary conditions at the finishing boundary
NP	Number of Pass; NP = 1 indicates linear solution
T22(N)*	$\bar{N}_\xi = N_\xi / (P.R)$
T7(N)	$\bar{N}_\theta = N_\theta / (P.R.)$

T9(N)	$\bar{M}_\theta = M_\theta / (P.R.h)$
Y(1,N)	$\bar{\xi} = \xi / \xi_o$
Y(2,N)	$\bar{u} = uEh / (P.R^2)$
Y(3,N)	$\bar{\beta} = \beta$
Y(4,N)	$\bar{w} = wEh / (P.R^2)$
Y(5,N)	$\bar{V} = V / (P.R)$
Y(6,N)	$\bar{H} = H / (P.R)$
Y(7,N)	$\bar{M}_\xi = M_\xi / (P.R.h)$
ST1	$\bar{\sigma}_{ci} = \sigma_{ci} / E$, normalized circumferential stress at the inner surface of the shell
ST2	$\bar{\sigma}_{co} = \sigma_{co} / E$, normalized circumferential stress at the outer surface of the shell
ST3	$\bar{\sigma}_{ai} = \sigma_{ai} / E$, normalized axial stress at the inner surface
ST4	$\bar{\sigma}_{ao} = \sigma_{ao} / E$, normalized axial stress at the outer surface

* N denotes points in a segment at which the variables are evaluated.

APPENDIX-B

PROGRAM LISTING

```
* -----  
*      PROGRAM FOR SHELL ANALYSIS  
* -----  
  
REAL*8 X(21,7),Y(7,21),Z(7,6),Y1(7,21),Y2(21,3),Y3(21,3)  
REAL*8 H(32),IG(20),APH(20),X7(21,7),AK(4),T22(21),Z2(3,1)  
REAL*8 AY(3,1),BY(3,1),F(7,21),X2(3,1),RO(21)  
REAL*8 TS1(3,3),TS2(3,3),TS3(3,3),TS4(3,3),TF1(3,3),TF2(3,3)  
REAL*8 TF3(3,3),TF4(3,3),A14(3,1),A15(3,1),A16(3,1),A17(3,1)  
REAL*8 A18(3,3),C(21,3,3),A(21,3),E(21,3,3),B(21,3),X1(3,1)  
REAL*8 C1(21),C2(21),T7(21),T9(21),T10(21),R(21),PH(21)  
REAL*8 Z1(3,1),A1(3,3),A2(3,3),A3(3,3),A4(3,3),A6(3,3)  
REAL*8 A7(3,3),A8(3,3),A9(3,1),A10(3,1),A11(3,1),A12(3,1)  
REAL*8 XX(3,1),XY(3,1),U(6,6),ZZXX(21),ZZNN(21),XYX4(21)  
REAL*8 ROO(21),YYN(21),XYX2(21),T3,T,T21,TM  
REAL*8 PB2,RC,AKL,EL,FL,DR,TO,TL,ZZ,FF,P3,DP,PHI,ALP  
OPEN(1,FILE='INPUT',STATUS='OLD')  
OPEN(3,FILE='OUT',STATUS='UNKNOWN',RECL=1400)  
OPEN(4,FILE='AX',STATUS='UNKNOWN',RECL=1400)  
OPEN(5,FILE='RD',STATUS='UNKNOWN',RECL=1400)  
OPEN(7,FILE='SHAPE',STATUS='UNKNOWN',RECL=1400)  
NP=0  
IN=1  
SOB2=0.  
  
SS=1.  
N2=6  
  
N3=3  
  
PB2=1.5707963268  
  
FOC=1.
```

```

*-----
*===== PART A. (READING IN INFORMATION)=====
*-----

```

```

      READ(1,110)EM1,SOB1,XL
      WRITE(3,110)EM1,SOB1,XL
25    READ(1,59)M
      WRITE(3,59)M
      READ(1,110)AN,EM
      WRITE(3,110)AN,EM
      READ(1,1100) T
      WRITE(3,1100) T
1100  FORMAT(10F7.2)
      MO=M+1
      DO 169 I=1,MO
      DO 170 J=1,7
170    X(I,J)=0.
169   CONTINUE
      READ(1,41)(XX(I,1),I=1,3)
      WRITE(3,41)(XX(I,1),I=1,3)
      READ(1,41)(XY(I,1),I=1,3)
      WRITE(3,41)(XY(I,1),I=1,3)
      READ(1,59)IS1,IS2,IS3
      WRITE(3,59)IS1,IS2,IS3
      READ(1,59)IF1,IF2,IF3
      WRITE(3,59)IF1,IF2,IF3

```

```

*-----
*
*                               INITIALIZATION BLOCK
*-----

```

```

      FR1=SQRT(FOC)
      FR2=SQRT(FOC+1.)
      ZFZ=FR2+SQRT(1.)
      YFY=FR1
      RC=XL+(FR2+FOC*ALOG(ZFZ/YFY))*(1.-XL)
      DP=PB2
      ANGB=DP
      DR=1./RC
      SEGL=1./REAL(M)*(1.-XL/RC)
      X(1,1)=1.
      DO 171 I =1,M
171    X(I+1,1)=X(I,1)-SEGL
      WRITE(3,41)((X(J,I),I=1,7),J=1,MO)

```

```

*-----

```

* PART B.(TREATMENT OF BOUNDARY CONDITION)

```

DO 21 I=1,N3
DO 21 J=1,N3
TS1(I,J)=0.0
TS2(I,J)=0.0
TS3(I,J)=0.0
TS4(I,J)=0.0
TF4(I,J)=0.0
TF3(I,J)=0.0
TF2(I,J)=0.0
21 TF1(I,J)=0.0
IF(IS1)23,23,24
23 TS1(1,1)=1.0
TS4(2,2)=1.0
GO TO 27
24 TS2(1,2)=1.0
TS3(2,1)=1.0
27 IF(IS2)28,28,29
28 TS1(2,2)=1.0
TS4(3,3)=1.0
GO TO 30
29 TS2(2,3)=1.0
TS3(3,2)=1.0
30 IF(IS3)33,33,34
33 TS1(3,3)=1.0
TS4(1,1)=1.0
GO TO 35
34 TS2(3,1)=1.0
TS3(1,3)=1.0
35 IF(IF1)36,36,37
36 TF2(1,2)=1.0
TF3(2,1)=1.0
GO TO 38
37 TF1(1,1)=1.0
TF4(2,2)=1.0
38 IF(IF2)39,39,40
39 TF2(2,3)=1.0
TF3(3,2)=1.0
GO TO 819
40 TF1(2,2)=1.0
TF4(3,3)=1.0
819 IF(IF3)84,84,87
84 TF2(3,1)=1.0
TF3(1,3)=1.0
GO TO 88
87 TF1(3,3)=1.0
TF4(1,1)=1.0
88 CONTINUE

```

* -----

* PART C. (CALCULATION OF CONSTANTS)

* -----

```
DO 31 J=1,M
31 H(J)=(X(J+1,1)-X(J,1))*0.05
405 CONTINUE
DP=ANGB
DR=1./RC
26 DO 1 J1=1,M
TZ=1.+AN
T1=RC*(1.-AN*AN)
T21=EM*T
TO=1./(12.*T1*EM*T*T)
TL=RC/T/EM
TM=EM*T*T
PR=EM*T
N=1
DO 32 I=1,7
32 Y(I,N)=X(J1,I)
DO 300 I=1,21
IF(I-21)312,306,306
312 Y(1,I+1)=Y(1,I)+H(J1)
306 PH(I)=DP
RO(I)=DR
ZZXX(I)=2.*FOC*(1.-XL)/DTAN(DP)
ZZ=PH(I)
DO 310 J=1,4
```

```

      FF=0.5*(RC/FOC)/(1.-XL)*(SIN(ZZ))**3.
      AK(J)=H(J1)*FF
      GO TO (311,311,314,310),J
311   V=.5
      GO TO 316
314   V=1.
316   ZZ=PH(I)+V*AK(J)
310   CONTINUE
      DP=PH(I)+(AK(1)+AK(4)+2.*(AK(3)+AK(2)))/6.
      DR=(1.-FOC*(1.-XL)/TAN(DP)*1./TAN(DP))/RC
300   CONTINUE
      DR=RO(21)
      DP=PH(21)
      N1=1
* -----
*   INTEGRATION OF FUNDAMENTAL SET STARTS
* -----
60    NO=0
46    CONTINUE
      IF(NP-1)111,111,199
199   T2=Y(2,N)/RO(N)
      T3=PH(N)-Y(3,N)
      C1(N)=DCOS(T3)
      C2(N)=DSIN(T3)
      T4=(DSIN(PH(N))-DSIN(T3))/RO(N)
      T5=Y(6,N)*C1(N)+Y(5,N)*C2(N)
      T22(N)=T5

```

```

T8=T1*T5-AN*T2
T6=(Y(7,N)-AN*TO*T4)/TO
T7(N)=(T2+AN*T8)/T1
T9(N)=TO*(T4+AN*T6)
T10(N)=TL+T8
R(N)=TL*RO(N)+Y(2,N)
F(2,N)=T10(N)*C1(N)-DCOS(PH(N))*TL
F(3,N)=T6
F(4,N)=T10(N)*C2(N)-DSIN(PH(N))*TL
F(5,N)=-T10(N)*(Y(5,N)*C1(N)/R(N)-PR*C1(N))
F(6,N)=-T10(N)*((Y(6,N)*C1(N)-T7(N))/R(N)+PR*C2(N))
F(7,N)=(T10(N)*C1(N)/R(N))*(T9(N)-Y(7,N))-T10(N)
1*(Y(6,N)*C2(N)-Y(5,N)*C1(N))*TM
GO TO 200

```

```

111 C1(N)=DCOS(PH(N))
    C2(N)=DSIN(PH(N))
    T2=Y(2,N)/RO(N)
    T4=Y(3,N)*C1(N)/RO(N)
    T5=Y(6,N)*C1(N)+Y(5,N)*C2(N)
    T22(N)=T5
    T8=T1*T5-AN*T2
    T6=Y(7,N)/TO-AN*T4
    T7(N)=(T2+AN*T8)/T1
    T9(N)=(T4+AN*T6)*TO
    F(2,N)=T8*C1(N)+Y(3,N)*C2(N)*TL
    F(3,N)=T6
    F(4,N)=T8*C2(N)-Y(3,N)*C1(N)*TL

```

```

F(5,N)=- (Y(5,N)/RO(N)-RC)*C1(N)
F(6,N)=- (Y(6,N)*C1(N)-T7(N))/RO(N)-RC*C2(N)
TX=- (Y(7,N)-T9(N.))/RO(N)
F(7,N)=TX*C1(N)-RC*T*(Y(6,N)*C2(N)-Y(5,N)*C1(N))
200  IF(N-2)42,43,43
43   IF(N-6)44,47,45
44   N=N+1
      GO TO 46
42   DO 81 J=2,6
      P2=FLOAT(J-1)
      P3=P2*H(J1)
      Y(1,J)=Y(1,1)+P3
      DO 81 I=2,7
81   Y(I,J)=Y(I,1)+P3*F(I,1)
      N=2
      IP=1
      GO TO 46
47   DO 48 I=2,7
      Z(I,2)=Y(I,1)+(H(J1)/1440.)*(493.*F(I,1)+1337.
1*F(I,2)-618.*F(I,3)+302.*F(I,4)-83.*F(I,5)+9.*F(I,6))
      Z(I,3)=Y(I,1)+(H(J1)/90.)*(28.*F(I,1)+129.*F(I,2)
1+14.*F(I,3)+14.*F(I,4)-6.*F(I,5)+F(I,6))
      Z(I,4)=Y(I,1)+(3.*H(J1)/160.)*(17.*F(I,1)+73.*F(I,2)
1+38.*(F(I,3)+F(I,4))-7.*F(I,5)+F(I,6))
      Z(I,5)=Y(I,1)+(4.*H(J1)/90.)*(7.*(F(I,1)+F(I,5))
1+32.*(F(I,2)+F(I,4))+12.*F(I,3))

```

```

48   Z(I,6)=Y(I,1)+(5.*H(J1)/288.)*(19.*(F(I,1)+F(I,6))
      1+75.*(F(I,2)+F(I,5))+50.*(F(I,4)+F(I,3)))
      R1=0.
      IP=IP+1
      DO 49 I=2,7
      DO 49 J=2,6
      R1=DABS(Y(I,J)-Z(I,J))+R1
49   Y(I,J)=Z(I,J)
      IF(IP-15)141,45,45
141  IF(R1-.1E-07)45,45,50
50   N=2
      GO TO 46
45   IF(NO-1)53,53,55
53   N=N+1
      IF(N-21)61,61,62
61   Y(1,N)=Y(1,N-1)+H(J1)
      DO 51 I=2,7
51   Y(I,N)=Y(I,N-6)+(.3*H(J1))*(11.*(F(I,N-5)+F(I,N-1))
      1-14.*(F(I,N-4)+F(I,N-2))+26.*F(I,N-3))
99   NO=2
      IP=1
      GO TO 46
55   R1=0.
      IP=IP+1
      DO 56 I=2,7
      Z(I,1)=Y(I,N-6)+(.3*H(J1))*(F(I,N-6)+5.*F(I,N-5)+F(I,N-4)+6.*
      1F(I,N-3)+F(I,N-2)+5.*F(I,N-1)+F(I,N))

```



```

R1=R1+DABS(Y(I,N)-Z(I,1))
56  Y(I,N)=Z(I,1)
    IF(IP-10)142,60,60
142  IF(R1-.1E-07)60,46,46
62   IF(NP-1)662,762,912
912  IF(AA-.10)911,911,914
914  IF(NP-10)662,911,911
911  IN=2
    GO TO 764
762  RRR=0.
    DO 763 I=2,7
763  RRR=RRR+DABS(Y(I,21)-X(J1+1,I))
    IF(RRR-.1)764,764,766
766  WRITE(3,767)
767  FORMAT(2X,/, ' SEGMENT IS TOO LONG',/)
764  CONTINUE

```

```

* -----
*           PART D. OUTPUT OF RESULTS
* -----

```

```

WRITE(3,508)
WRITE(3,507)
DO 793 N=1,21,4
ST1= T7(N)+T9(N)*6.
ST2= T7(N)-T9(N)*6.
ST3= T22(N)+Y(7,N)*6.
ST4= T22(N)-Y(7,N)*6.
ROO(N)=RC*RO(N)

```

```

ZZNN(N)=ZZXX(N)-EM*Y(4,N)*2000.
YYN(N)=ROO(N)+EM*Y(2,N)*2000.
WRITE(7,105) ZZXX(N),ROO(N),ZZNN(N),YYN(N)
793  WRITE(3,105)Y(1,N),Y(2,N),Y(4,N),T9(N),Y(7,N),T22(N),T7(N),
1ST1,ST2,ST3,ST4
GO TO 1

```

```

C=====

```

```

C  INTEGRATION OF DERIVED SET STARTS

```

```

C=====

```

```

662  N1=N1+1
      N=1
      Y1(1,N)=X(J1,1)
      DO 63 I=2,7
63    Y1(I,N)=0.
      Y1(N1,N)=1.
90    NO=0
76    CONTINUE
      IF(NP-1)502,502,202
202   T2=Y1(2,N)/RO(N)
      T3=Y1(3,N)*C1(N)/RO(N)
      T4=Y1(6,N)*C1(N)+Y1(5,N)*C2(N)-Y1(3,N)*(Y(5,N)*C1(N)
1-Y(6,N)*C2(N))
      T5=T1*T4-AN*T2
      T6=Y1(7,N)/TO-AN*T3
      Q1=(T2+AN*T5)/T1
      T8=TO*(T3+AN*T6)
      F(2,N)=T5*C1(N)+T10(N)*Y1(3,N)*C2(N)

```

$$F(4,N)=T5*C2(N)-T10(N)*Y1(3,N)*C1(N)$$

$$F(3,N)=T6$$

$$TA=(Y(6,N)*C1(N)-T7(N))/R(N)$$

$$F(6,N)=-T5*(TA+PR*C2(N))-T10(N)*((Y1(6,N)*C1(N) \\ 1+Y1(3,N)*Y(6,N)*C2(N)-Q1-TA*Y1(2,N))/R(N)-PR*Y1 \\ 1(3,N)*C1(N))$$

$$F(5,N)=-F(2,N)*(Y(5,N)/R(N)-PR)-T10(N)*C1(N)*(Y1(5,N) \\ 1-Y(5,N)*Y1(2,N)/R(N))/R(N)$$

$$TX=(T9(N)-Y(7,N))/R(N)$$

$$F(7,N)=F(2,N)*(TX+TM*Y(5,N))+T10(N)*(C1(N)*(TM*Y1(5,N) \\ 1+(-Y1(7,N)+T8-TX*Y1(2,N))/R(N))-TM*C2(N)*Y1(6,N)) \\ 1-TM*F(4,N)*Y(6,N)$$

GO TO 203

502 $T2=Y1(2,N)/RO(N)$

$$T4=Y1(3,N)*C1(N)/RO(N)$$

$$T5=Y1(6,N)*C1(N)+Y1(5,N)*C2(N)$$

$$T8=T1*T5-AN*T2$$

$$T6=Y1(7,N)/TO-AN*T4$$

$$T7(N)=(T2+AN*T8)/T1$$

$$T9(N)=(T4+AN*T6)*TO$$

$$F(2,N)=T8*C1(N)+Y1(3,N)*C2(N)*TL$$

$$F(3,N)=T6$$

$$F(4,N)=T8*C2(N)-Y1(3,N)*C1(N)*TL$$

$$F(5,N)=-Y1(5,N)/RO(N)*C1(N)$$

$$F(6,N)=-Y1(6,N)*C1(N)-T7(N))/RO(N)$$

$$TX=-Y1(7,N)-T9(N))/RO(N)$$

$$F(7,N)=TX*C1(N)-RC*T*(Y1(6,N)*C2(N)-Y1(5,N)*C1(N))$$

```

203  IF(N-2)72,73,73
73   IF(N-6)74,77,75
74   N=N+1
      GO TO 76
72   DO 82 J=2,6
      P2=FLOAT(J-1)
      P3=P2*H(J1)
      Y1(1,J)=Y1(1,1)+P3
      DO 82 I=2,7
82   Y1(I,J)=Y1(I,1)+P3*F(I,1)
      N=2
      IP=1
      GO TO 76
77   DO 78 I=2,7
      Z(I,2)=Y1(I,1)+(H(J1)/1440.)*(493.*F(I,1)+1337.*F(I,2)
1-618.*F(I,3)+302.*F(I,4)-83.*F(I,5)+9.*F(I,6))
      Z(I,3)=Y1(I,1)+(H(J1)/90.)*(28.*F(I,1)+129.*F(I,2)+14.
1*F(I,3)+14.*F(I,4)-6.*F(I,5)+F(I,6))
      Z(I,4)=Y1(I,1)+(3.*H(J1)/160.)*(17.*F(I,1)+73.*F(I,2)
1+38.*(F(I,3)+F(I,4))-7.*F(I,5)+F(I,6))
      Z(I,5)=Y1(I,1)+(4.*H(J1)/90.)*(7.*(F(I,1)+F(I,5))+32.
1*(F(I,2)+F(I,4))+12.*F(I,3))
78   Z(I,6)=Y1(I,1)+(5.*H(J1)/288.)*(19.*(F(I,1)+F(I,6))
1+75.*(F(I,2)+F(I,5))+50.*(F(I,4)+F(I,3)))
      R1=0.
      IP=IP+1
      DO 79 I=2,7

```

```

DO 79 J=2,6
R1=DABS(Y1(I,J)-Z(I,J))+R1
79  Y1(I,J)=Z(I,J)
    IF(IP-15)143,75,75
143  IF(R1-.1E-06)75,75,80
80   N=2
    GO TO 76
75   IF(NO-1)83,83,85
83   N=N+1
    IF(N-21)91,91,92
91   Y1(1,N)=Y1(1,N-1)+H(J1)
    DO 95 I=2,7
95   Y1(I,N)=Y1(I,N-6)+(.3*H(J1))*(11.*(F(I,N-5)+F(I,N-1))
1-14.*(F(I,N-4)+F(I,N-2))+26.*F(I,N-3))
101  NO=2
    IP=1
    GO TO 76
85   R1=0.
    IP=IP+1
    DO 86 I=2,7
    Z(I,1)=Y1(I,N-6)+(.3*H(J1))*(F(I,N-6)
1+5.*F(I,N-5)+F(I,N-4)+6.*F(I,N-3)+F(I,N-2)+5.*F(I,N-
1  1)+F(I,N))
    R1=R1+DABS(Y1(I,N)-Z(I,1))
86   Y1(I,N)=Z(I,1)
    IF(IP-10)144,90,90
144  IF(R1-.1E-07)90,76,76

```

```

92   DO 22 J=1,N2
22   U(N1-1,J)=Y1(J+1,21)
      IF(N1-7)662,96,96
104  FORMAT (7E14.8)
59   FORMAT (31I2)
508  FORMAT (/ ,2X,'DISTANCE',3X,' DISPLACEMENTS',9X,'MOMENTS',
      19X,'STRESS', ' RESULTANTS',5X,'CIRCUM. STRESS',7X,
      1'AXIAL STRESS')
507  FORMAT (1X,' FROM APEX',2X,'RADIAL',5X,'AXIAL',3X,
      1'CIRCUM.',5X,'AXIAL',3X,'CIRCUM.',5X,'AXIAL',4X,'INNER',5X,
      1'OUTER',5X,'INNER',5X,'OUTER',/)
41   FORMAT (7E11.5)
110  FORMAT (10E11.5)
105  FORMAT (12E10.4)
505  FORMAT (//,2X,' NO. OF PASS= ',I2,' RESIDUE= ',E11.5,
      1' LOAD(P/E)= ',E11.5,' EM1= ',E11.5,/)
* -----
*   SOLUTION OF MATRIX EQUATIONS STARTS
* -----
96   N1=J1
      DO 4 I=1,N3
      DO 4 J=1,N3
      A1(J,I)=U(I,J)
      A2(J,I)=U(I+3,J)
      A3(J,I)=U(I,J+3)
      A4(J,I)=U(I+3,J+3)
      X1(I,1)=X(N1,I+1)

```

```

X2(I,1)=X(N1,I+4)
Y3(N1+1,I)=Y(I+1,21)
4  Y2(N1+1,I)=Y(I+4,21)
DO 20 I=1,N3
AY(I,1)=Y3(N1+1,I)
20  BY(I,1)=Y2(N1+1,I)
CALL MATM(A1,X1,A9,N3,N3,1)
CALL MATM(A2,X2,Z1,N3,N3,1)
CALL MATS(A9,Z1,N3,1)
CALL MATSB(Z1,N3,1)
CALL MATS(AY,Z1,N3,1)
CALL MATM(A3,X1,A9,N3,N3,1)
CALL MATM(A4,X2,Z2,N3,N3,1)
CALL MATS(A9,Z2,N3,1)
CALL MATSB(Z2,N3,1)
CALL MATS(BY,Z2,N3,1)
IF(N1-1)6,6,7
6  CALL MATM(A1,TS1,A6,N3,N3,N3)
CALL MATM(A1,TS2,A7,N3,N3,N3)
CALL MATM(A2,TS3,A1,N3,N3,N3)
CALL MATS(A6,A1,N3,N3)
CALL MATM(A2,TS4,A6,N3,N3,N3)
CALL MATS(A6,A7,N3,N3)
CALL MATM(A3,TS1,A6,N3,N3,N3)
CALL MATM(A3,TS2,A8,N3,N3,N3)
CALL MATM(A4,TS3,A3,N3,N3,N3)
CALL MATS(A6,A3,N3,N3)

```

```

CALL MATM(A4,TS4,A6,N3,N3,N3)
CALL MATS(A6,A8,N3,N3)
DO 2 I=1,N3
DO 2 J=1,N3
A4(I,J)=A8(I,J)
2 A2(I,J)=A7(I,J)
CALL MATI(A2,A6,N3)
CALL MATM(A4,A6,A7,N3,N3,N3)
CALL MATI(A7,A8,N3)
CALL MATM(A1,XX,A9,N3,N3,1)
CALL MATS(Z1,A9,N3,1)
CALL MATSB(A9,N3,1)
CALL MATM(A3,XX,A10,N3,N3,1)
CALL MATS(Z2,A10,N3,1)
CALL MATM(A4,A6,A7,N3,N3,N3)
CALL MATM(A7,A9,A11,N3,N3,1)
CALL MATS(A11,A10,N3,1)
CALL MATSB(A10,N3,1)
GO TO 8
7 IF(N1-M)3,5,5
5 CALL MATM(TF1,A1,A6,N3,N3,N3)
CALL MATM(TF3,A1,A7,N3,N3,N3)
CALL MATM(TF2,A3,A1,N3,N3,N3)
CALL MATS(A6,A1,N3,N3)
CALL MATM(TF4,A3,A6,N3,N3,N3)
CALL MATS(A6,A7,N3,N3)
CALL MATM(TF1,A2,A6,N3,N3,N3)

```



```

CALL MATM(TF3,A2,A18,N3,N3,N3)
CALL MATM(TF2,A4,A2,N3,N3,N3)
CALL MATS(A6,A2,N3,N3)
CALL MATM(TF4,A4,A6,N3,N3,N3)
CALL MATS(A6,A18,N3,N3)
CALL MATM(TF1,Z1,A14,N3,N3,1)
CALL MATM(TF3,Z1,A15,N3,N3,1)
CALL MATM(TF2,Z2,Z1,N3,N3,1)
CALL MATS(A14,Z1,N3,1)
CALL MATM(TF4,Z2,A14,N3,N3,1)
CALL MATS(A14,A15,N3,1)
DO 19 I=1,N3
Z2(I,1)=A15(I,1)
DO 19 J=1,N3
A3(I,J)=A7(I,J)
19  A4(I,J)=A18(I,J)
3   CALL MATM(A1,A8,A7,N3,N3,N3)
CALL MATS(A2,A7,N3,N3)
CALL MATI(A7,A6,N3)
CALL MATM(A1,A8,A7,N3,N3,N3)
CALL MATM(A7,A10,A9,N3,N3,1)
CALL MATS(Z1,A9,N3,1)
CALL MATSB(A9,N3,1)
CALL MATM(A3,A8,A7,N3,N3,N3)
CALL MATM(A7,A10,A11,N3,N3,1)
CALL MATS(A4,A7,N3,N3)
CALL MATM(A6,A9,A12,N3,N3,1)

```

```

CALL MATM(A7,A12,A10,N3,N3,1)
CALL MATS(A11,A10,N3,1)
CALL MATS(Z2,A10,N3,1)
CALL MATSB(A10,N3,1)
CALL MATM(A3,A8,A7,N3,N3,N3)
CALL MATS(A4,A7,N3,N3)
CALL MATM(A7,A6,A1,N3,N3,N3)
CALL MATI(A1,A8,N3)
IF(N1-M)8,9,9
9 CALL MATS(XY,A10,N3,1)
8 DO 5000 I=1,N3
DO 5000 J=1,N3
E(N1,I,J)=A6(I,J)
C(N1,I,J)=A8(I,J)
A(N1,I)=A9(I,1)
B(N1,I)=A10(I,1)
5000 CONTINUE
1 CONTINUE
WRITE(7,*) '//NC'
WRITE(7,*) EM
IF(NP-1)117,115,117
117 GO TO(718,108),IN
718 AA=0.
DO 15 I1=1,M
N1=M-I1+1
DO10 I=1,N3
DO 10 J=1,N3

```

```

A6(I,J)=E(N1,I,J)
A8(I,J)=C(N1,I,J)
A9(I,1)=A(N1,I)
10  A10(I,1)=B(N1,I)
    IF(N1-M)11,12,12
12  CALL MATM(A8,A10,A11,N3,N3,1)
    CALL MATS(A11,A9,N3,1)
    CALL MATM(A6,A9,A12,N3,N3,1)
    CALL MATM(TF1,A11,A14,N3,N3,1)
    CALL MATM(TF2,XY,A15,N3,N3,1)
    CALL MATM(TF3,A11,A16,N3,N3,1)
    CALL MATM(TF4,XY,A17,N3,N3,1)
    DO 89 I=1,N3
    X(MO,I+1)=A15(I,1)+A14(I,1)
89  X(MO,I+4)=A17(I,1)+A16(I,1)
    GO TO 16
11  CALL MATS(A12,A10,N3,1)
    CALL MATM(A8,A10,A11,N3,N3,1)
    CALL MATS(A11,A9,N3,1)
    CALL MATM(A6,A9,A12,N3,N3,1)
    DO 17 I=1,N3
17  X(N1+1,I+1)=A11(I,1)
    IF(N1-1)93,93,16
93  CALL MATM(TS1,XX,A14,N3,N3,1)
    CALL MATM(TS2,A12,A15,N3,N3,1)
    CALL MATM(TS3,XX,A16,N3,N3,1)
    CALL MATM(TS4,A12,A17,N3,N3,1)

```

```

DO 98 I=1,N3
X(1,I+1)=A15(I,1)+A14(I,1)
98 X(1,I+4)=A17(I,1)+A16(I,1)
GO TO 18
16 DO 13 I=1,N3
13 X(N1,I+4)=A12(I,1)
18 DO 15 I=1,N3
AA=DABS(Y3(N1+1,I)-X(N1+1,I+1))+AA
15 AA=DABS(Y2(N1+1,I)-X(N1+1,I+4))+AA
115 NP=NP+1
RES=AA/SS
SS=AA
WRITE(3,505)NP,AA,EM,EM1
WRITE(6,*)EM,EM1,AA,SOB2,RC
IF(NP-5)151,152,152
152 IF(RES-1.)151,151,153
153 DO 154 I=2,7
DO 154 J=1,MO
154 X(J,I)=X7(J,I)
EM=EM-EM1
EM1=EM1/2.
NP=3
151 WRITE(3,104)((X(J,I),I=1,7),J=1,MO)
IF(AA.LT.0.1) THEN
5505 EEM=ABS(EM)
DO 5508 J = 1,MO
XYX4(J) = EM*X(J,4)

```

```

5508 XYX2(J) = EM*X(J,2)
      WRITE(4,5507) EEM,(XYX4(J),J =1,MO)
      WRITE(5,5507) EEM,(XYX2(J),J =1,MO)
5507 FORMAT (31E12.5)
      ELSE
      ENDIF
      GO TO 405
108   DO 155 I=2,7
      DO 155 J=1,MO
155   X7(J,I)=X(J,I)
      IN=1
      NP=3
      AA=1.
      SOB2=SOB2+1.
      EM=EM+EM1
      IF(ABS(EM1)-.1E-10) 109,109,1011
1011  IF(SOB2-SOB1)405,405,109
109   WRITE(3,1270)EM,EM1,SOB2
1270  FORMAT(//'EM= ',E14.8,'EM1= ',E14.8,' SOB2= ',F6.0)
      STOP
      END
C*****
C  SUBROUTINES-----
C*****
      SUBROUTINE MATS (A5,B5,L,K)
      REAL*8 A5(3,3),B5(3,3)
      DO 99 L1=1,L

```

```
DO 99 K1=1,K
99 B5(L1,K1)=A5(L1,K1)+B5(L1,K1)
RETURN
END
```

```
****
SUBROUTINE MATSB (A5,L,K)
REAL*8 A5(3,3)
DO 98 L1=1,L
DO 98 K1=1,K
98 A5(L1,K1)=-A5(L1,K1)
RETURN
END
```

```
****
SUBROUTINE MATM (A5,B5,C5,L,K,K2)
REAL*8 A5(3,3),B5(3,3),C5(3,3)
DO 97 L1=1,L
DO 97 K1=1,K2
C5(L1,K1)=0.
DO 97 J1=1,K
97 C5(L1,K1)=C5(L1,K1)+A5(L1,J1)*B5(J1,K1)
RETURN
END
```

```
****
SUBROUTINE MATI (A5,B5,K1)
REAL*8 A5(3,3),B5(3,3)
P=0.
DO 9 L=1,3
DO 9 K=1,3
GO TO (2,3,4),L
```

```

2      I1=L+1
      I2=L+2
      GO TO 5
3      I1=L+1
      I2=1
      GO TO 5
4      I1=1
      I2=2
5      GO TO (6,7,8),K
6      J1=K+1
      J2=K+2
      GO TO 9
7      J1=K+1
      J2=1
      GO TO 9
8      J1=1
      J2=2
9      B5(K,L)=A5(I1,J1)*A5(I2,J2)-A5(I2,J1)*A5(I1,J2)
      DO 11 L=1,3
11     P=P+A5(1,L)*B5(L,1)
      DO 12 L=1,3
      DO 12 K=1,3
12     B5(L,K)=B5(L,K)/P
      RETURN
      END

```

